

SRL-10-F-1994

**COST-EFFECTIVE RED WATER DISPOSAL
BY ELECTRON BEAM RADIOLYSIS**

Prepared by

James P. Moran, Ph.D.

SCIENCE RESEARCH LABORATORY, INC.
15 Ward Street
Somerville, MA 02143
(617) 547-1122

Contract No. DAAL03-92-C-0012

ARO Project No. P-30332-CH

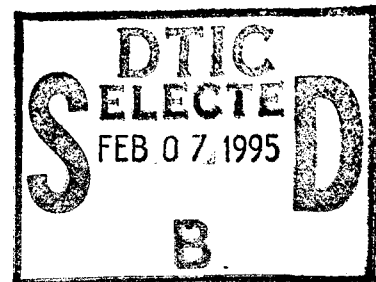
Period of Performance: April 15, 1992 to October 14, 1993

FINAL TECHNICAL REPORT

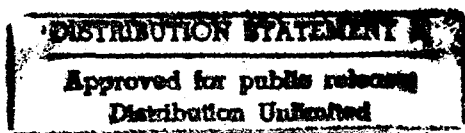
September 2, 1994

Prepared for

U.S. Army Research Office
Research Triangle Park, NC 27709



The views, opinions, and/or findings contained in this report are those of the author(s) and should not be construed as an official Department of the Army position, policy, or decision, unless so designated by other documentation.



REPORT DOCUMENTATION PAGE			Form Approved OMB No. 0704-0188	
Public reporting burden for this collection of information is estimated to average 1 hour per response, including the time for reviewing instructions, searching existing data sources, gathering and maintaining the data needed, and completing and reviewing the collection of information. Send comments regarding this burden estimate or any other aspect of this collection of information, including suggestions for reducing this burden, to Washington Headquarters Services, Directorate for Information Operations and Reports, 1215 Jefferson Davis Highway, Suite 1204, Arlington, VA 22202-4302, and to the Office of Management and Budget, Paperwork Reduction Project (0704-0188), Washington, DC 20503.				
1. AGENCY USE ONLY (Leave blank)	2. REPORT DATE June 28, 1994	3. REPORT TYPE AND DATES COVERED Final 15 Apr 92-14 Apr 94		
4. TITLE AND SUBTITLE Cost-Effective Red Water Disposal by Electron Beam Radiolysis			5. FUNDING NUMBERS DAAL03-92-C-0012	
6. AUTHOR(S) James P. Moran, Ph.D.				
7. PERFORMING ORGANIZATION NAME(S) AND ADDRESS(ES) Science Research Laboratory, Inc. 15 Ward Street Somerville, MA 02143			8. PERFORMING ORGANIZATION REPORT NUMBER SRL-10-F-1994	
9. SPONSORING/MONITORING AGENCY NAME(S) AND ADDRESS(ES) U. S. Army Research Office P. O. Box 12211 Research Triangle Park, NC 27709-2211			10. SPONSORING/MONITORING AGENCY REPORT NUMBER ARO 30332.1-CH	
11. SUPPLEMENTARY NOTES The view, opinions and/or findings contained in this report are those of the author(s) and should not be construed as an official Department of the Army position, policy, or decision, unless so designated by other documentation.				
12a. DISTRIBUTION/AVAILABILITY STATEMENT Approved for public release; distribution unlimited.			12b. DISTRIBUTION CODE	
13. ABSTRACT Key questions addressed in this study are: (1) What is the efficiency and projected cost for electron beam decontamination of red water and other waste water streams? (2) Does induction accelerator technology with associated high electron irradiation dose rates influence process efficiency? Reported results show that dose rate indeed affects decontamination efficiency. However, dose rates, at the lower end of the range which is practical for large scale induction accelerator systems, are as efficient as competing continuous electron beam systems. Said simply, no significant penalty is implicit in the				
14. SUBJECT TERMS Electron Beam Radiolysis, Red Water Disposal, Waste Water Streams, Accelerator Systems, Incineration, Decontamination			15. NUMBER OF PAGES 129	
			16. PRICE CODE	
17. SECURITY CLASSIFICATION OF REPORT UNCLASSIFIED	18. SECURITY CLASSIFICATION OF THIS PAGE UNCLASSIFIED	19. SECURITY CLASSIFICATION OF ABSTRACT UNCLASSIFIED	20. LIMITATION OF ABSTRACT UL	

application of this compact, reliable and low cost technology. The projected dose requirements for red water decontamination is 630 Mrads with a projected treatment cost of \$1.50 per gallon. This is comparable to the cost of incineration; consequently this technology does not present an attractive alternative. It may, however, offer an attractive means for decontamination of pink water which has composite contaminant concentrations of order 200 ppm. This observation is based on reported studies of a variety of volatile organics at concentrations between 40 and 400 ppm. Here the dosages required for reductions by a factor of ten range between 0.73 and 2.7 Mrads and the associated treatment costs are projected as \$1.70 to \$6.40 per thousand gallons. This is much less costly than competing conventional and advanced technologies. Induction accelerator technology as developed at SRL would, therefore, offer a cost effective system which is scalable to hundreds of millions of gallons per year.

TABLE OF CONTENTS

<u>Section</u>		<u>Page</u>
1.0	INTRODUCTION	1
	1.1 Summary of Experimental Results	7
2.0	CHEMISTRY OF ELECTRON BEAM RADIOLYSIS	15
	2.1 Production of H ₂ O ₂ and OH	15
	2.2 Possible Chemical Decomposition of Red Water	17
3.0	RED WATER BACKGROUND	23
	3.1 Composition, Hazard and Destruction of Red Water	24
	3.2 Chemical Analysis of Red Water	26
	3.3 TNT and Isomer Standards	28
4.0	EXPERIMENT DESCRIPTION	31
	4.1 Electron Beam	31
	4.2 Radiolysis Test Cell	44
	4.3 Flow System	49
	4.4 Diagnostics	54
5.0	EXPERIMENTAL RESULTS	59
	5.1 Mod 0.5 Experimental Results	60
	5.1.1 Mod 0.5 Red Water Tests	62
	5.1.2 Mod 0.5 VOC Tests	76
	5.2 Mod 1.5 Experimental Results	92
	5.2.1 Mod 1.5 Red Water Tests	95
	5.2.2 Mod 1.55 VOC Tests	96
6.0	PROCESS COST ANALYSIS	109
	6.1 Configuration and Operating Parameters	110
	6.2 Red Water Process Cost Estimate	113
	6.3 VOCs in Water, Process Cost Estimates	115
7.0	SUMMARY AND CONCLUSIONS	120
	7.1 Summary	120
	7.2 Conclusions	125
	REFERENCES	127

<input checked="" type="checkbox"/>
<input type="checkbox"/>
<input type="checkbox"/>

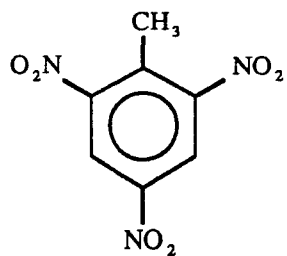
Availability Codes	
Dist	Avail and/or Special
A-1	

1.0 INTRODUCTION

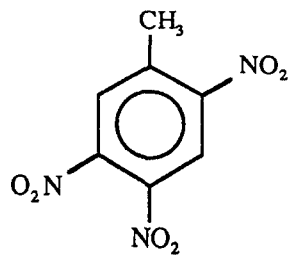
Trinitrotoluene (TNT) is by far the most important explosive in use in military weapons. It is very stable, neutral and does not attack metal. It is used in pure form, or mixed with ammonium nitrate to form Amatols, or with aluminum powder to form Tritonal, or with RDX to form Cyclonite, or with Composition B. It is also used in combinations to form Torpex, HBX and Triallene. Furthermore, TNT is an important component of many industrial explosives.

TNT is produced by nitration of toluene, meta-nitrotoluene or ortho-nitrotoluene with mixed nitric and sulfuric acid in several steps. Insoluble and unwanted isomeric forms are separated from 2,4,6 TNT (alpha TNT) by reaction with sodium sulfite in several stages of sulfite washing and separation. This preferentially replaces the NO^2 at asymmetric sites and renders soluble products. These are removed with the wash solution and they are major constituents of process waste water. Diagrams of symmetric TNT, three isomeric forms and the sodium sulfonate of one isomer are shown in Figure 1. The color of red water is thought to be due primarily to these sulfonates and their complexes. This is discussed further in Chapter 3. For reference, properties of TNT are shown here as Table 1 and representative composition of red water is shown in Table 2.

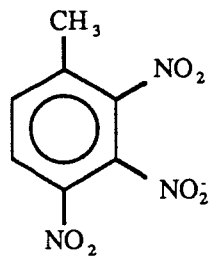
Unfortunately, all U.S. military production facilities of TNT have been closed. This includes the primary site at Radford Army Ammunition Plant (RAAP) in Radford,



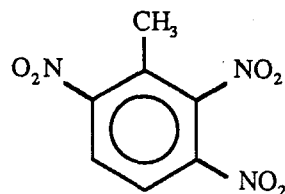
2, 4, 6-TNT
(α-TNT)



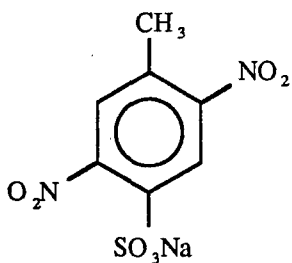
2, 4, 5-TNT



2, 3, 4-TNT



2, 3, 6-TNT

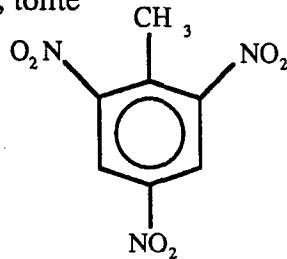


Sodium Sulphonate of 2, 4, 5-TNT

Figure 1: Isomers of TNT and Sodium Sulphonate of 2, 4, 5-TNT

**TABLE 1:
PROPERTIES OF TNT**

2, 4, 6-trinitrotoluene; Trinitrotoluol;
trinitrotoluene; Trotyl; tolite



Pale Yellow Crystals; If Granulated,	Flakes
Gross Formula:	$C_7H_5N_3O_6$
Molecular Weight:	227.1
Energy of Formation:	-44.2 kcal/kg = -184.8 kJ/kg
Enthalpy of Formation:	-62.5 kcal/kg = -261.5 kJ/kg
Oxygen Balance:	-73.9%
Nitrogen Percentage:	18.50%
Volume of Detonation Gases:	730 l/kg
Heat of Explosion	1050 kcal/kg = 4396 kJ/kg
H ₂ O gas:	1080 kcal/kg = 4533 kJ/kg
H ₂ O liquid:	1090 kcal/kg = 4564 kJ/kg
Specific Energy:	870 kJ/kg
Density, Crystals:	1.654 g/cm ³
Density, Molten:	1.47 g/cm ³
Solidification Point:	80.8°C = 177.4 °F
Melting Enthalpy:	23.1 kcal/kg = 96.6 kJ/kg
Specific Heat at 20°C = 68°F:	0.331 kcal/kg = 1.38 kJ/kg

Vapor Pressure:

millibar	Temp. (°C)	Temp. (°F)
0.057	81	178 (melting point)
0.14	100	212
4	150	302
14	200	392
86.5	250	482 (beginning of decomposition)

Lead Block Test:	300 cm ³ /10 g
Detonation Velocity, confined:	6900 m/s = 22,000 ft/s at p = 1.60 g/cm ³
Deflagration Point:	300 °C = 570 °F
Impact Sensitivity:	1.5 kpm = 15 Nm
Friction Sensitivity:	up to 36 kp = 353 N
Pistol Load	No Reaction
Critical Diameter of Steel Sleeve Test:	5 mm

**TABLE 2:
RED WATER SOLIDS**

Inorganic Salts	Percent by Weight
Na ₂ SO ₃ -Na ₂ SO ₄ (Sodium Sulfite - Sodium Sulfate)	32.3
NaNO ₂ (Sodium Nitrite)	11.2
NaNO ₃ (Sodium Nitrate)	1.5
Sodium Sulfide (NaHS-Na ₂ S)	May be present
Sodium Carbonate/Bicarbonate	May be present
	<hr style="width: 100%; border: 0.5px solid black;"/>
	45.0
 Nitro bodies	
Sodium Sulfonate of 2, 4, 5-TNT	22.7
Alpha-TNT-Sellite Complex	16.2
Sodium Sulfonate of 2, 3, 4-TNT	9.6
Sodium Sulfonate of 2, 3, 6-TNT	2.0
Sodium Sulfonate of 2, 3, 5-TNT	Trace
2, 4, 6-TNBA (Trinitrobenzoic Acid) Sodium Salt	1.0
White Compound Sodium Salt	1.0
TNBAL-Bisulfite Addition Compound (Trinitrobenzaldehyde)	1.0
TNBOH (Trinitrobenzyl Alcohol)	1.0
Sodium Nitroformate	0.5
3, 4-DNBA (Dinitrobenzoic Acid) Sodium Salt	Trace
2, 3-DNBA (Dinitrobenzoic Acid) Sodium Salt	Trace
TNB (Trinitrobenzene-Sellite Complex)	Trace
Dissolved 2, 4-DNT (Dinitrotoluene)	Trace
Dissolved α-TNT (Trinitrotoluene)	Trace
	<hr style="width: 100%; border: 0.5px solid black;"/>
	55.0
	<hr style="width: 100%; border: 0.5px solid black;"/>
	100.0

Virginia. Closures have been mandated until methods have been developed and deployed for environmentally acceptable disposal of red water. The U.S. Army is exploring the option of incineration of red water which is expensive both in terms of plant construction cost and operating cost. Consequently the army, and in particular personnel at Picatinny Arsenal (Dr. R. Goldberg) and at RAPP (Mr. Chip Batton), are actively seeking alternatives for cost effective destruction of red water contaminants. They have obtained the samples of red water from the ICI explosives facility in Canada which were used in the current studies. The first sample was accompanied by the listing in Table 2 which was described as a compilation of information.

The broad objective of this effort is to develop an experimental basis for a new, low cost process for removing contaminants in waste water using pulsed electron beams from a new generation of compact, reliable and inexpensive induction accelerators. Some current methods of water contaminant removal such as activated carbon absorption and air stripping merely transfer the contaminants to a different phase.^(1,2) Current methods of contaminant destruction include ozonation, ultraviolet photolysis, photocatalysis, supercritical oxidation, electron beam radiolysis, biodegradation and incineration.^(3,4) Among emerging technologies electron beam radiolysis appears an attractive option since the process of radical formation in water and radical attack on contaminants and contaminant by-products is energy efficient and relatively nonselective. Radiolysis is safe and compatible with high throughput operation. It has been demonstrated effective and efficient in the destruction of a variety of volatile organic contaminants over a broad range

of initial concentrations (0.1-400 ppm)⁽⁴⁻⁶⁾ and in the decontamination and disinfection of potable water and waste water even with the presence of suspended solids.⁽⁷⁻¹⁰⁾ A variety of electron accelerator technologies have been employed in the irradiation of gases and liquids including Van de Graaff, Cockcroft-Walton, insulating core transformers, Dynamitrons, radio frequency (rf) linear accelerators, and linear induction accelerators.^(6,11,12) All except perhaps the last have limitations in reliability, excessive size, initial cost, scalability in average power or in serviceability. Commercial implementation has been impeded due to these limitations.

The current broad interest in the disinfection and detoxification of contaminated military, industrial and municipal waste water by direct electron beam radiolysis rests on the promise of complete and thermally efficient destruction of contaminant by-products as well as original contaminants. With such a wide variety of electron accelerator technologies being applied in these studies, acceptance and implementation must await a comparative assessment in terms of overall cost and the demonstration of practical and reliable operation of pilot and full scale systems in the field. This effort addresses these issues for water decontamination by direct electron beam radiolysis using a linear induction accelerator. The characteristics of short pulse lengths (tens of nanoseconds) and low interstage voltage differences (of order 100 keV) allow compact and inexpensive construction. High pulse rates (5-10 kHz) provide very high average power. Despite the significant current interest in electron beam radiolysis for water decontamination, Science Research Laboratory, Inc. (SRL) alone is currently working with induction accelerators.

Experimental studies conducted at Science Research Laboratory (SRL) examine the effectiveness of electron beam radiolysis on the destruction of red water constituents and of the building blocks, benzene and toluene. Additional studies with trichloroethylene and methylene chloride were also conducted to provide comparisons with electron beam radiolysis experiments at other facilities and to broaden the context of these studies. A part of this additional work was supported by the Electric Power Research Institute. These studies report the first use of a linear induction accelerator for electron beam generation for this application. A key objective is to determine destruction efficiency at the high dose rates which are characteristic of this technology. A closed contaminated water system has been constructed in which a flowing stream is irradiated while passing in direct contact with the electron beam foil window. This novel feature provides both efficient and uniform irradiation and effective foil cooling. The closed system allows evaluation of contaminants reduction both due to radiolysis destruction and to dissolution to the vapor phase.

1.1 Summary of Experimental Results

Radiolysis experiments and analyses were conducted in two segments, first in the period November 1992 - February 1993, then in the period November 1993 - February 1994. The first segment was conducted with the injector portion of the induction accelerator which produced an electron beam at a nominal current of 500 A and voltage of

0.5 MeV with a pulse duration of 35 nsec. The second segment was conducted after the addition and checkout of an accelerator module which increased the voltage to a nominal 1.5 MeV. The radiolysis cell was modified to accommodate the increased electron energy and was also upgraded to improve dose uniformity and dosimetry.

The primary goal in the first segment was the determination of the efficiency of destruction of red water and VOC contaminants at fixed electron beam pulse conditions both with and without the addition of an oxidizing additive, hydrogen peroxide. These tests were conducted at a single dose rate of 10^{13} Rads/sec. Red water was irradiated after water dilution by factors of ten and one hundred. VOCs were irradiated at equal initial concentrations of 400 ppm. Tests during the second segment explored the effects of dose rate on destruction efficiency, at 7×10^{11} and 1.4×10^{11} , and also broadened the study of efficiency dependence on initial contaminant concentrations down to 40 ppm. In each test segment, accelerator radiolysis operation exceeded ten hours with an accumulation of over one million pulses over a period of several weeks with no difficulties in system performance and no apparent deterioration of the foil window. This has important practical implications for system reliability and for simplification of system configuration.

Destruction of major red water constituents as well as TNT and its isomers was determined by high performance liquid chromatography (HPLC) with UV absorption detection. Red water composition was found to be complex, as expected, with at least

thirty distinguishable peaks. Samples of symmetric TNT and of four of its five isomers were obtained from Dr. R. Spangord of Stanford Research Institute. These were analyzed and identified in the HPLC chromatograms. Destruction of VOCs, benzene, toluene, trichloroethylene and methylene chloride was determined by gas chromatographic analysis and mass spectrometric detection (GCMS). Mass balance assessment by total carbon analysis was carried out for the first test segment and results showed preservation of carbon in soluble forms to a factor of approximately 2.5 while source contaminant concentrations were reduced by nearly three decades. Consequently to conserve resources this analysis was not performed in the second test segment.

During the first test segment four test series were conducted with red water (1 and 2) duplicate runs with red water initially diluted 1:10; (3) initial dilution 1:100; (4) initial dilution 1:10 with the addition of 9200 ppm of hydrogen peroxide. Samples were taken after each of five or six passes through the radiolysis cell to provide records of degree of destruction versus cumulative dosage to maximum levels ranging from 20 to 29 MRads. Samples for 1:10 dilution retained strong red coloring at all dose levels, although color did diminish with increasing dose and the run with peroxide added showed significantly greater reduction in color. The series at 1:100 dilution showed dramatic color change with increasing dosage going from bright red to pale yellow. In all cases results of HPLC analysis showed significant reduction in all resolvable peaks with increasing dosage including those identified with TNT and its isomers. For 1:10 dilution, peaks were reduced approximately linearly with increasing dose to a reduction of 50-60% at the

maximum dose of 19 MRads. For the series with 1:10 dilution and hydrogen peroxide added the peaks did not all follow the same pattern. Some showed approximately linear reduction by levels of 65-70% at the maximum dose of 29 MRads while others showed more rapid and nonlinear destruction patterns. The series with initial dilution of 1:100 showed roughly exponential decay with cumulative dosage for those peaks examined to date with final reductions by factors of 25 to >100. This is consistent with the VOCs destruction studies during this test segment as described below since 1:100 dilution would bring the red water contaminant concentrations to the range of several hundreds of ppm. Credit is due for the success of our subcontractor, Jordi Associates Inc., in development of a very repeatable HPLC separation process for these very complex red water samples. In all cases the color change caused by radiolysis was compared to a series of unirradiated reference samples at selected levels of water dilution. These comparisons showed a quantitative correlation between color change and HPLC measured contaminant destruction.

During the first test segment five test series were conducted with VOCs dissolved in water: (1) initial concentrations of 200 ppm of benzene and 200 ppm of toluene; (2) initial concentration of 400 ppm of toluene; (3) initial concentration of 400 ppm of benzene; (4) initial concentration of 400 ppm of toluene with stoichiometric hydrogen peroxide (2660 ppm) added; (5) initial concentration of 400 ppm of trichloroethylene. Each group was irradiated in increments during each of six or seven passes through the radiolysis cell. Samples were taken after each pass to provide records of VOC

destruction with increasing radiolysis dose to limits of six to seven MRads. Visual observations showed formation of slight amber color and a cloudy precipitate which increased initially with increased dosage and then decreased with further increases in cumulative dosage for all benzene and toluene cases. With peroxide added to toluene these features were less pronounced and the peak in color and precipitate occurred at lower cumulative dose, which suggests that peroxide may accelerate the destruction process. This was verified by subsequent GCMS analysis. This analysis showed VOC destruction by as much as three decades for the above dose range and a roughly exponential decay with increasing dose. Preliminary estimates of destruction efficiency range from 1.5 to 3.0 MRads per decade of VOC removal. Addition of hydrogen peroxide improved the destruction efficiency by approximately a factor of two. Although evolved gas was not analyzed at this time its measured volume determined that it did not constitute a significant part of the depleted VOCs.

During the second test segment, from November 1993 through February 1994, both red water and VOC's were studied. A second sample (approx. 1 kg) of undiluted red water was obtained for these tests early in 1993 by the same sources as the first sample. The specific gravity of this sample was approximately 1.15. Radiolysis tests were conducted on undiluted red water and with no oxidizing additive. It was passed repeatedly through the closed flowing system with an average dose of 10.5 MRads applied in each pass. With 19 passes in total the accumulated dosage was 200 MRads. Samples of red water with no irradiation and with a dose of 200 MRads were each diluted 1:100

with water and were then compared to reference samples at dilution's of 1:100 and 1:333. This comparison showed no color change in the red water as a result of irradiation. On the basis of our earlier correlation between color change and HPLC measured contaminant destruction we concluded that no significant destruction of contaminants occurred as a result of 200 MRads of electron beam irradiation. One may speculate that recombination may play a role in contaminant survival in undiluted red water. Clearly either dilution or addition of an oxidizing agent is desirable for effective decontamination.

During the second test segment seven test series were conducted with VOCs dissolved in water: (1) initial concentrations of 400 ppm of benzene and a dose rate of 7×10^{11} Rads/sec; (2) a duplication of the above; (3) initial concentration of 400 ppm of benzene and a dose rate of 1.4×10^{11} ; (4) initial concentration of 100 ppm of benzene and a dose rate of 7×10^{11} Rads/sec; (5) initial concentration of 100 ppm of benzene and a dose rate of 1.4×10^{11} ; (6) initial concentration of 40 ppm of benzene and a dose rate of 7×10^{11} Rads/sec; (7) initial concentration of 5000 ppm of methylene chloride and a dose rate of 7×10^{11} Rads/sec. Each group was irradiated in increments during each of six to ten passes through the radiolysis cell. Samples were taken after each pass to provide records of VOC destruction with increasing radiolysis dose up to limits ranging from four to eight MRads. Visual observations showed formation of a white cloudy precipitate which resulted from radiolysis and which increased with increased dosage for cases (1) through (5). No precipitate formed for cases (6) and (7). This precipitate appears quite stable and remains in suspension for weeks or longer. It does not appear to dissolve by water

dilution. Samples were stored for possible future analysis. Only small amounts of evolved gas were observed such that dissolution to vapor does not account for a significant fraction of source contaminant or contaminant products of radiolysis.

GCMS analysis of residual source contaminant concentration showed a marked dependence of fractional destruction on both initial concentration and on dose rate as summarized in the following table.

**Summary of Benzene Destruction by One and Two Decades
for Several Initial Concentrations and Dose Rates**

Benzene Init Conc (ppm)	400	400	400	100	100	40
Dose Rate (10^{12} Rads/sec)	10	0.7	0.14	0.7	0.14	0.7
Dose for Destruction (MRads):						
First Decade of Destruction	3.1	2.5	2.1	0.91	0.58	0.37
Second Decade of Destruction	1.7	1.0	0.62	0.45	0.33	0.36
Two Decades of Destruction	4.8	3.5	2.7	1.36	0.91	0.73

The first column above was taken from previous measurements at significantly higher dose rate. Dependencies on both concentration and dose rate are evident. Progress of destruction is not logarithmic except at the lowest initial concentration, as seen by differences in required dose between the first and second decades. Destruction effectiveness is consistent with existing measurements of other investigators at much lower dose rates, i.e. at initial concentrations of 100 and 40 ppm. This suggests that high dose rates which are characteristic of linear induction accelerators are suitable for efficient water decontamination. Reaction products, though not identified, would appear to have

an influence on the continued progress of destruction. For example the dose for the second decade of destruction in the second column (i.e. reduction from 40 ppm to 4 ppm) of 1.0 MRads is much larger than the 0.37 MRad dose for destruction from 40 ppm to 4 ppm in the last column. Trends in the above table are summarized as: required radiolysis dose per decade of destruction increases with increasing contaminant initial concentration and with increasing dose rate; required dose per unit mass of contaminant destruction decreases with increasing contaminant initial concentration. In all benzene studies (cases 1-6) destruction was observed over a range of three to four orders of magnitude. Test results with methylene chloride at an initial concentration of 5000 ppm are consistent with these trends. Several reaction products were detected in the methylene chloride analysis and these will be reported. The presence and persistence of these products and the high dose required for source contaminant destruction point to the potential benefit of addition of an oxidizing agent to drive reactions more rapidly to completion. This was observed in studies at SRL with hydrogen peroxide added to toluene at high concentrations in water as previously reported.

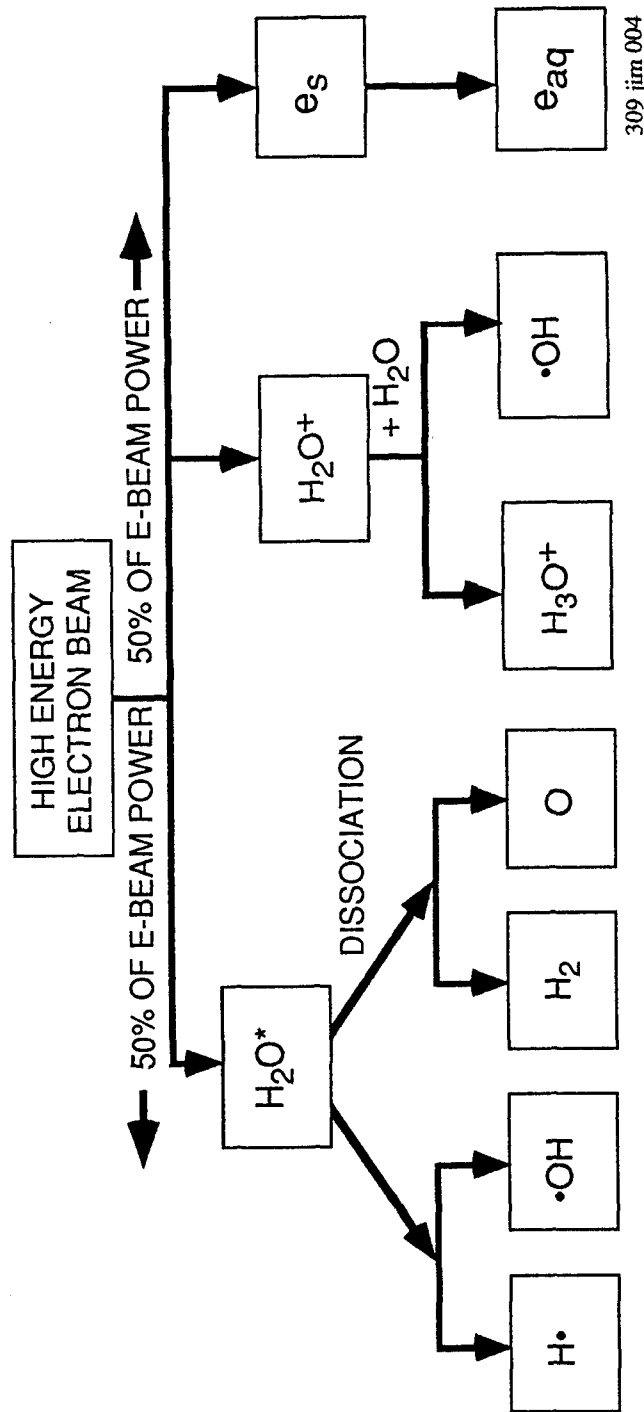
2.0 CHEMISTRY OF ELECTRON BEAM RADIOLYSIS

The chemistry of electron beam detoxification is complex, but SRL modeling of relevant chemical and radiological processes, summarized in this report, indicates that organic compounds can be efficiently and completely oxidized to produce carbon dioxide, hydrogen and water. The concentration of organic contaminants in process water varies widely with concentrations usually in the 0.1-1000 ppm range for VOCs, but as high as 10% by weight for red water. When aqueous solutions at these concentration levels are irradiated by electrons, direct interactions between the electrons and solute molecules are small. Most of the energy is absorbed by the water, producing both oxidizing and reducing radicals that efficiently destroy the toxic contaminants in the water.

2.1 Production of H_2O_2 and OH

When a high energy electron beam irradiates water, approximately 50% of the electron beam power ionizes the water molecules forming H_2O^+ and approximately 50% of the beam power results in excited water molecules, H_2O^* . These primary reactions and subsequent secondary reaction products are shown in the hierarchy of Table 3. In these reactions e_p , the primary high energy beam electron survives to repeat the process many thousands of times and e_s , the secondary electron rapidly becomes hydrated in the aqueous solution. Included in Table 3 is a tabulation of the G values for forming the various

Table 3: Various ions and radicals formed by electron beam irradiation of water



309 jim 004

G Values of Various Ions and Radicals

Product	H•	•OH	H ₂	H ₂ O ₂	H ₃ O ⁺	OH ⁻	e _{aq}
G Value	0.6	2.8	0.45	0.7	3.1	0.4	2.7

species, where the G value is defined as the number of species produced for every 100 eV of electron beam energy absorbed.

From the G values given in Table 3, a total of 15.4 hydrogen atoms and 7.7 oxygen atoms are produced in the form of radicals and ions for every 100 eV of electron beam energy absorbed. This results in 7.7 H_2O molecules dissociated for every 100 eV of electron beam energy absorbed by the water. The maximum total yield for the formation of hydrogen peroxide will be half of this value, i.e.

$$G(H_2O_2) = 3.85 \quad (1)$$

where $G(H_2O_2)$ measures the efficiency of formation of hydrogen peroxide by electron beam radiolysis. However, the oxidizing and reducing species initially formed by electron beam irradiation are even more reactive than H_2O_2 and will be considerably more effective in oxidizing and thereby destroying hydrocarbons in contaminated water.

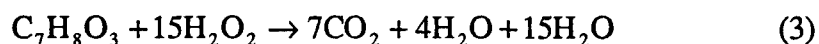
2.2 Possible Chemical Decomposition of Red Water

Major components of red water are isomeric TNT and sodium sulfonates of these isomers. By irradiating the red water with an electron beam, sodium sulfonate of 2,4,5 TNT can be reduced to $NaHSO_4$, NO_2 , water and carbon dioxide. The chemical reactions may proceed along the following pathway: Four hydroxyl radicals oxidize the sodium

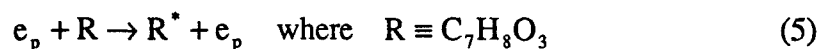
sulfonate of TNT to produce NO_2 and NaHSO_4 . This chemical reaction is shown in Fig. 2 and is given by



The NO_2 will escape as a gas and the NaHSO_4 will precipitate as a harmless salt. The remaining alcohol $\text{C}_7\text{H}_5(\text{OH})_3$ will react with H_2O_2 in a chain reaction and result in water and carbon dioxide as represented by the following chemical reaction



In the absence of an oxidizing additive the water radiolysis product H_2 is formed to provide the required surplus H_2O_2 . Reaction (3) just shows the final product of a complex chain reaction which can be described as follows. The electron beam will simultaneously dissociate H_2O_2 to form two hydroxyl radicals and excite the alcohol R according to



The hydroxyl radicals will react with the H_2O_2 to produce another rather stable radical HO_2 from the following reaction

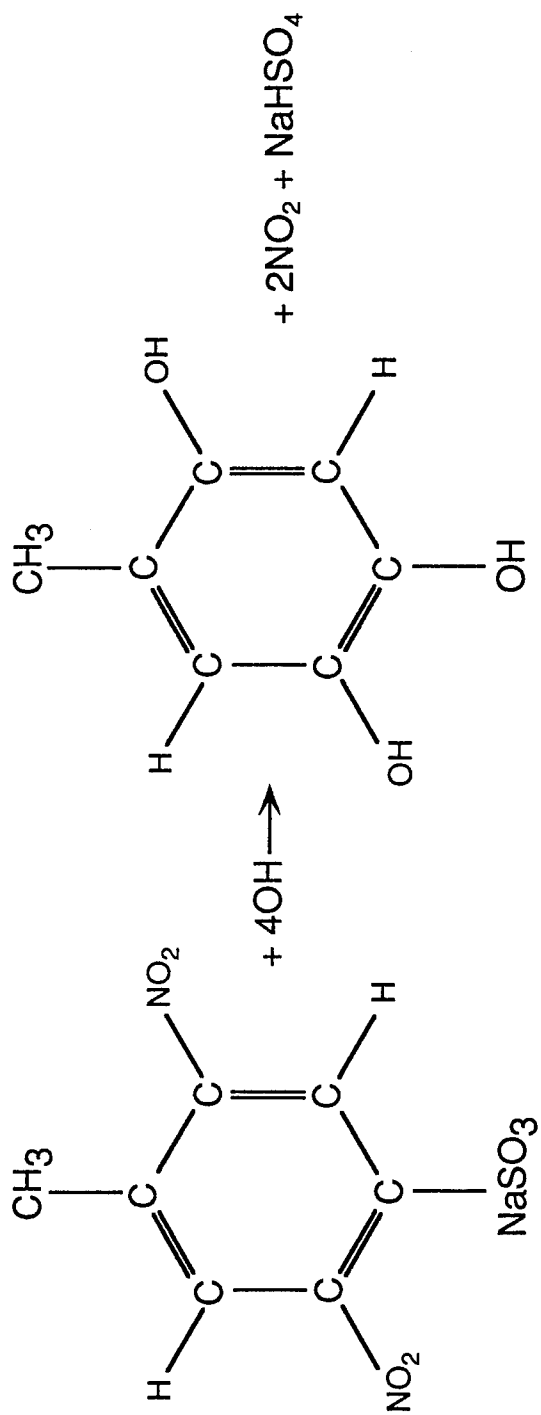
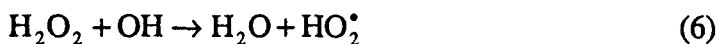
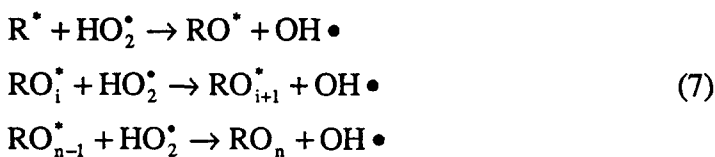


Figure 2: Sodium Sulfonate of TNT may be oxidized by 4 OH radicals to produce NO₂ gas, NaHSO₄ and C₇H₅(OH)₃



The HO_2 radical will oxidize the excited alcohol R^* as represented by the following reactions



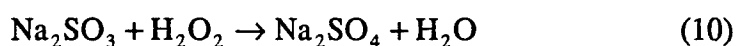
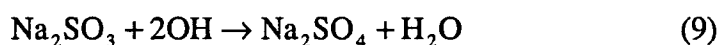
The OH radicals will of course react with the hydrogen peroxide to form HO_2 as shown in reaction (6) thus forming a chain reaction. RO_n is just the complete oxidization of the alcohol to form carbon dioxide and water, i.e.



Next let us consider the required energy for this process. From the G values given in Fig. 1 it requires about 12.5 eV per OH radical in water.⁽¹³⁾ From Equation (2) one determines that 4 OH radicals are required to oxidize each sodium sulfonate of TNT molecule and from Equation (3) we find we need 15 molecules of H_2O_2 to develop the chain reaction to completely oxidize the resulting alcohol molecule. From Eq. (1) it appears that one requires 26 eV per H_2O_2 molecule or 390 eV of electron beam energy absorbed per sodium sulfonate molecule. From this analysis one can conclude that 450 eV

of electron beam irradiation to completely oxidize each molecule of the organic in red water. As stated previously the initial radicals formed by the electron beam irradiation are far more reactive than H_2O_2 and so they are probably much more efficient in destroying the sodium sulfonate of TNT. In fact the existing data on electron beam irradiation shows that only 100 eV of electron beam energy is required to destroy each organic molecule.⁽¹⁴⁾

The destruction of inorganic salts such as Na_2SO_3 and Na_2SO_4 will require substantially less energy. Na_2SO_3 can easily be oxidized by two OH radicals or one H_2O_2 molecule to produce Na_2SO_4 which is a stable salt



So we can conclude that it will take approximately 15 eV to destroy each inorganic molecule.

Bounds on cost for electron beam treatment of red water may be estimated from this analysis with the following assumptions: total contaminant concentration of 10% by weight; organic portion of 55%; representative molecular weight of 284; investment for destruction of an organic molecule of 100-450 eV; investment for an inorganic molecule of 5-15 eV; electron beam transport efficiency of 80%; electron beam production electrical

efficiency of 60%; and a total energy plus system operating cost of \$0.11 per kwh. The resulting cost range is \$0.45-\$2.00 per 1000 gallons of treated red water and the associated radiolysis dose range is 160-700 MRads. Cost analysis in Section 6 indicates the projected lower bound is considerably less than the alternative of incineration whereas the upper bound is comparable to incineration.

3.0 RED WATER BACKGROUND

Considerable background work was conducted to address a variety of questions about red water:

- What is the composition and how does it vary with time and with source?
- What causes the red color?
- What is the origin and knowledge of the samples obtained by SRL?
- What is known about toxicity and hazard?
- How is it presently destroyed?
- What methods are used for chemical analysis?
- How may we obtain TNT and sulfonated TNT standards for analysis?

These question were researched by SRL staff and by a consultant chemical engineer Dr. Deborah Savage of Tellus Institute in Boston, MA. The first level of inquiries were directed to Dr. Richard Loda of the DARPA Defense Sciences Office, Dr. Richard Paur of the Army Research Office in North Carolina, Mr. Chip Batton at RAAP, and Dr. Robert Goldberg of the Production Based Modernization Agency at Picatinny Arsenal in New Jersey. These led in part to further inquiries. Don Kunkle of Aerojet Propulsion Division at Sacramento participated in a red water destruction study under U.S. Army support. Bill Peters of the MIT Energy Laboratory works with Professor Jeff Testor on a U.S. Army supported study of water decontamination by supercritical oxidation. Fred Heim is a chemist at RAAP with historical experience on red water analysis. Ron Spangord of Stanford Research Institute. has extensive experience in red

water analysis and in preparation of TNT standards. Professor Oliver Hao of University of Maryland Civil Engineering Department studied red water decontamination by wet air oxidation. This background work is summarized below under subject headings. We do not attempt to provide a complete thread of contacts or sources of specific information.

3.1 Composition, Hazard and Destruction of Red Water

SRL obtained a comprehensive report from Chip Batton of RAAP⁽¹⁵⁾ which includes discussion of manufacture of TNT, waste composition and some chemical analysis. We also obtained approximately one kilogram of red water which originated from a TNT manufacturing plant operated by ICI of Quebec, Canada. Chip Batton enclosed several sheets, including Table 2, describing red water composition, which he described as a compilation of information. Since the TNT manufacturing process at RAAP was developed at least in part by ICI he felt the RAAP generated compilation, including estimates of 15% solids and a specific gravity of 1.1, was probably representative of the ICI supplied sample. SRL has also confirmed the specific gravity of approximately 1.15 for the supplied sample. Ersin Kutloughlu of ICI in Toronto, Ontario confirmed this specific gravity however both he and Chip point out that dissolved solids may vary significantly. This is partly a result of the feed stock which is currently toluene. ICI has used ortho-nitrotoluene in the past; this produces a lower waste water solid content. Constantine Matusoff of ICI Quebec commented on limited analysis of eight drums of red water with specific gravity between 1.2 and 1.4, and sulfate concentrations

of 5-6%. To summarize we do not know the composition of the test sample, but may link it to the data compilation only by its specific gravity.

The deep red color is ascribed by Fred Heim of RAAP to complexes of symmetric and non-symmetric TNT and sellite (Na_2SO_4). He has observed generally that addition of anions to an aromatic ring will produce color. At the pH of red water, between 7 and 10, he suspects all potentially acidic compounds are fully ionized to anionic form. He feels that red water is highly complex, and no single chromatographic process would provide thorough characterization. Constantine Matusoff feels the red color is partly due to TNT itself and also due to complexes between sellite and TNT isomers. Incidentally both Fred and Ersin agree that the character of red water changes with time.

Red water is currently incinerated at ICI in Canada. They do no analysis of the water, only the ash residue. Persons contacted have no detailed knowledge of hazards or toxicity. Reference 15 cites problems of fire only in places where water evaporates to leave solid residue. Solids will burn with a nominal heat value of 3200 BTU/lbm. Environmental concerns include the strong color which is conspicuous even at a dilution of 1:1000. SRL did not obtain any specific or quantitative explanation of environmental impact. It is listed by RCRA (K047) due to its reactivity. It is said to be toxic to fish and certain trace constituents such as dinitrotoluene isomers are priority pollutants under the Clean Water Act.

3.2 Chemical Analysis of Red Water

SRL has explored chromatographic analytical processes for separation of major constituents of red water. These constituents are not volatile and are not significantly extracted by methylene chloride over a pH range of 2 to 11. Consequently standard Gas Chromatographic/Mass Spectrometric (GCMS) analysis was not applicable. High Pressure (Performance) Liquid Chromatography (HPLC) seemed more promising. SRL obtained segments of a report by Aerojet Propulsion Division (U.S. Army Contract DAAH01-91-C-0738)⁽¹⁶⁾ in which red water analysis was reported. They were successful in HPLC quantification of TNT isomers but not their sulfonated compounds. They were most successful in tracking sulfonated isomers with Nuclear Magnetic Resonance and Capillary Electrophoresis. They did, however, cite work by Chow at the University of Illinois who successfully separated sulfonated isomers of TNT using HPLC. They also referenced Ron Spangord of Stanford Research Institute as a source for isomers of TNT which could provide standards for identification of at least some HPLC peaks.

Teresa Chow worked with Marvin Pawony at the University of Illinois on the analysis of red water constituents using reverse phase HPLC. They used a Hamilton Model PLP-1 column, UV detection at 254 nm and sample injection of 10 μ l. Cetyltrimethylammoniumbromide (0.3%) was used as the ion paring agent. Three solvents were used, constant acetonitrile elution at 35%, gradient elution of meahanol at 25 to 65% and water at 40 to 0% over a time of 30 minutes. There were key differences between

Aerojet and Chow processes which motivated our further exploration of this powerful diagnostic tool.

A search for a qualified and capable laboratory to perform this specialized analysis on a very complex mixture led directly to Howard Jordi of Jordi Associates in Bellingham Ma. SRL contacted 14 laboratories and in many cases were referred to Jordi Associates after we described our needs. Howard accepted this work as a research project and began with a review of our background study and communications with Teressa Chow and Deborah Savage. He concluded that Chow's work was sound and developed his procedures on that basis. The final process is described in Table 4 and the process diagram is shown in Figure 3. He used UV absorption detection at three wavelengths as shown. Absorption at 214 nm would serve to isolate carbonyls and double bonds, absorption at the 214 nm mercury line is historical and absorption at 340 nm would identify aromatic rings with electronegative attachments. Good peak separation was obtained for approximately 30 bands after the process was optimized to conditions in Figure 3. Good resolution and good peak correlation was obtained for detection at 254 nm and 340 nm. All samples were analyzed twice and repeatability was excellent; comparisons between 50 peaks in 20 pairs of duplicate runs showed differences of less than 3% in 90% of the cases.

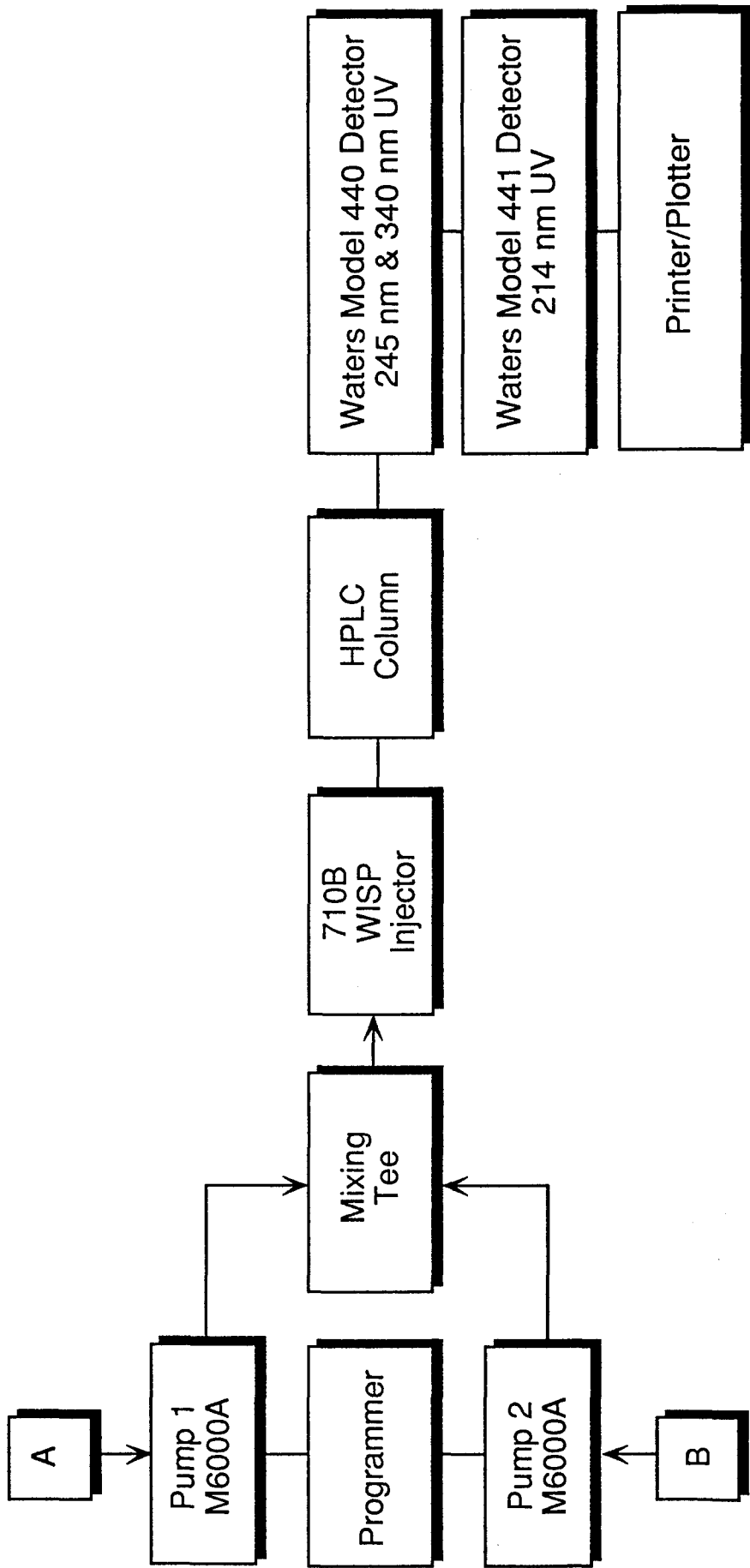
Table 4: Red Water Chemical Analysis

Dr. H. Jordi: Jordi Associates Inc., Bellingham, MA

- **High Performance Liquid Chromatography (HPLC)**
 - Reverse Phase, H₂O + MeOH + ACN on Polydivinylbenzene
 - Ion Pairing Agent, CTMABr (0.3%)
 - Linear Gradient Elution
 - Filtration at 0.45 µm
 - Absorption Detection at 214 nm, 254 nm, 340 nm
- **Gel Permeation Chromatography (GPC)**
 - Jordi Jel Column
 - Solvent, 50/50 MeOH/1M - NaOH
 - Absorption Detection at 400 nm
 - Index of Refraction Detection

3.3 TNT and Isomer Standards

Both Don Kunkle of Aerojet and Teresa Chow of the University of Illinois obtained TNT isomer standards from Ron Spanggord of the Stanford Research Institute. The Aerojet group used these to develop the sulfonated species. Ron Spanggord developed the sulfonates for Teresa Chow. Although this work was done some years ago Ron Spanggord had small samples of crystalline TNT and four of its five isomers. He provides small (a few mg) samples to SRL and we sent them to Jordi Associates for analysis. These were tested individually and as a mixed solution; they eluted closely in time and provided identification of a major peak cluster in the red water analysis. This



A = 60 / 20 / 20 / 0.3 H₂O / MeOH / ACN / CTMA Br

B = 50 / 50 / 0.3 MeOH / ACN / CTMA

30 min Linear Gradient A / B 40 / 60 → 0/100

Figure 3: Block diagram of HPLC system used

provided added confidence in the HPLC analysis but of course it did not add greatly to our understanding of this complex mixture.

4.0 EXPERIMENT DESCRIPTION

The test apparatus consists of a flowing contaminated water channel which is exposed to direct electron beam irradiation through a thin (0.038 mm) titanium foil window. The flowing channel cell is attached directly to a conflat flange on an existing electron beam apparatus complete with electron source, linear induction accelerator, beam shaping magnets, vacuum pumps, gauges and valving. The contaminated water flows in direct contact with the foil window and thereby provides highly effective removal of the small fraction of electron beam energy which is deposited in the foil.

Tests were conducted in two segments which were separated by approximately one year. During this interval the electron accelerator was upgraded from a nominal operating voltage of 500 keV to 1.5 MeV. During this time significant changes were also made in the configuration of the radiolysis cell. Both operating capabilities will be described and test results will be distinguished by descriptors Mod 0.5 and Mod 1.5.

4.1 Electron Beam

SRL's SNOMAD-IV linear induction accelerator has a current capability of producing 50 nsec electron beam pulses at multi-kilohertz pulse rates at pulse energies of 36 J at 1.5 MeV. These capabilities far exceed the requirements of the current effort but serve to illustrate the scalability of the existing technology.

A photograph of the 500 keV injector is shown in Figure 4. The right side of this compact, oil-filled housing contains the pulse forming network. The left side contains the injector accelerator which terminates at the dispenser cathode within the vacuum housing in the bottom central portion of the photograph. Operation of the injector module alone provided Mod 0.5 capability with representative voltage and current traces shown in Figures 5 and 6 for the current studies. The voltage pulse width is 50 nsec while the current pulse width is 37 nsec. Consequently most of the delivered electron beam energy is near peak voltage. This insures efficient foil penetration and fair deposition uniformity across the water channel.

Representative Mod 0.5 test parameters are shown in the first column in Table 5 for an extended set of runs. The fractions of electron beam energy deposited in foil, water and channel back wall are scaled from deposition calculations using the TIGER code. Deposition calculations at 500 keV beam voltage and for two titanium foil thicknesses are shown in Figures 7a and 7b. The associated deposition in the Titanium foil is 9840 keV/cm. Deposition at slightly reduced voltage is estimated by scaling range as voltage to the 3/2 power. The fraction deposited in the back wall is removed mainly by water cooling within the radiolysis cell so does not play an important role in the heat balance of the irradiated water. Fractions deposited in the contaminated water and in the foil are removed primarily by the contaminated water and this heating is determined by measured temperature rise between water inlet and exit. The estimate of 16% foil heating

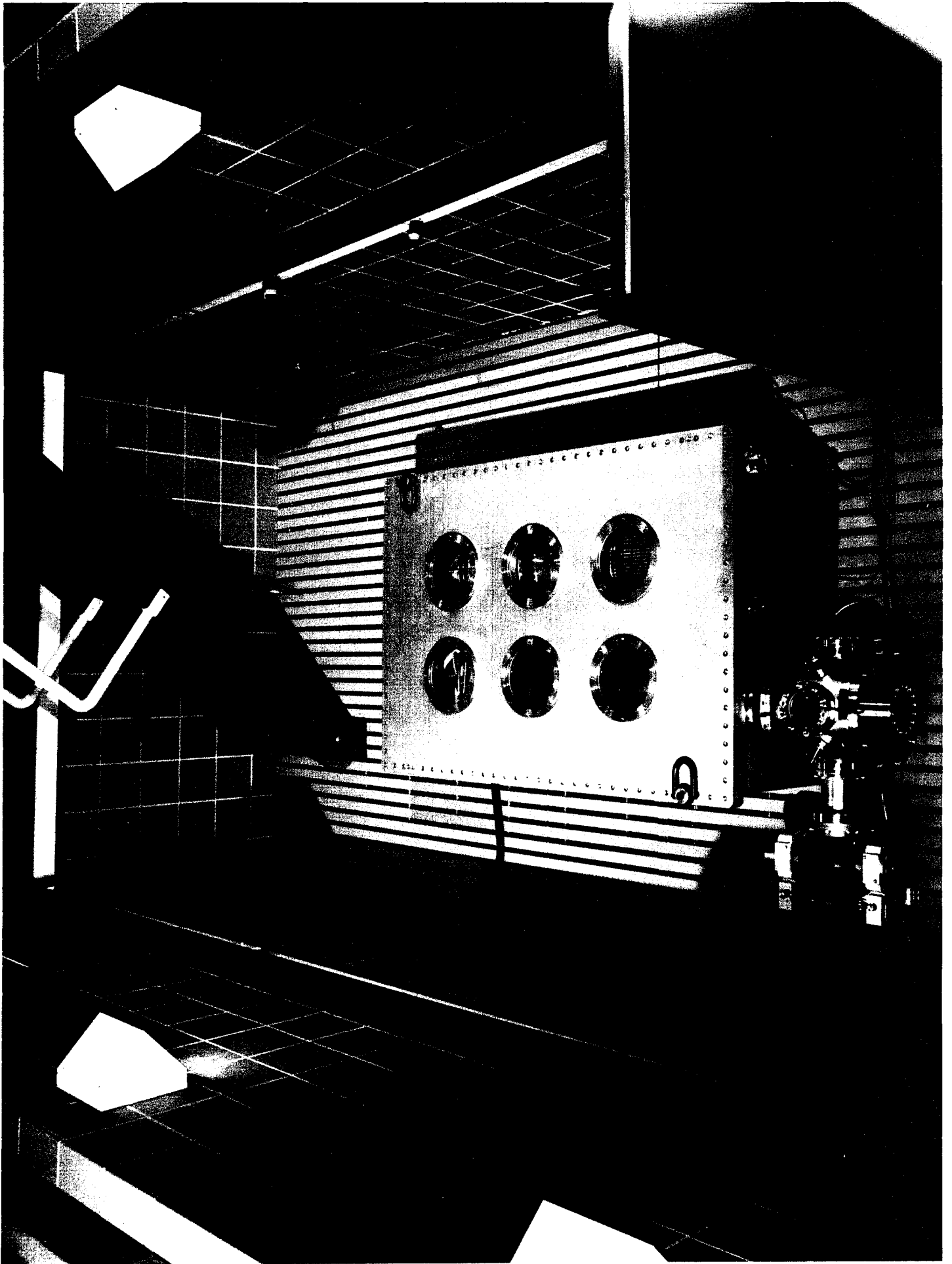


Figure 4: SNOMAD-IV 500 keV Electron Beam Injector Module

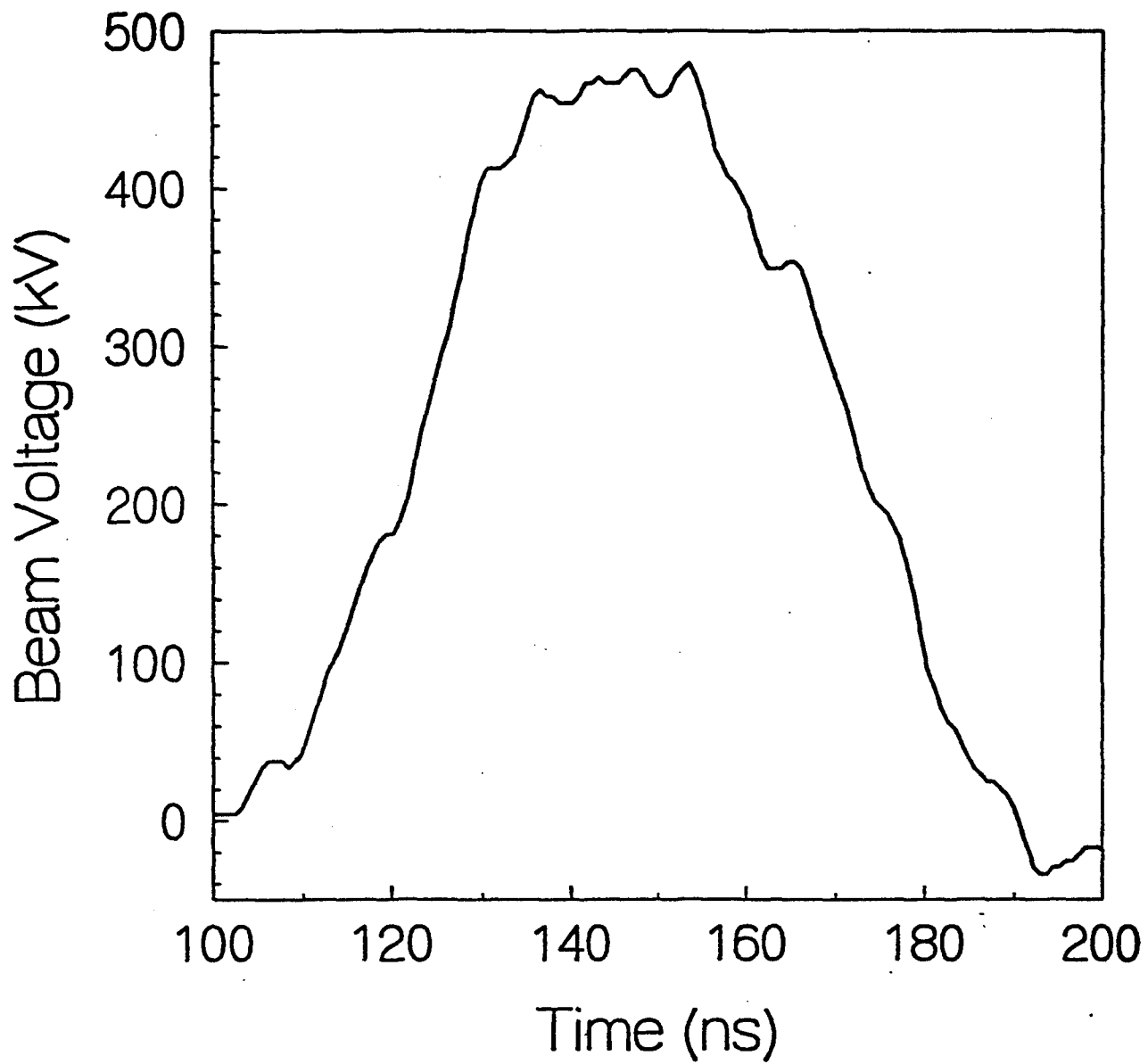


Figure 5: Injector voltage measurement using a capacitive voltage divider.

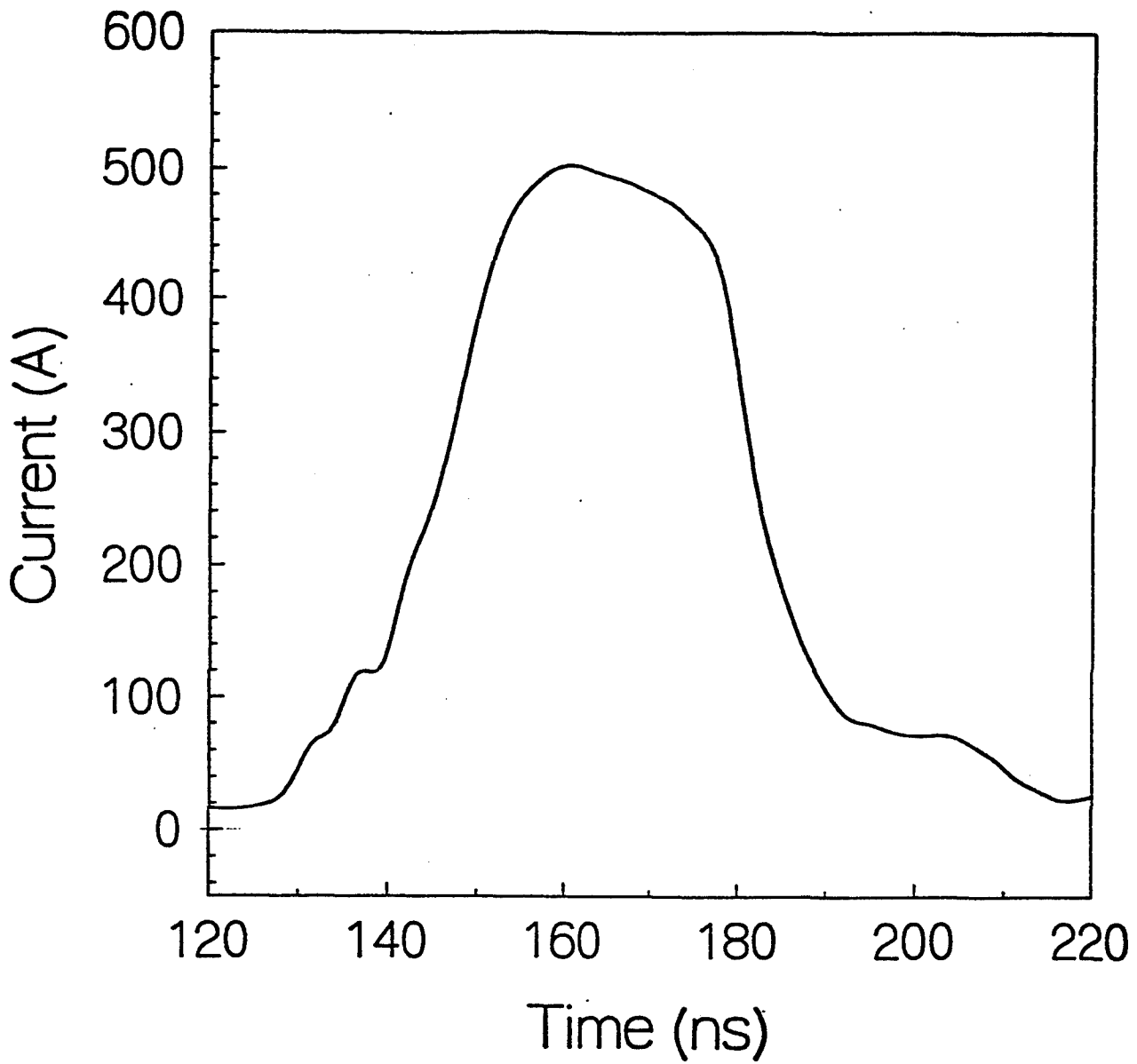


Figure 6: Current after integrating the dB/dt signal from a single turn pickup loop.

is therefore applied to measurements to determine irradiation dose level. The dose per electron beam pulse is determined from the measured temperature rise of water in passage through the test cell under repetitive pulse operation as 0.366 MRad. Dose rate is inferred from pulse length and dose per pulse as 10^{13} Rads/sec. Clearly pulse rates far below system capability are sufficient to meet test requirements. With this excess capability in dosage we chose to sacrifice beam energy to the back wall to improve dose uniformity as suggested by Figs. 7a and 7b.

Table 5: Representative SNOMAD-IV Test Parameters

	Mod 0.5	Mod 1.5
Injector Voltage (kV)	460	420
Accelerator Voltage (kV)	0	800
Electron Beam Current (A)	480	326
Pulse Width FWHM (nsec)	35	32
Pulse Energy (J)	8	12.5
Energy Fluence to Foil (J/cm ²)	0.44	0.12
Percent Deposited in Foil (%)	16	5
Water Channel Depth (MM)	0.71	4.6
Deposited in Opposite Wall (%)	25	0
Deposited in Cell Water (%)	59	95
Dose (kRads)	366	25
Irradiated Volume (cc)	0.11	13.6

The injector was integrated with one accelerator module to provide the Mod 1.5 operational capability as shown in Figure 8. The 0.5 MeV injector in the upper left corner is coupled to the vacuum core of the 1.0 MeV accelerator which contains 14 accelerator stages. The pulse shaping circuitry within the module is shown on the right. A series of beam shaping magnets (5) are positioned along the beam tube at the exit of the accelerator. The test cell is located at the end of this tube and in this configuration it is a

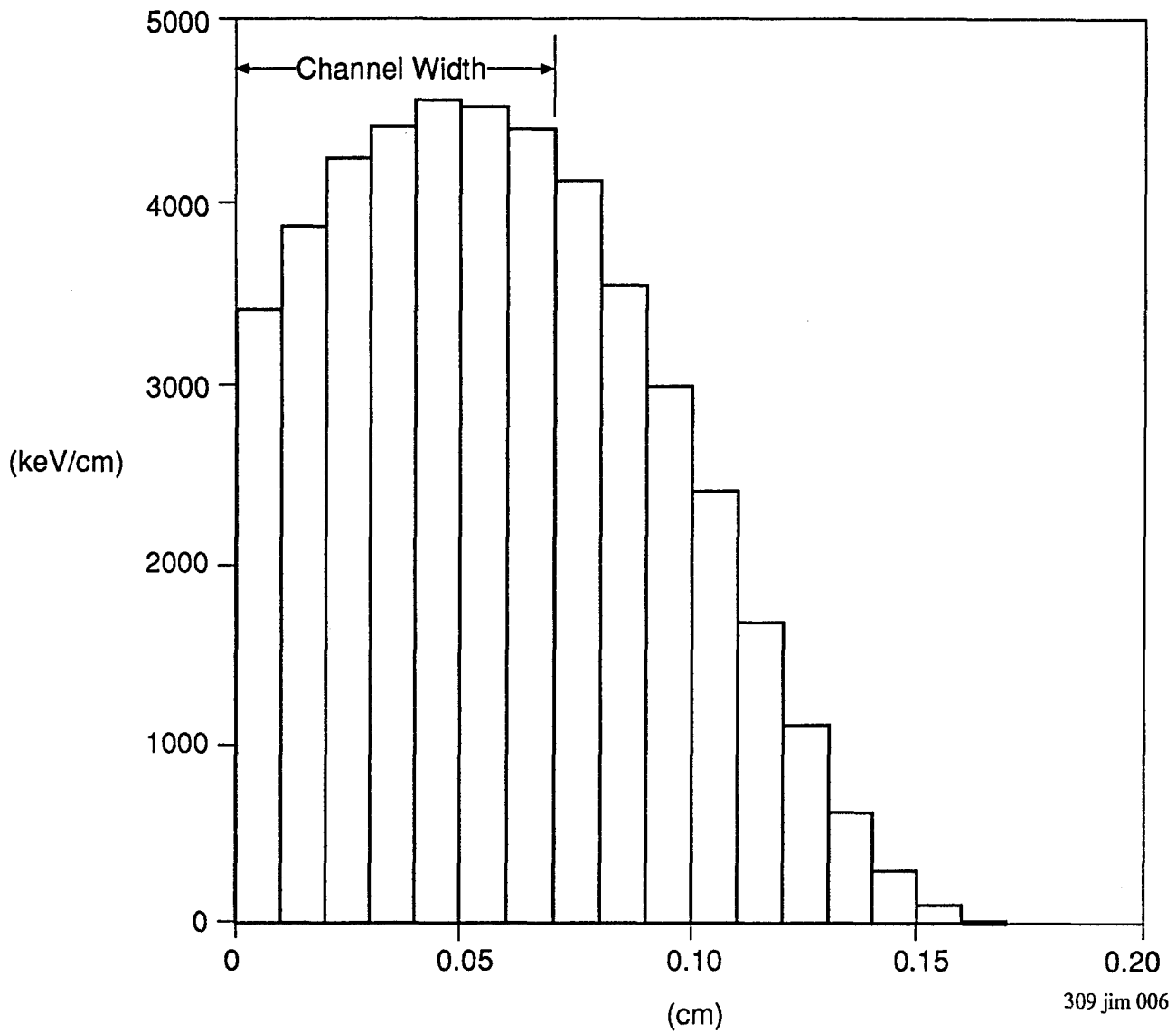


Figure 7.a: 500 keV deposition in water (0.0254 mm Ti)

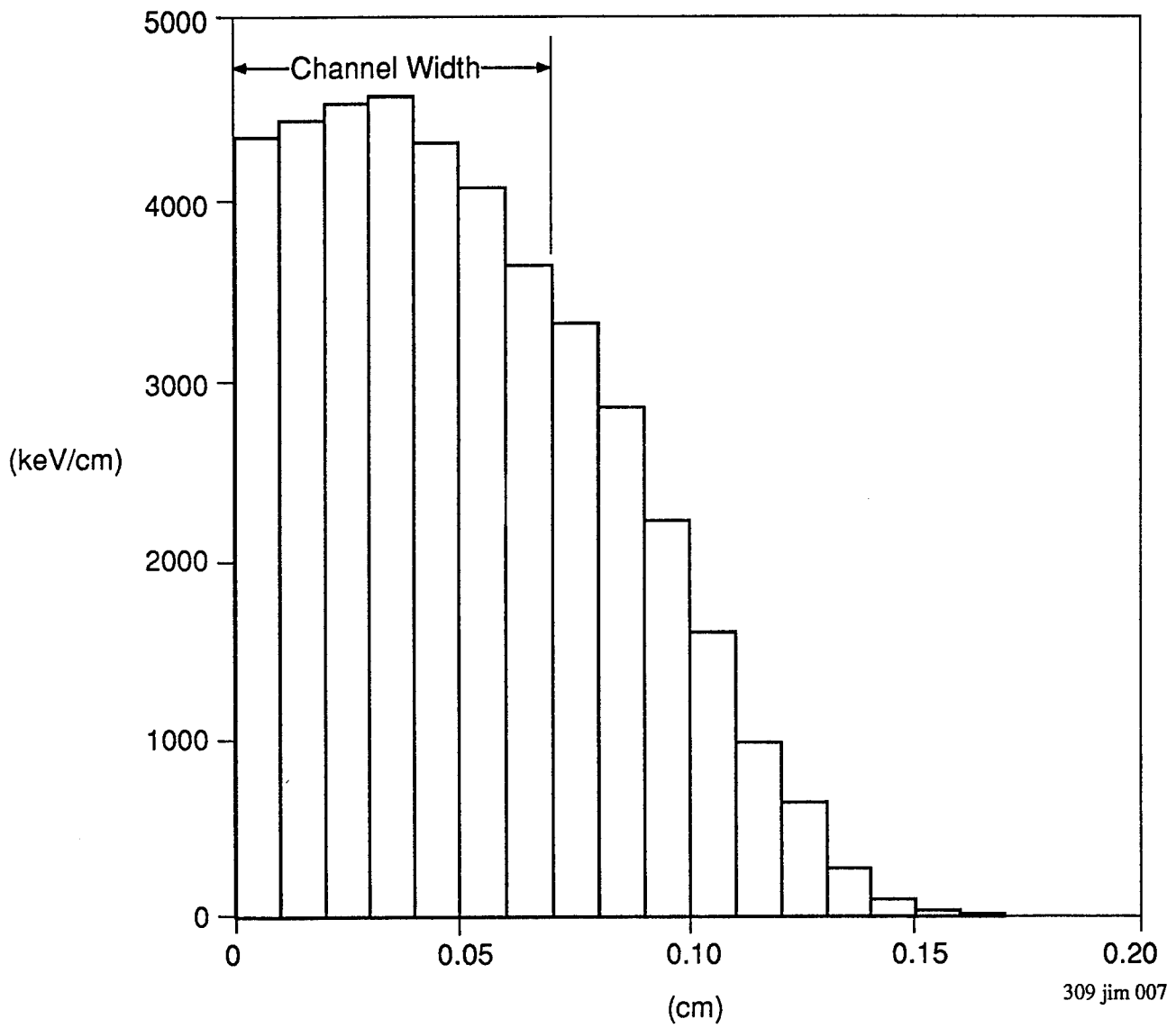
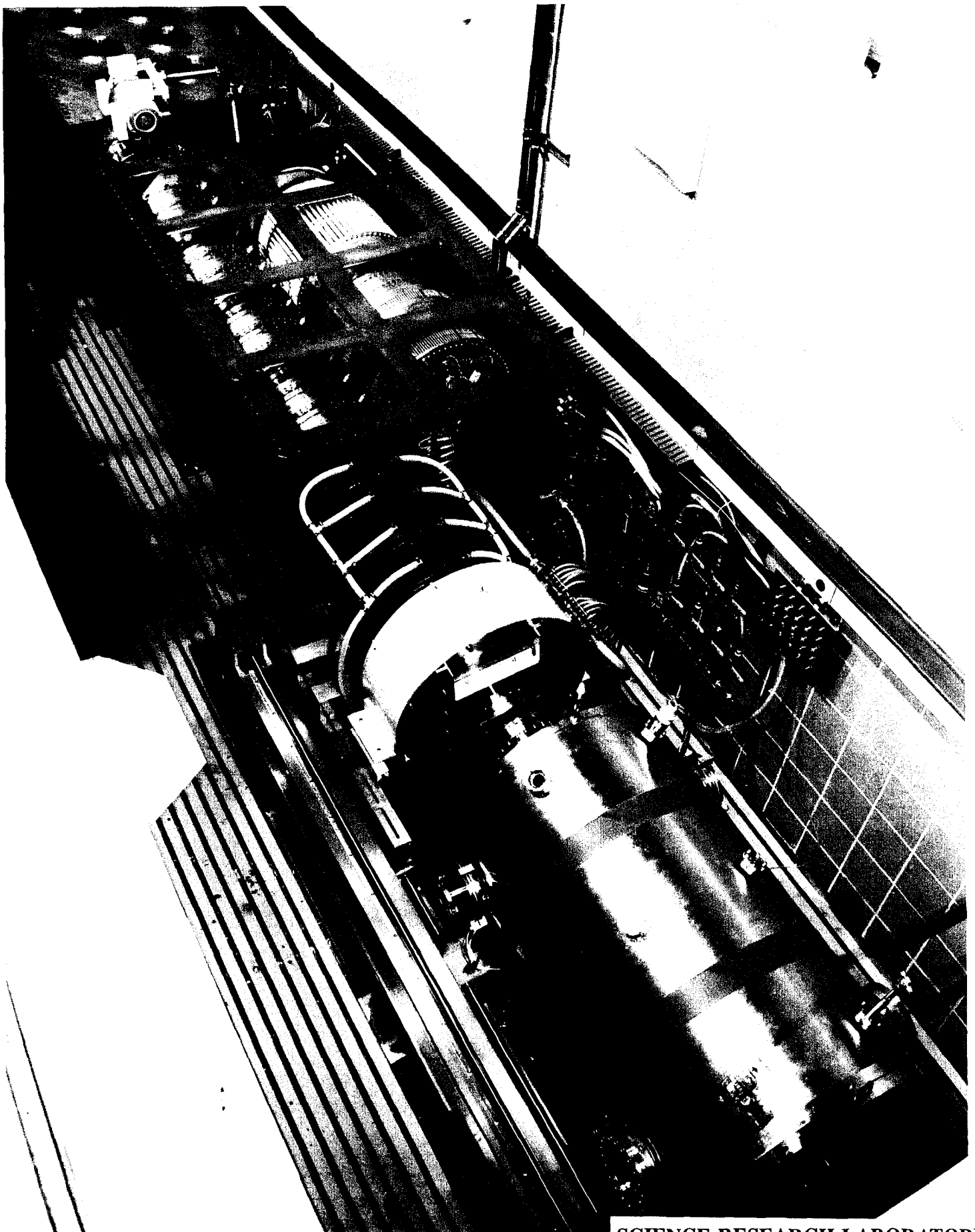


Figure 7.b: 500 keV deposition in water (0.0508 mm Ti)



SCIENCE RESEARCH LABORATORY

Figure 8: SNOMAD-IV 1.5 MeV Electron Beam Accelerator with 0.5 MeV Injector and One 1.0 MeV Accelerator Module

large stainless steel cylinder. In the radiolysis studies this cylinder is replaced by a small test cell which mount directly to the flange of a gate valve at the end of the electron beam tube. Traces of injector voltage, accelerator voltage and electron beam current are shown in Figures 9a, 9b, and 9c respectively. The peak injector voltage is 0.42 MeV and the pulse width is 45 nsec FWHM. The accelerator peak voltage is 0.8 MeV and the pulse width is 37 nsec. Peak current is 326 A and the current pulse width is 32 nsec. This decreasing order in pulse widths insures that most electrons arrive at the test cell at high and relatively uniform energy. Consequently, only a small fraction of electron energy is deposited in the 0.038 mm thick foil window. Foil stopping power is quite insensitive to electron energy in this voltage range as was verified by application of the TIGER code. A nearly constant stopping power of 6.0 MeV/cm of titanium was calculated over a range of 1.2 to 1.5 MeV. Calculated energy deposition profiles within the radiolysis cell after passage through the foil are shown in Figure 10 for four accelerator voltages. The total depth of the cell channels, 0.46 mm, is somewhat larger than electron range even at the peak operating voltage of 1.22 MeV. Consequently, unlike Mod 0.5, we expect negligible electron energy deposition to the cell wall opposite the foil in this test series. Still, uniform mean dose to all water is assured by thorough flow mixing between passes in series through five channels which form the radiolysis cell.

Nominal Mod 1.5 test parameters are shown in the second column in Table 5. Here we estimate 5% of the electron beam energy is deposited in the foil and a negligible fraction is deposited in the opposite cell wall. The electron beam spot size was much

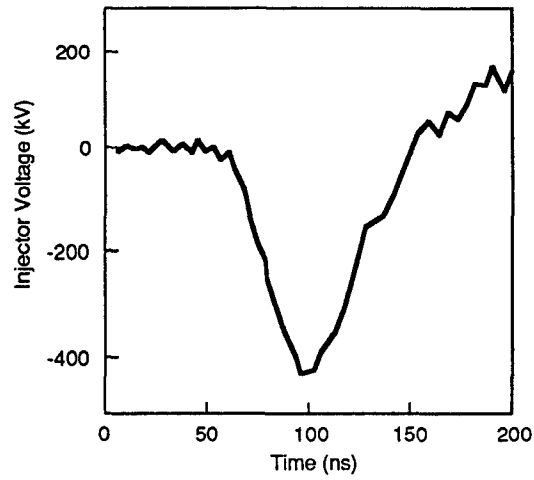


Figure 9.a: Injector voltage pulse shape

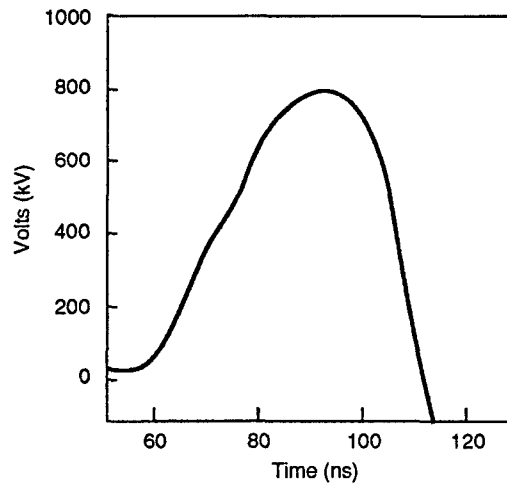


Figure 9.b: Accelerator voltage pulse shape

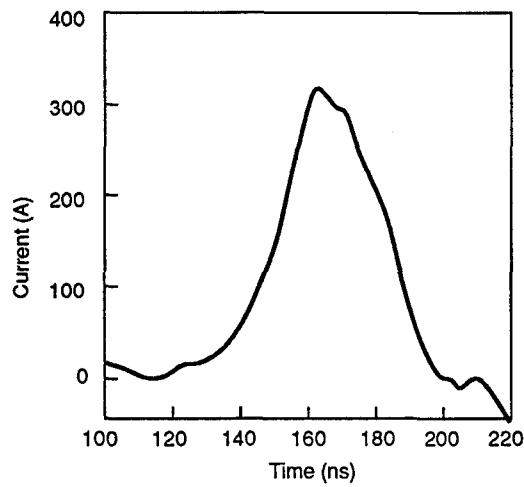


Figure 9.c: Electron gun current pulse shape

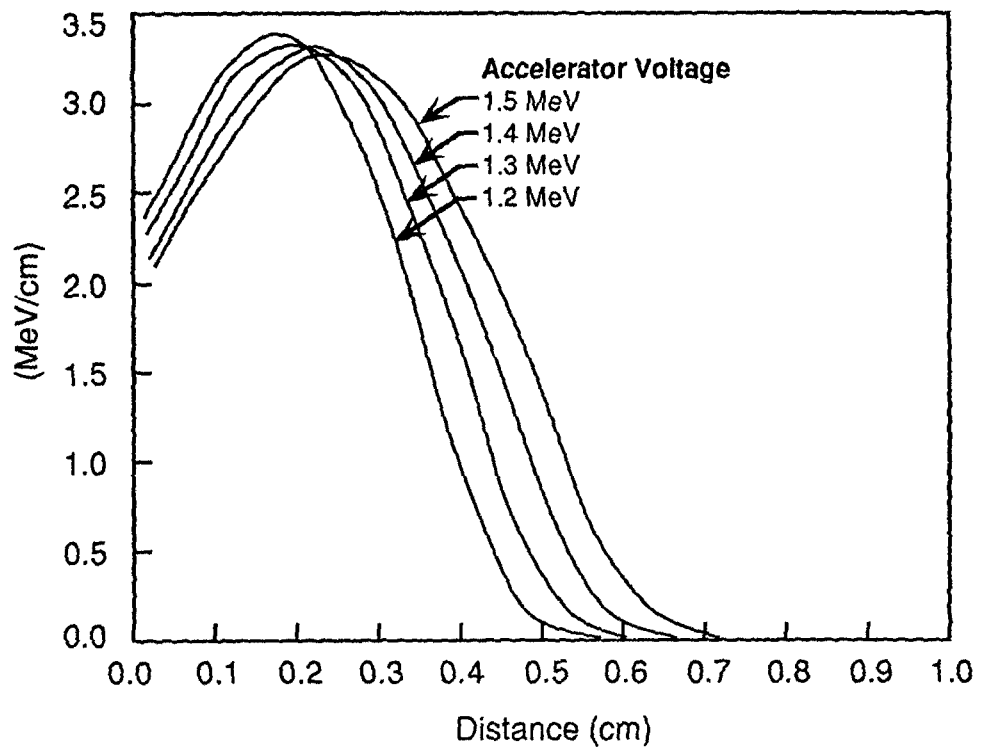


Figure 10: Electron energy deposition in water (0.381 mm Ti)

larger in these Mod 1.5 tests, both to accommodate a larger cell foil window area and to provide a reduced dose rate of 7×10^{11} Rads/sec. Beam spot size is controlled by the beam shaping magnets which were described above. The dose per pulse is much lower in the Mod 1.5 configuration and the cell volume is much larger. These upgrades allow more pulses and therefore improved dose uniformity during cell passage for any specified cumulative dose level. Tests were also conducted at a lower dose per pulse of 5 kRads and consequently a lower dose rate of 1.4×10^{11} . This was achieved by operating the dispenser cathode at reduced heater power and thus reduced temperature. As before, dosage was determined from measured water temperature rise in passage through the radiolysis cell. This continuous dose monitoring was essential, particularly at the lower dose level, since repeatability in gun current control is very difficult using gun temperature control. In this test series we also measured dosage at low pulse rates with a Radiochromatic System as supplied by Far West Technology (FWT). Tests employed small patches of radiation sensitive plastic film which were inserted at several locations immediately outside the foil window. Transmission measurements were made at 510 and at 600 nm before and after direct electron beam irradiation. The change in transmission due to irradiation was compared to a calibration curve which was generated for our instrument by Energy Sciences (Wilmington, MA). Energy Sciences exposed samples of SRL film and of their own film to a 150 kV electron beam. The doses were measured using their own NIST-calibrated FWT meter. Samples at 0.3-6.0 MR doses provided the SRL film calibration data. These tests were conducted at the beginning and end and

during one interruption within the Mod 1.5 test period. Average dose per pulse at 25 kRads was repeatable to within +/- 12% on this basis.

4.2 Radiolysis Test Cell

The Mod 0.5 radiolysis test cell is shown in section and in partial blowup in Figure 11. The hardware assembly is shown in Figure 12 with the flow channel swung back like an open clam shell to expose the Titanium foil disc. A standard Conflat flange was mounted to the 0.5 MeV electron beam injector system and the test cell was mounted over a 9.5 cm diameter circular hole in its center. A 0.038 cm thick Titanium foil was bonded to an OFHC Copper adapting flange over a 0.5 cm by 3.0 cm opening. This opening defined the electron beam window aperture to the waste water channel which was on the opposite side of and in direct contact with the foil. The bulk of the electron beam energy was deposited in the adapting flange and was removed through water cooling channels. Waste water entered and exited the radiolysis cell through fittings as shown. Sheathed and electrically insulated thermocouples were inserted through fittings to allow direct measurements of waste water temperature rise between entry and exit plenums. Uniform laminar flow was established in the radiolysis region by the placement of 0.25 mm deep flow contractions between the 0.71 mm deep flow channel and the plenums.

An OFHC Copper back plate which contained the flow channel and plenums was also cooled through the channels in the adapting flange in the assembled configuration.

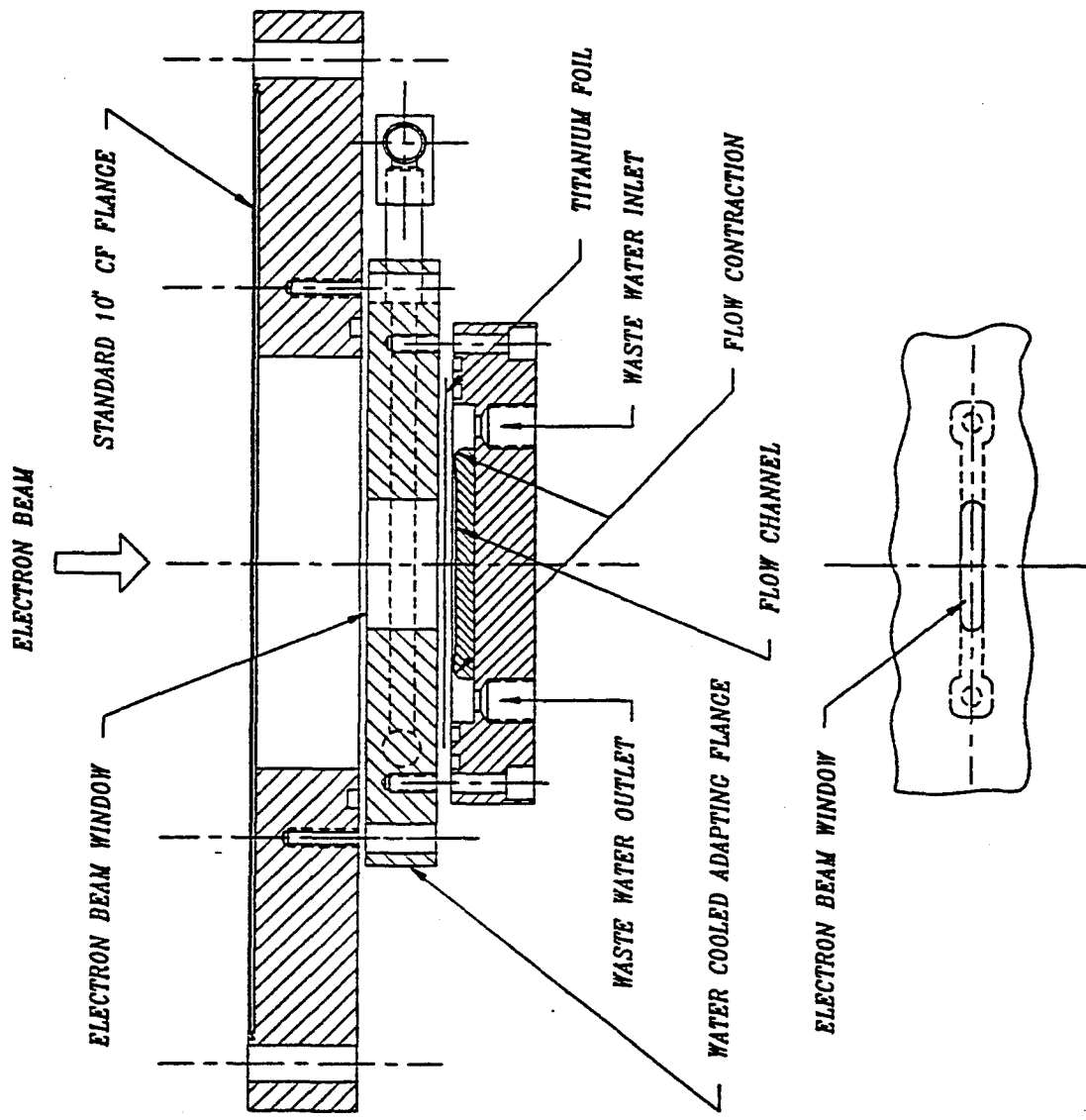


Figure 11: Radiolysis Cell Assembly (Mod 0.5)

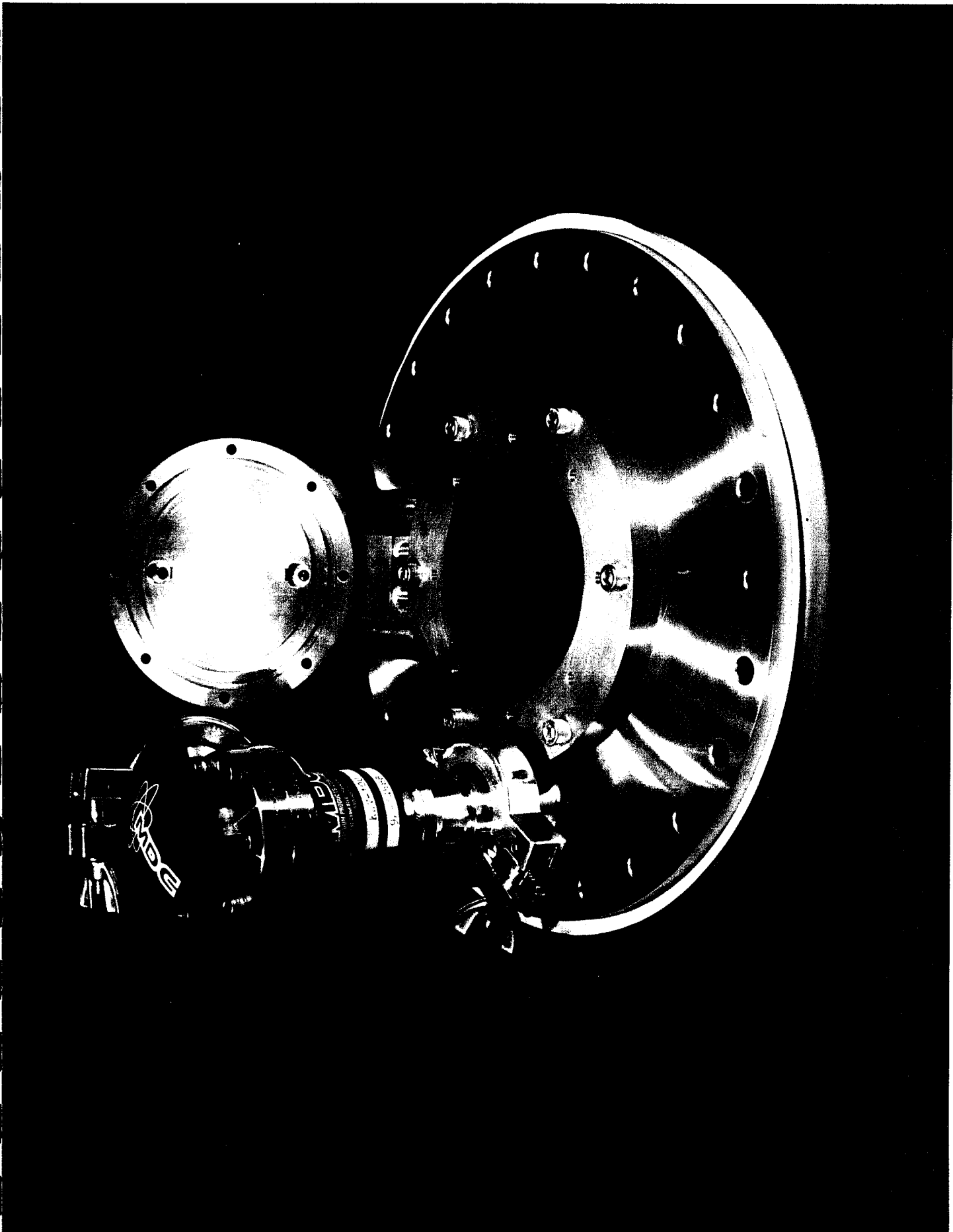


Figure 12: Photograph of Radiolysis Cell (Mod 0.5)

The waste water was in intimate contact with channel walls. Consequently careful heat transfer analysis was developed to insure that waste water temperature rise measurements reflected water and foil heating and were not compromised by heating or cooling through the channel walls. Coolant water inlet temperature was controlled to minimize channel wall heat transfer. Water cooling was designed for a maximum pulse rate of 1.0 kHz or 8 kW of heat removal. Four water channels of 0.22 in diameter are equally spaced on 0.71 in centers in the adapting flange. Cooling channels were connected in series to accept a cooling flow rate of 5.0 gpm at a pressure drop of 50 psi. These coolant supply conditions were provided by the existing chiller which cools the electron beam shaping magnets.

The Mod 1.5 radiolysis test cell is shown in the photograph in Figure 13 in exploded view. Extensive modifications are evident in this figure. The water cooled OFHC Copper base, shown mounted on the conflat flange, has five 9.0 mm wide electron beam passages and are separated by the above mentioned series of four water cooling channels. The foil window, with five matching segments, is mounted on a separated stainless steel disc. The radiolysis cells are five matching channel segments in the topmost OFHC Copper piece in Figure 13. Contaminated water enters and exits at the back side of this piece and the sheathed thermocouples as described above provide measurements of entry and exit water temperatures. The contaminated water passes in series through the five radiolysis channels and the flow links which couple these channels are not visible behind the viton gasket which is in view. These channel links draw from the top of a

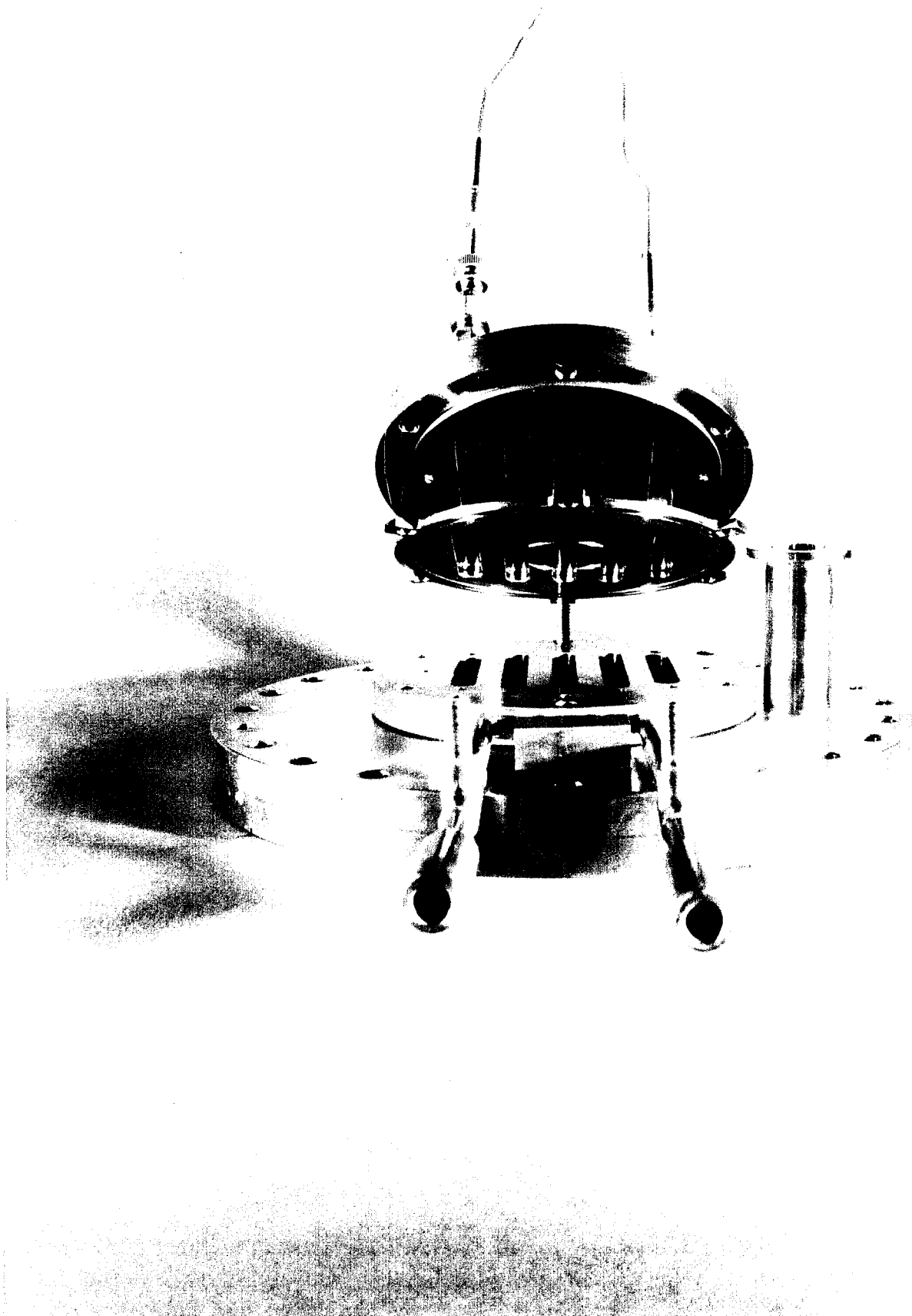


Figure 13: Radiolysis Cell (Mod 1.5)

channel and reinsert at the bottom of the next channel. This provides thorough mixing between channel passes and thus insures uniform mean dosage to all processed water. In addition this routing prevents formation of vapor pockets in the radiolysis cells as a result of vapor dissolution or production. The radiolysis cell is thermally isolated from the water cooled test cell base in three ways. It is held in position by a stainless steel ring with a circular "knife edge" contact. It is separated from the foil holder by an insulating gasket. The foil holder is in turn isolated from the base piece by minimum mechanical contact outboard of the vacuum O-ring and by a vacuum gap of 0.015 in inboard of the O-ring. In this configuration the radiolysis cell will reach an approximately adiabatic condition under uniform electron beam conditions in a time of several hundred seconds. Under ideal conditions the measure of contaminated water temperature rise would then provide an unambiguous determination of radiolysis dose. Under actual conditions there is some steady heat removal to the water cooled base plate. However this effect was measured, and corrected independently during operation with no electron beam and with a controlled temperature difference between coolant water and test cell water.

4.3 Flow System

Present studies address destruction by electron beam radiolysis of red water and of volatile organic contaminants both with and without the addition of an oxidizing agent, Hydrogen Peroxide. The flow system allows contaminated water to be premixed or mixed during delivery to the radiolysis cell. A schematic of the flow system and instrumentation is shown in Figure 14. In these studies the options of air or oxygen addition to the

contaminated water and the separate source containment of Hydrogen Peroxide were not employed. We focus therefore on the flow route from contaminated source (w/wo Peroxide addition) through valving to a peristaltic pump, then through the irradiation cell and valving to the processed reservoir. During system shake down, valves V1 and V2 and valves V3 and V4 were replaced by two remotely controlled three way valves. During system start up, HPLC grade water flowed from the source as shown through the system to a dump beaker. At the start of electron beam pulsing both three way valves were switched to cause flow from contaminated to processed reservoirs. At the termination of radiolysis these valves were returned to their original positions to allow flushing of the system. This procedure prevented mixing of processed and unprocessed water from one run to the next but introduced a small and measurable amount of dilution in each run. The total volume between three way valves was 9.6 cc for Mod 0.5 operation and 27 cc for Mod 1.5 operation. Volumes of processed samples ranged from 1500 to 200 cc and this dilution has been taken into account in reported results. An early version of the flow system is shown in Figure 15 prior to the addition of automatic three way valves. It is built on (tiers) shelving which is lowered into the test vault. The source pouch is shown on the top shelf; supply and return valving are beneath the top shelf; the supply purge water, the peristaltic pump, pressure gauge and relief valve are shown on the second shelf and the radiolysis cell (Mod 0.5) which mounts on the electron gun is shown on the lower shelf. The basic plumbing has not changed during this study although automatic valves

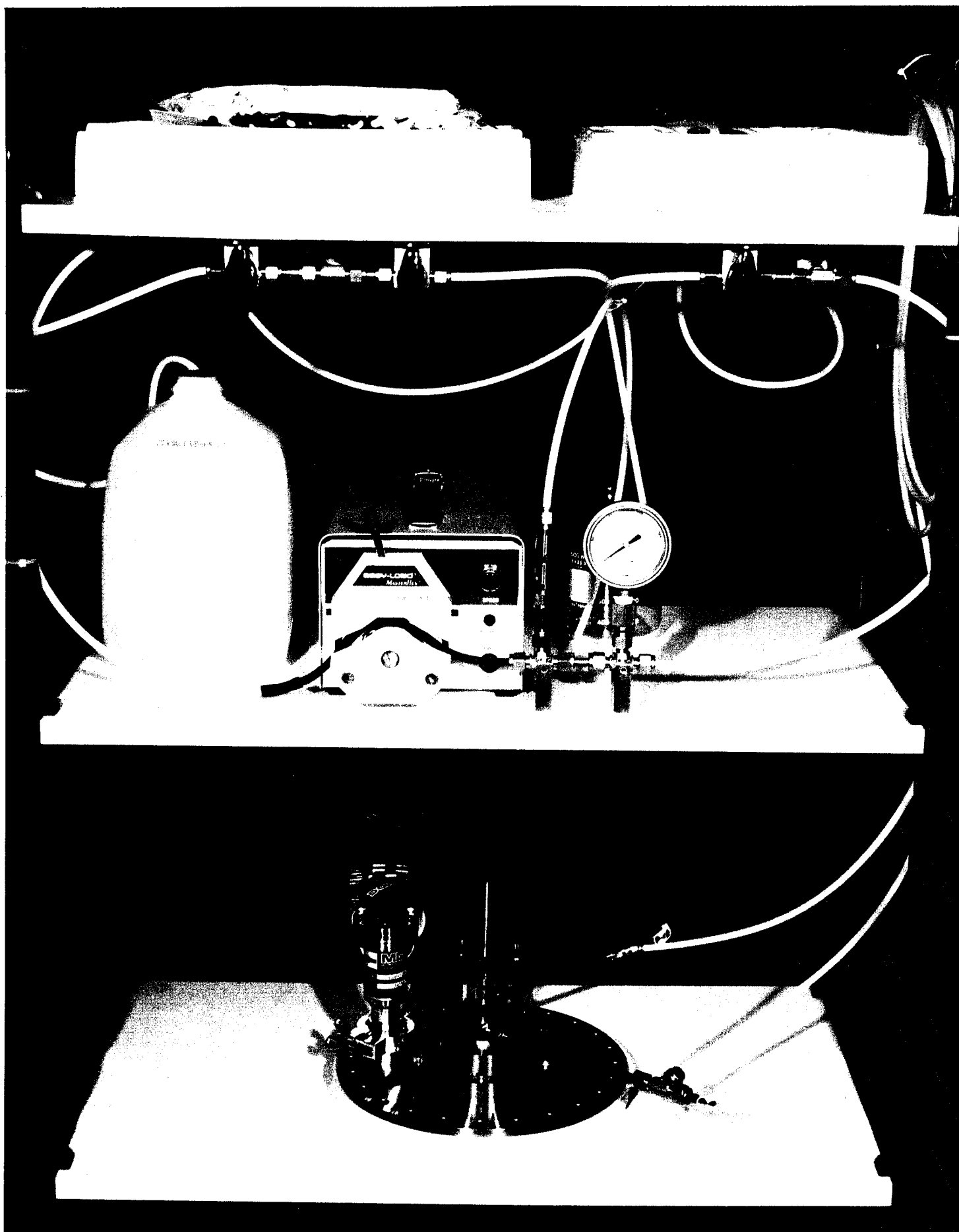


Figure 15: Photograph of Test Apparatus

were added and line sizing was reduced from 1/8 in ID to 1/16 in ID to reduce the dilution by purge flow.

The source and processed reservoirs are Teflon pouches with stainless steel valves and Teflon coated silicone septa made by BGI Inc of Waltham, MA. Source samples were prepared by first filling the pouch with a measured amount of HPLC grade filtered water, as supplied by our subcontractor E3I in Somerville, MA and with a minimum of air space (of order 3 cc). The desired amounts of contaminant and Peroxide were then injected through the septum. Working the flexible pouch drove the contaminant into solution. This was verified by inspection since even very small beads of undissolved contaminant were visible due to differences in index of refraction. Of course red water mixing was straightforward since it was already a water solution.

Most lines were 1/16 in ID Teflon. Short sections such as that in the peristaltic pump were Viton. Valves and fittings were either Stainless or Teflon. The radiolysis cell exposed the test stream to titanium, OFHC copper, stainless steel, viton and small amounts of low temperature solder. The pump head (Masterflex L/S) with a variable speed drive (Masterflex 1-100 RPM std. drive) provided a range in flow rate from 0.8 to 167 cc/min which well exceeded our requirements. Measured line pressure loss did not exceed 10 psi. and consequently placed little added stress to the electron beam foil. Extensive flow and radiolysis tests were conducted with pure water during checkout and trouble shooting testing in both test segments. Inspection and GCMS analysis confirmed

that the system hardware did not introduce identifiable contaminants to the processed water.

4.4 Diagnostics

Temperatures were monitored at four locations periodically during each run: contaminated water in, radiolysis cell (the element containing the contaminated water channel(s)), coolant water in and base plate (the element containing coolant water channels) as indicated by T2, T9, T6 and T8 respectively in Fig. 14. Type J, Iron/Constantan, thermocouple signals were displayed on an Omega Model 2176A digital thermometer. Temperature difference between radiolysis cell exit and inlet was continuously measured during each run with a pair of sheathed and electrically insulated Type J thermocouples. This was the primary diagnostic for determining radiolysis dosage. High voltage transients were suppressed by Zener diodes of both polarities between both signal leads and ground. Signals were amplified by either 200x or 1000x through an EG&G PARC Model 113 differential amplifier with an internal low frequency band pass of 3 Hz and were displayed on a LaCroix 9400A digital oscilloscope. A Tungsten/Rhenium thermocouple exposed directly to the incident electron beam in vacuum with one side grounded locally served to monitor mean electron beam power flux. This signal was amplified 100x with 3 Hz cutoff and displayed on the same oscilloscope in Mod 0.5 tests. Use of this monitoring diagnostic was precluded in the Mod 1.5 tests due to interference by the larger area electron beam.

Coolant water inlet temperature was manually controlled so that the cell back plate temperature, T9, was nearly equal to contaminated water inlet temperature, T2. Heat transfer analysis showed this condition minimized heat transfer between contaminated water and cell walls in Mod 0.5 tests. Runs where this condition was most closely met were used as an ongoing calibration of the system. Repeatable electron beam conditions showed repeatable Tungsten/Rhenium thermocouple readings in Mod 0.5 tests. Therefore this signal, when coupled with measured flow rate, provided dose determinations when this condition was not met. Cell design for Mod 1.5 tests relied on nearly adiabatic steady state operation. Correction for nonadiabatic losses were applied as described in Section 4.2. In the Mod 1.5 test series we also measured dosage at low pulse rates with a Radiochromatic System as supplied by Far West Technology as described above in Section 4.1. Contaminated water flow rate was controlled by a ten turn potentiometer on the Masterflex drive console. Flow rate calibration was done for each run from measurements of run duration and weight of processed water.

Both source and processed radiolysis samples were chemically analyzed in selected cases. Red water samples were analyzed by Jordi Associates using HPLC procedures as described in Section 3.2 and in Figure 3 and Table 4. VOC samples were analyzed by Energy and Environmental Engineering Inc of Somerville, MA for total carbon concentration (TC) and for concentrations of certain volatile organic compounds as listed

in Table 6. Details of TC and VOC analysis were provided by Dr. Nicholas Corso of E3I and are summarized here in Table 7.

TABLE 6:
E3I Form 1A
Volatile Organic Analysis Data Sheet

Client Sample No.

10/26/92 A

Client Name:	Science Research Laboratory	E3I Sample ID:	930126-1
Client Project:	141	E3I File Name:	F4637
		Associated Blank:	F4628
Matrix:	Water		
Level:	Low	Date Received:	11/02/92
		Date Extracted:	
Sample wt/vol:	5.0 mL	Date Analyzed:	11/05/92
% Moisture:	NA		
		Dilution Factor:	1.0

Gas No.	Compound	Conc. Units (µg/L)	Q
74-87-3	Chloromethane	10	U
74-83-9	Bromomethane	10	U
75-01-4	Vinyl Chloride	10	U
75-00-3	Chloroethane	10	U
75-09-2	Methylene Chloride	4	JB
67-64-1	Acetone	10	U
75-15-0	Carbon Disulfide	5	U
75-35-4	1, 1-Dichloroethene	5	U
75-34-3	1, 1-Dichloroethane	5	U
540-59-0	1, 2-Dichloroethane (total)	5	U
67-66-3	Chloroform	3	J
78-93-3	2-Butanone	10	U
107-02-2	1, 2-Dichloroethane	5	U
71-55-6	1, 1, 1-Trichloroethane	5	U
56-23-5	Carbon Tetrachloride	5	U
108-05-4	Vinyl Acetate	10	U
75-27-4	Bromodichloromethane	5	U
78-87-5	1, 2-Dichloropropane	5	U
10061-01-5	cis-1, 3-Dichloropropene	5	U
79-01-6	Trichloroethene	5	U
124-48-1	Dibromochloromethane	5	U
79-00-5	1, 1, 2-Trichloroethane	5	U
71-43-2	Benzene	29	
10061-02-6	trans-1, 3-Dichloropropene	5	U
75-25-2	Bromoform	5	U
108-10-1	4-Methyl-2-pentanone	10	U
591-78-6	2-Hexanone	10	U
127-18-4	Tetrachloroethene	5	U
79-34-5	1, 1, 2, 2-Tetrachloroethane	5	U
108-88-3	Toluene	2	J
108-90-7	Chlorobenzene	5	U
100-41-4	Ethylbenzene	5	U
100-42-5	Styrene	5	U
133-02-7	Xylene (total)	5	U

309 jim 021

Qualifiers

- U: Analyzed for, but not detected
- B: Found in associated blank as well as sample
- J: Estimated value, below quantitation limit
- E: Estimated value, above calibration limit

Table 7: VOC Chemical Analysis

N. Corso: Energy and Environmental Engineering Inc., Somerville, MA

- **Total Carbon (TC)**
 - Dohrman DC-80 Total Organic Carbon System
 - UV Promoted Persulfate Oxidation
 - IR Detection
 - Samples Not Sparged Prior to Analysis

- **Gas Chromatography (GCMS)**
 - Hewlett-Packard 5890 Gas Chromatograph
 - Hewlett-Packard 5790 Mass Selective Detector
 - Column, 60/80 Carbopack B/1% SP-1000
 - Sample Introduction, Takmar LCS-2 Purge and Trap
 - Temperature Programmed, 40 to 200°C at 10°C/min
 - Calibration Range, 10-160 ppb

5.0 EXPERIMENTAL RESULTS

Radiolysis experiments and analyses were conducted in two segments, first in the period November 1992 - February 1993, then in the period November 1993 - February 1994. The first segment was conducted with the injector portion of the induction accelerator which produced an electron beam at a nominal voltage of 0.5 MeV. The second segment was conducted after the addition and checkout of an accelerator module which increased the voltage to a nominal 1.5 MeV. The radiolysis cell was modified to accommodate the increased electron energy and was also upgraded to improve dose uniformity and dosimetry. Representative gun operating conditions are listed in Table 5 and were discussed in Section 4.1.

Representative electron beam voltage and current traces were discussed above and shown in Figs. 5 and 6 (Mod 0.5) and Fig. 9 (Mod 1.5). Flow rates were determined for each run by accounting of processed water weight and run duration. Dose level, the key experimental parameter, was determined primarily by contaminated water heating as discussed above. Key temperature and temperature rise measurements were recorded continuously during each run.

5.1 Mod 0.5 Experimental Results

The primary goal of tests during this segment was the determination of the efficiency of destruction of red water and VOC contaminants at fixed electron beam pulse conditions both with and without the addition of an oxidizing additive, hydrogen peroxide. These tests were conducted at a single dose rate of 10^{13} Rads/sec. Red water was irradiated after water dilution by factors of ten and one hundred. VOCs were irradiated at equal initial concentrations of 400 ppm. In each test segment accelerator radiolysis operation exceeded ten hours with an accumulation of over one million pulses over a period of several weeks with no difficulties in system performance and no apparent deterioration of the foil window. This has important practical implications for system reliability and for simplification of system configuration.

A representative record of water temperature rise between radiolysis cell entry and exit and of temperature of the Tungsten/Rhenium thermocouple on the vacuum side of the foil are shown in Figure 16 as upper and lower traces respectively. This run, referred to as Run 11/19/92-P4, extended 510 sec during which 379 g (44.6 cc/min) of contaminated water were irradiated at a pulse rate of 25 Hz. The event sequence is: start of distilled water flow (drop in T3-T2), start of electron beam pulsing and simultaneous switching to contaminated water flow (abrupt rise in T3-T2), end of electron beam pulsing and simultaneous switching back to distilled water flow, end of distilled water flow. Cooling water flow operated continuously. The temperature rise through the radiolysis channel is

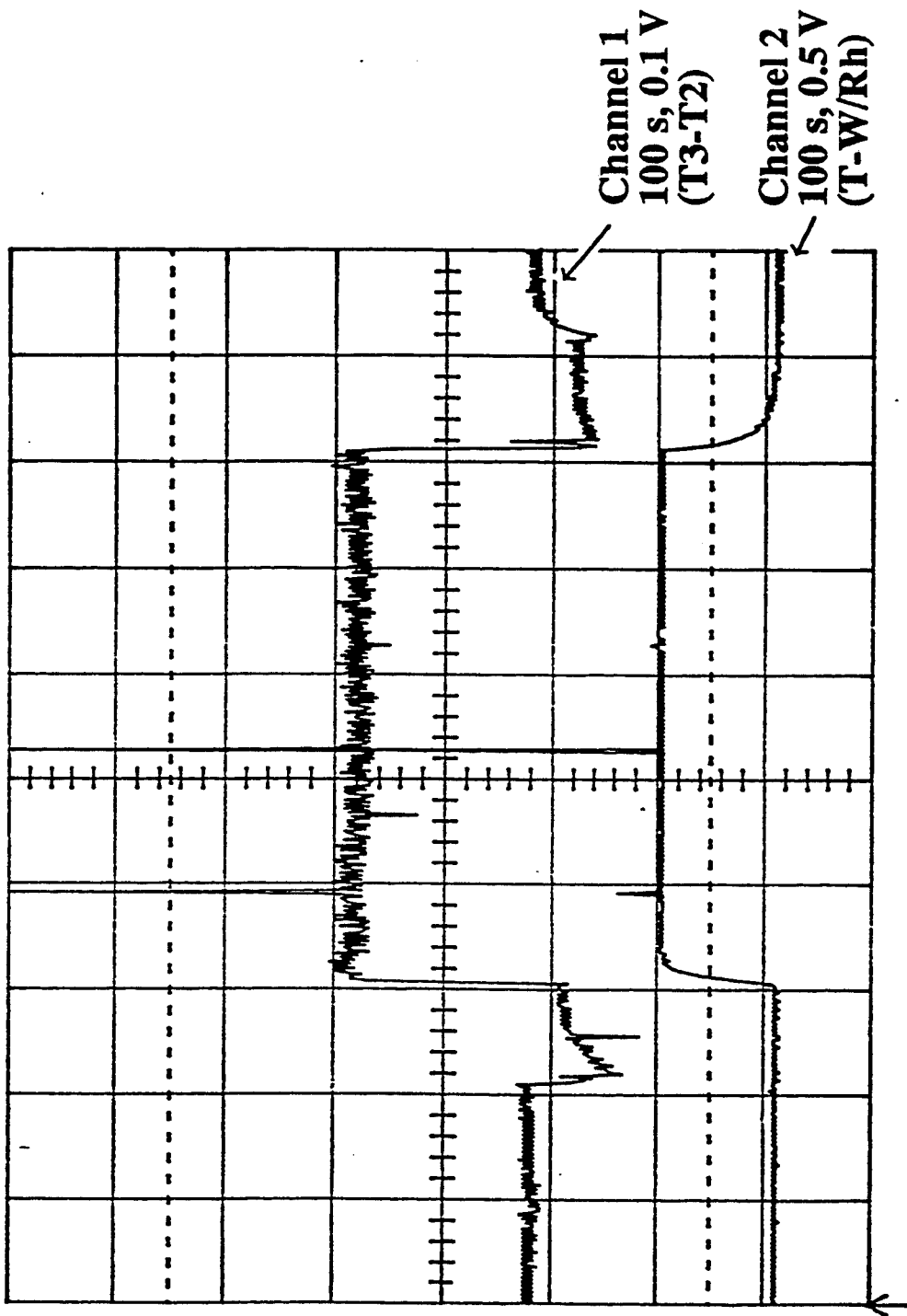


Figure 16: Temperature rise and temperature traces during run 11/19/92 - P4

3.85°C (Gain=1000, 52 $\mu\text{v}/^\circ\text{C}$). With an estimated 16% heating from the foil the resulting dose level is 1.33 MRad. The Tungsten/Rhenium thermocouple shows very steady electron beam operation although the absolute temperature rise of 320°C is not subjected to analysis.

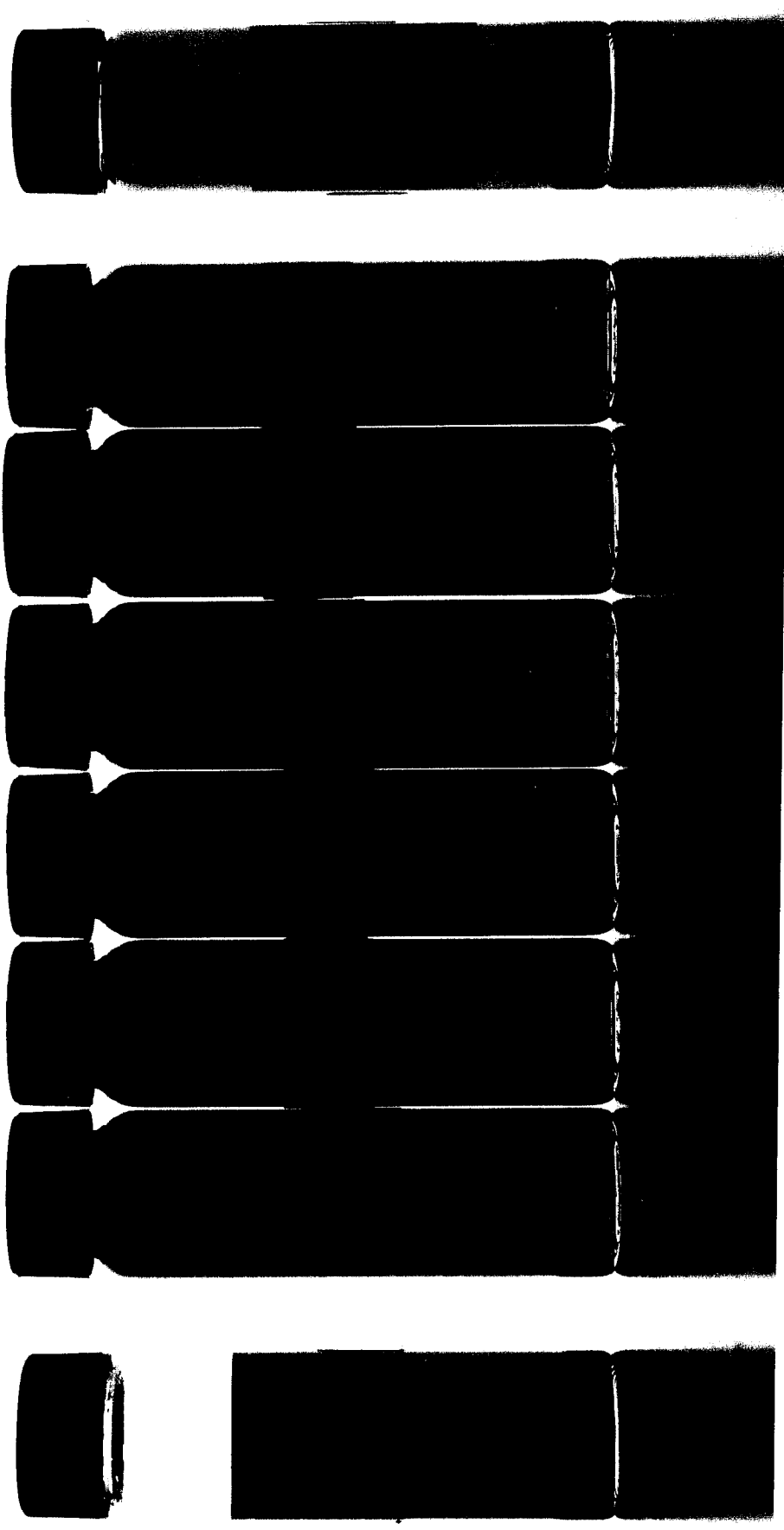
5.1.1 Mod 0.5 Red Water Tests

During the first test segment four test series were conducted with red water (1 and 2) duplicate runs with red water initially diluted 1:10; (3) initial dilution 1:100; (4) initial dilution 1:10 with the addition of 9200 ppm of hydrogen peroxide. A summary of these test operating conditions is shown in Table 8. Samples were taken after each of five or six passes through the radiolysis cell to provide records of degree of destruction versus cumulative dosage to maximum levels ranging from 20 to 29 MRads.

Samples for 1:10 dilution retained strong red coloring at all dose levels although color did diminish with increasing dose. Change in color with increasing dose is shown in Figure 17 for tests of 11/19/92. All samples were diluted by an additional factor of ten after irradiation to provide suitable contrast for this comparison. For reference the photo also shows two unirradiated red water samples diluted by 1:100 and by 1:333. The 1:100 diluted standard matches the source sample in color and the 1:333 diluted standard is clearly lighter than the irradiated sample at a dose of 19.4 MRads. Although the samples

Table 8: Mod 0.5 Red Water Radiolysis Test Conditions

Source Composition Run Ident. Number	Pulse Rate (Hz)	Run Time (sec)	Processed Mass (g)	Dose - Differential (Mrad)	Dose - Cumulative (Mrad)	Evolve Gas (cc)
Diluted to 9.9%						
11/2/92 - P1	72	1530	405	0.48	0.48	
11/2/92 - P2	35	1200	269	4.86	5.34	
11/2/92 - P3	35	985	202	4.93	10.27	
11/2/92 - P4	35	640	134	5.00	15.27	
11/2/92 - P5	35	365	79	4.51	19.78	
Diluted to 10%						
11/19/92 - P1	35	1560	348	4.46	4.46	---
11/19/92 - P2	35	1190	268	4.48	8.94	25
11/19/92 - P3	35	910	202	3.90	12.84	25
11/19/92 - P4	35	615	130	3.62	16.46	25
11/19/92 - P5	35	305	66	2.98	19.44	15
Diluted to 1.09%						
11/11/92 - P1	35	2430	510	4.37	4.37	
11/11/92 - P2	35	1780	397	4.86	9.23	
11/11/92 - P3	35	1160	254	4.65	13.88	
11/11/92 - P4	35	930	204	4.51	18.39	
11/11/92 - P5	35	570	127	4.65	23.04	
Diluted to 10% + Stoic. Hydrogen Peroxide						
11/12/92 - P1	35	1430	321	4.86	4.86	110
11/12/92 - P2	35	1290	298	4.72	9.58	130
11/12/92 - P3	35	1120	256	4.79	14.34	75
11/12/92 - P4	35	900	187	5.00	19.34	65
11/12/92 - P5	35	675	135	4.65	23.99	50
11/12/92 - P6	35	---	109	4.65	28.64	---



Ref: Standard Dilution 100:1

Source: Dilution 10:1

Irradiated Samples: Differential Dose (MRAD)

4.46	4.48	3.90	3.62	2.98
------	------	------	------	------

Irradiated Samples: Cumulative Dose (MRAD)

4.46	8.94	12.8	16.5	19.4
------	------	------	------	------

Ref: Standard Dilution 333:1

Note: Source and Irradiated Samples Were Diluted Additional 10:1 to Allow Sufficient Transparency for Visual Comparison

Figure 17: Red Water at 10:1 Dilution Irradiated by an Electron Beam: Mod 0.5 Tests of 11/19/92

were not photographed the tests of 11/12/92 with peroxide added showed significantly greater reduction in color. The series at 1:100 dilution showed dramatic color change with increasing dosage going from bright red to pale yellow as shown in Figure 18. In this photo we have again included unirradiated, diluted red water samples for comparison. At the maximum cumulative dose of 19.4 MRads the color corresponds to a reference water dilution of approximately 2000:1. If color were an indicator of contaminant destruction this would then correspond to a destruction by a factor of twenty. HPLC measurements of contaminant destruction, reported below, show color is a fair indicator.

Small samples of symmetric TNT and four of its isomers, 3-4-5, 2-3-4, 2-3-6 and 2-4-5 were obtained from R. Spanggord of SRI. These were analyzed by H. Jordi partly to validate his HPLC process development and also to identify at least some of the many peaks in red water analysis. Results with absorption detection at 254 nm are shown in Figure 19. The separate peaks are closely spaced as expected and the peaks for a mixture of all five species match those of the individual samples to an extent that even shows repeatability of an unidentified contaminant.

In all cases results of HPLC analysis showed significant reduction in all resolvable peaks with increasing dosage including those identified with TNT and its isomers. An example of contaminant destruction is provided by a comparison of Figures 20 and 21. In these elution traces time increases from left to right and absorption detection is shown for bands at 340 and 254 nm. These traces correspond to source and maximum radiolysis

Red Water Irradiated by an Electron Beam

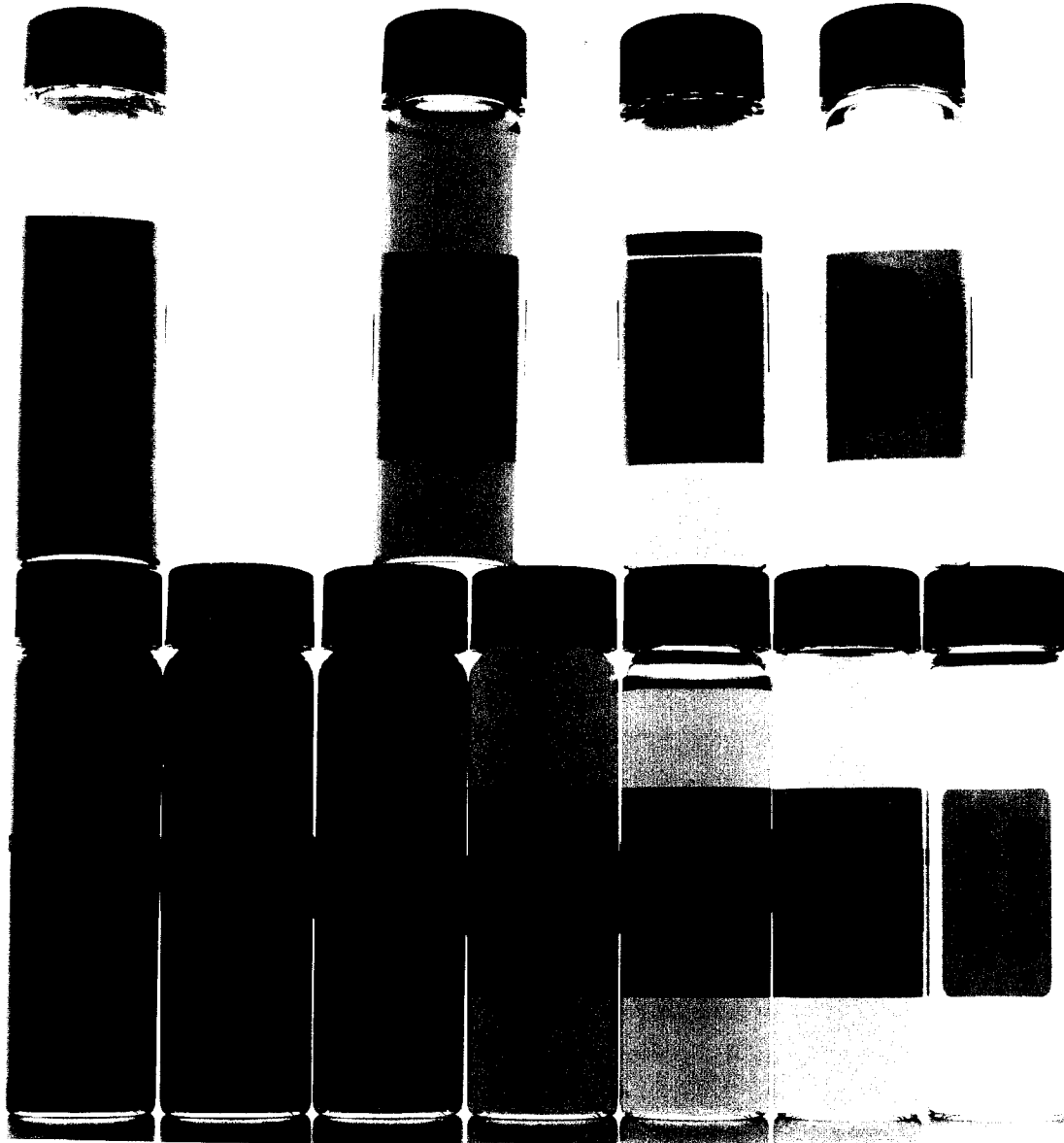
REFERENCE STANDARD PREPARED BY WATER DILUTION

100:1

333:1

1000:1

3330:1



SOURCE:
DILUTION
100:1

IRRADIATED SAMPLES: DIFFERENTIAL DOSE (MRAD)

4.4	4.5	3.9	3.6	3.0
-----	-----	-----	-----	-----

REF:
EMPTY
VIAL

IRRADIATED SAMPLES: CUMULATIVE DOSE (MRAD)

4.4	8.9	12.8	16.5	19.4
-----	-----	------	------	------

263 jj 002

Figure 18: Red Water at 100:1 Dilution Irradiated by an Electron Beam: Mod 0.5 Tests of 11/12/92

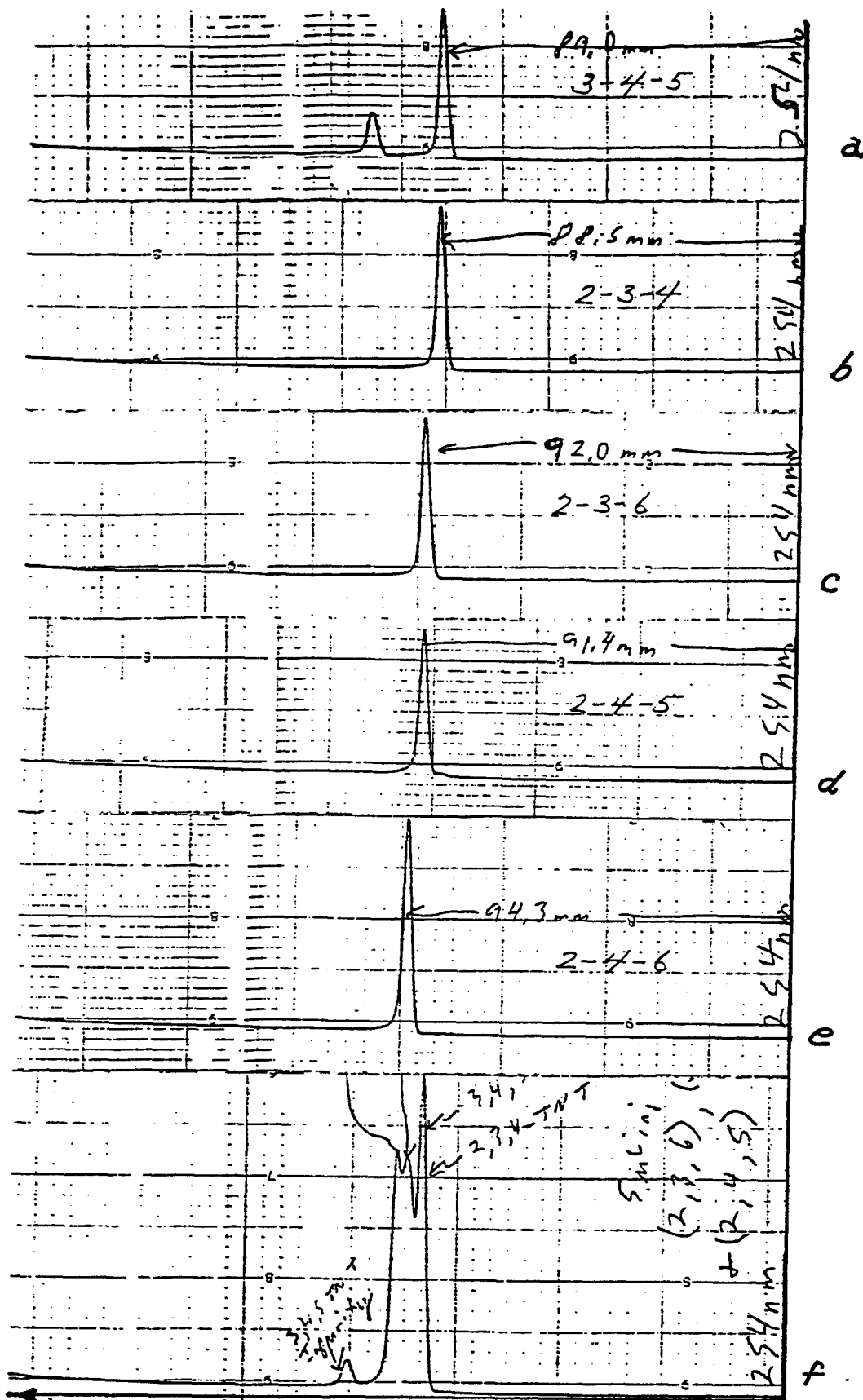


Figure 19: HPLC peak elution of TNT isomers absorption at 254 nm.

Dilution 1:10

No Irradiation

Absorption at

340 nm (Upper)
254 nm (Lower)

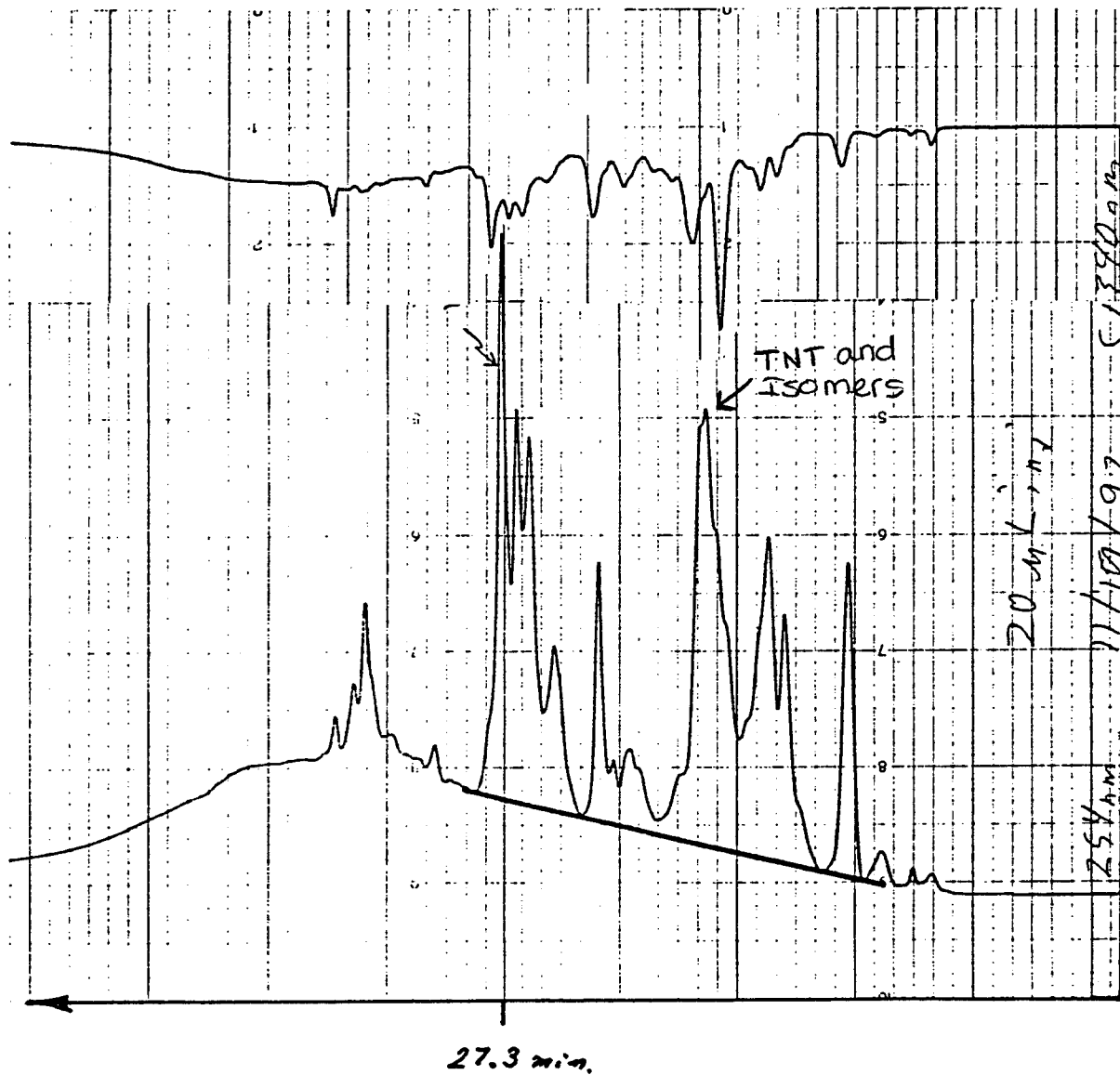


Figure 20: HPLC analysis of red water before radiolysis.

Dilution 1:10

Dosage = 19.4 MRads

Absorption at

340 nm (Upper)
254 nm (Lower)

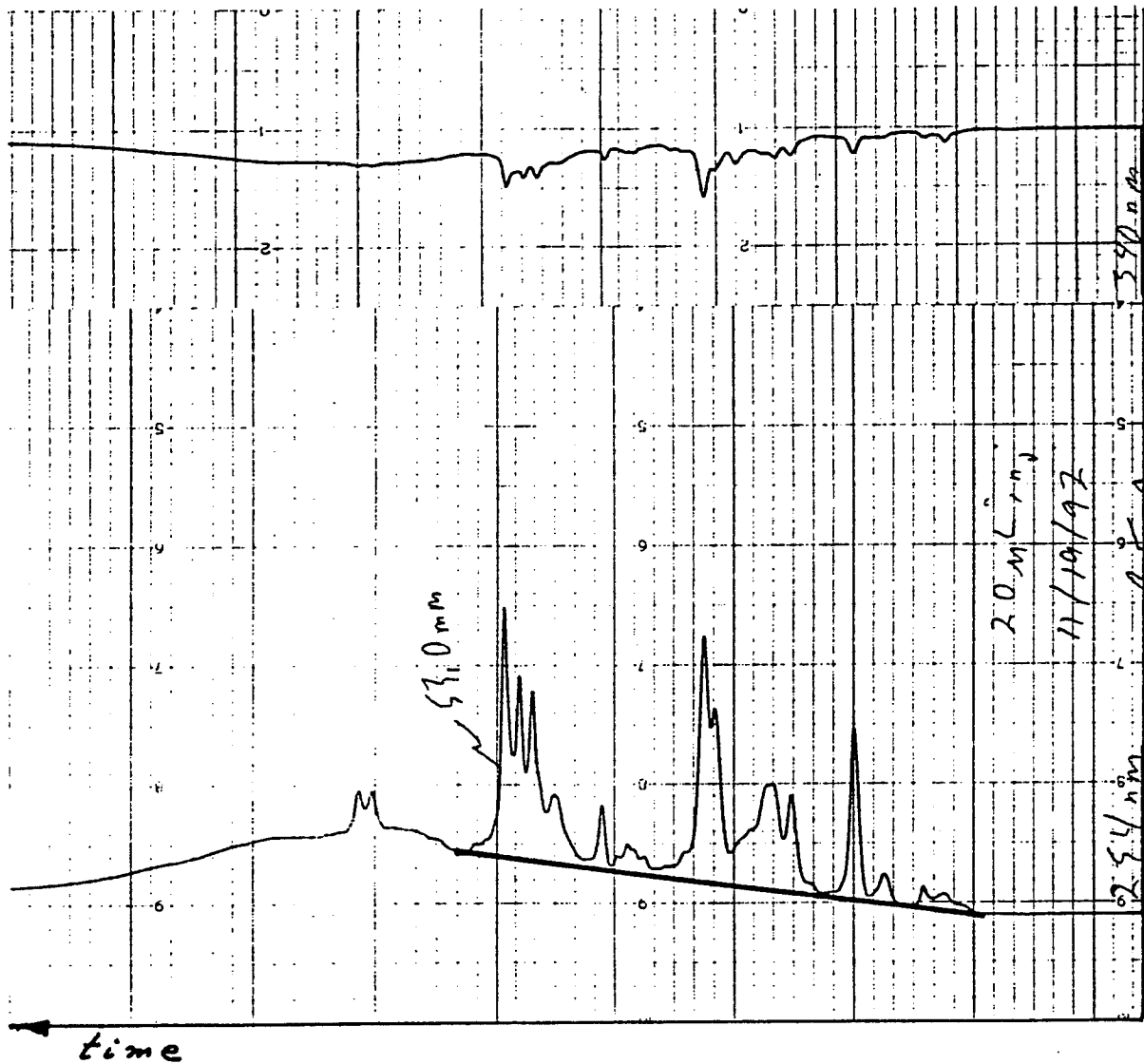


Figure 21: HPLC analysis of red water after radiolysis.

dose (P5) respectively of tests 11/19/92 and may be compared to the photograph in Figure 17. More than 30 peaks are identifiable for the unirradiated sample and more than 25 are still resolvable for the irradiated sample. There is also a very broad peak over which others are superimposed; this was associated with oligomers of the fundamental species. The isomer group is present with a very strong signal although one other later peak is stronger. The most noticeable feature in this comparison is the uniform fractional reduction of all peaks by radiolysis. This feature was verified by examination of the traces for all tests of 11/19/92. Consequently it was convenient to summarize these tests as a plot of the strongest peak (eluted at 27.3 min) versus dose in Figure 22. This shows that for 1:10 dilution, peaks were reduced approximately linearly with increasing dose to a reduction of 50-60% at the maximum dose of 19.4 MRads. Comparison of color change with dosage in Figure 17 against unirradiated diluted standards suggests that color change is a fair indicator of overall contaminant destruction.

For the series with 1:10 dilution and with the addition of 9200 ppm of hydrogen peroxide the peaks did not all follow the same pattern. Some showed approximately linear reduction by levels of 65-70% at the maximum dose of 29 MRads while others showed more rapid and nonlinear destruction patterns. Consequently these results were summarized by recording changes in the three major peaks with dosage as reported in Figure 23. The peak at 27.3 min elution time shows a maximum reduction to 4.5% of its initial height. Those at 17.9 min (TNT isomer cluster) and 11.7 min show reductions to 33% and 35% of their respective initial heights. A comparison of chromatographs for

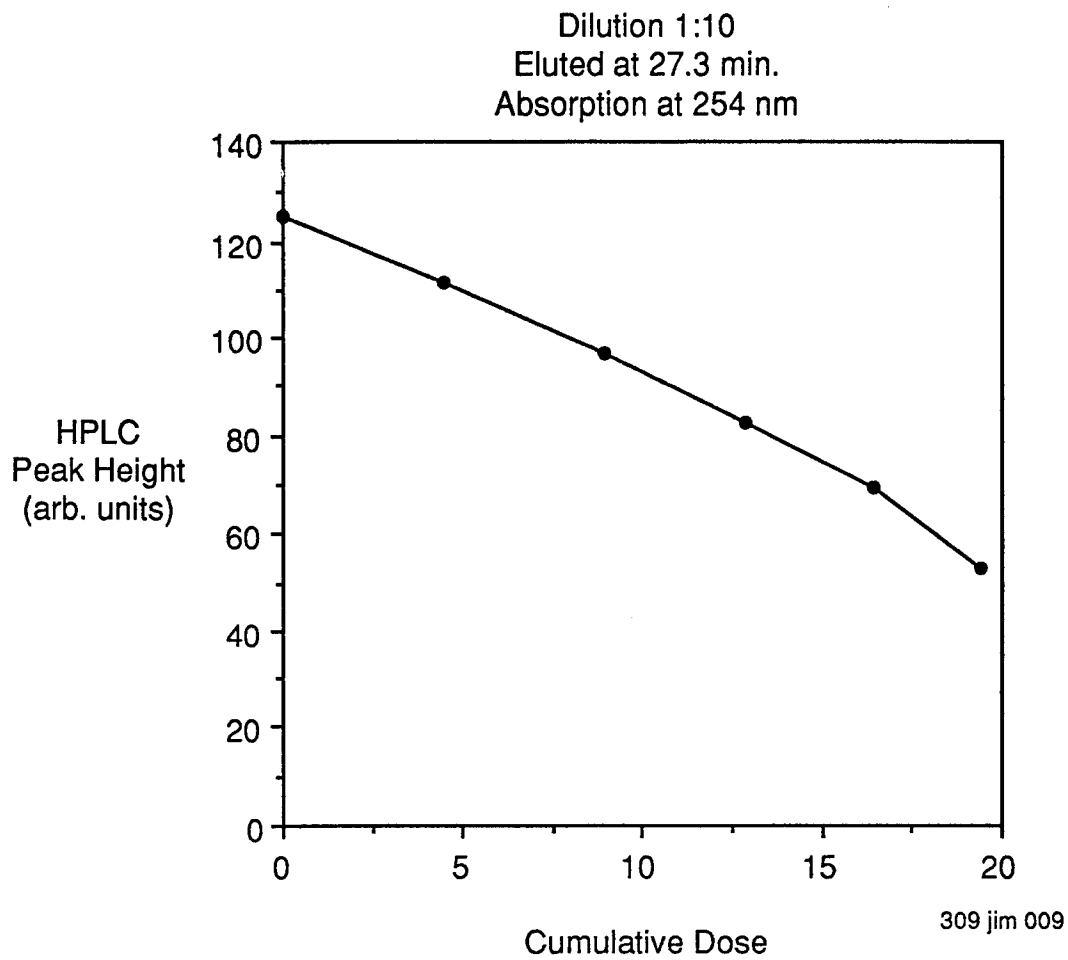


Figure 22: Red water species destruction with increasing radiolysis dosage:
MOD 0.5 test of 11/19/92

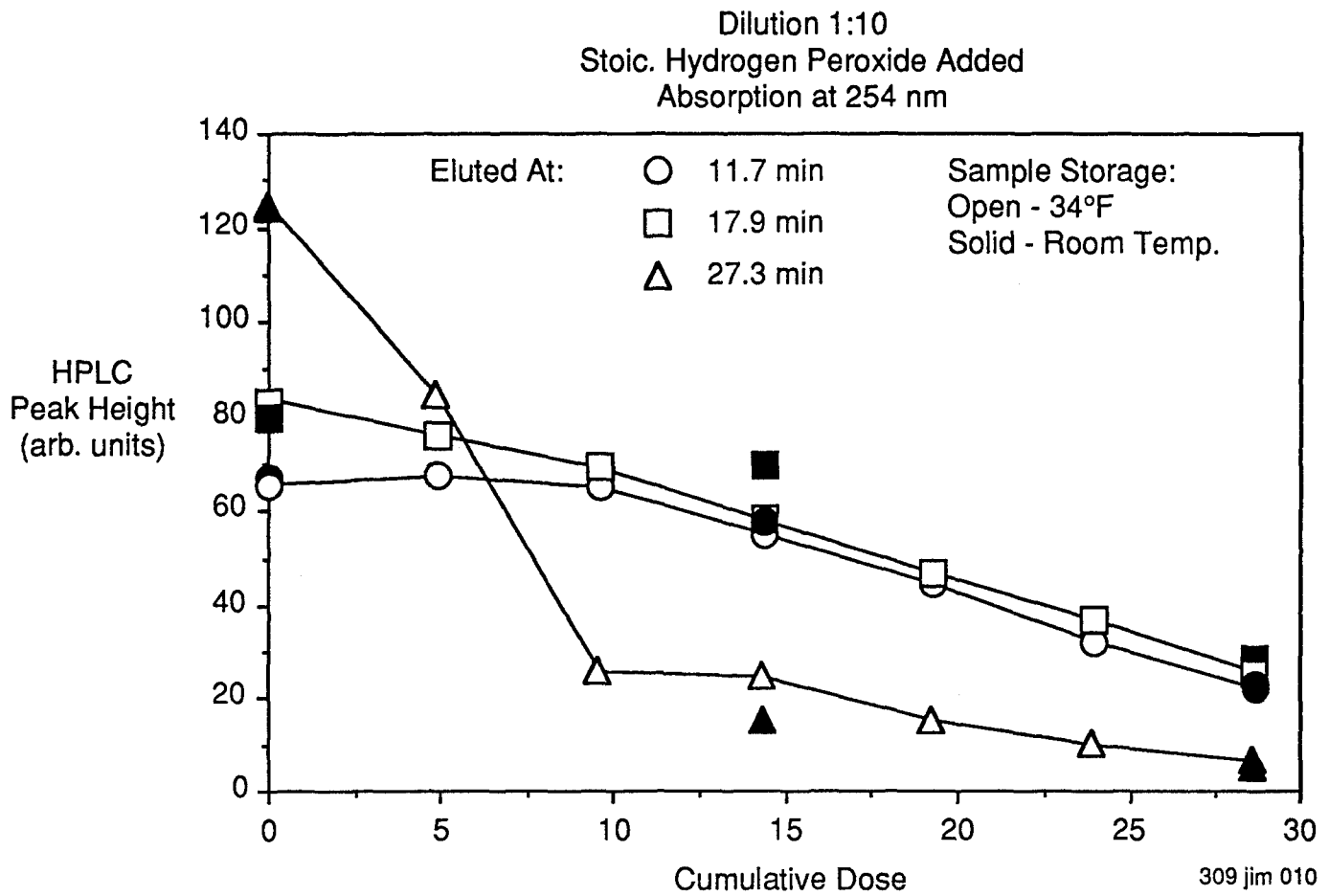


Figure 23: Red water species destruction with increasing radiolysis dosage: MOD 0.5 test of 11/12/92

unirradiated samples with and without the addition of hydrogen peroxide showed good quantitative agreement. We conclude that the significant differences in chromatographs for irradiated samples are a direct result of the combination of irradiation and peroxide addition and not a result of the oxidizing action of peroxide alone. The composition of both irradiated and unirradiated samples was not sensitive to storage temperature over a period of approximately 30 days. This is shown in Figure 23 where open and solid symbols represent storage at 34°F and at room temperature respectively. Color comparisons indicated that composition did not change significantly during storage of approximately 30 days between irradiation and analysis. Significant amounts of gas evolved during irradiation only for tests with peroxide added as shown in Table 8. This was presumably the result of breakdown of peroxide itself although we did not analyze the trapped vapor phase products in these experiments. The complex influence of peroxide on radiolysis of red water and the potential benefits of process cost reduction by peroxide addition point up the importance of further studies in this area.

The test series with initial dilution of 1:100 showed roughly exponential decay with cumulative dosage for those peaks examined to date with final reductions by factors of 25 to >100. These results were also summarized by recording the three major elution peaks as a function of cumulative dosage as shown in Figure 24. The exponential form is indicated in semilog format. Maximum reductions in the three reported elution peaks at a dosage of 23 MRads are 0.4%, 3.9% and 3.0% of their respective unirradiated peaks at elution times of 28.3, 17.9 and 11.7 min. Again reference to color of these irradiated

Dilution 1:100
Absorption at 254 nm

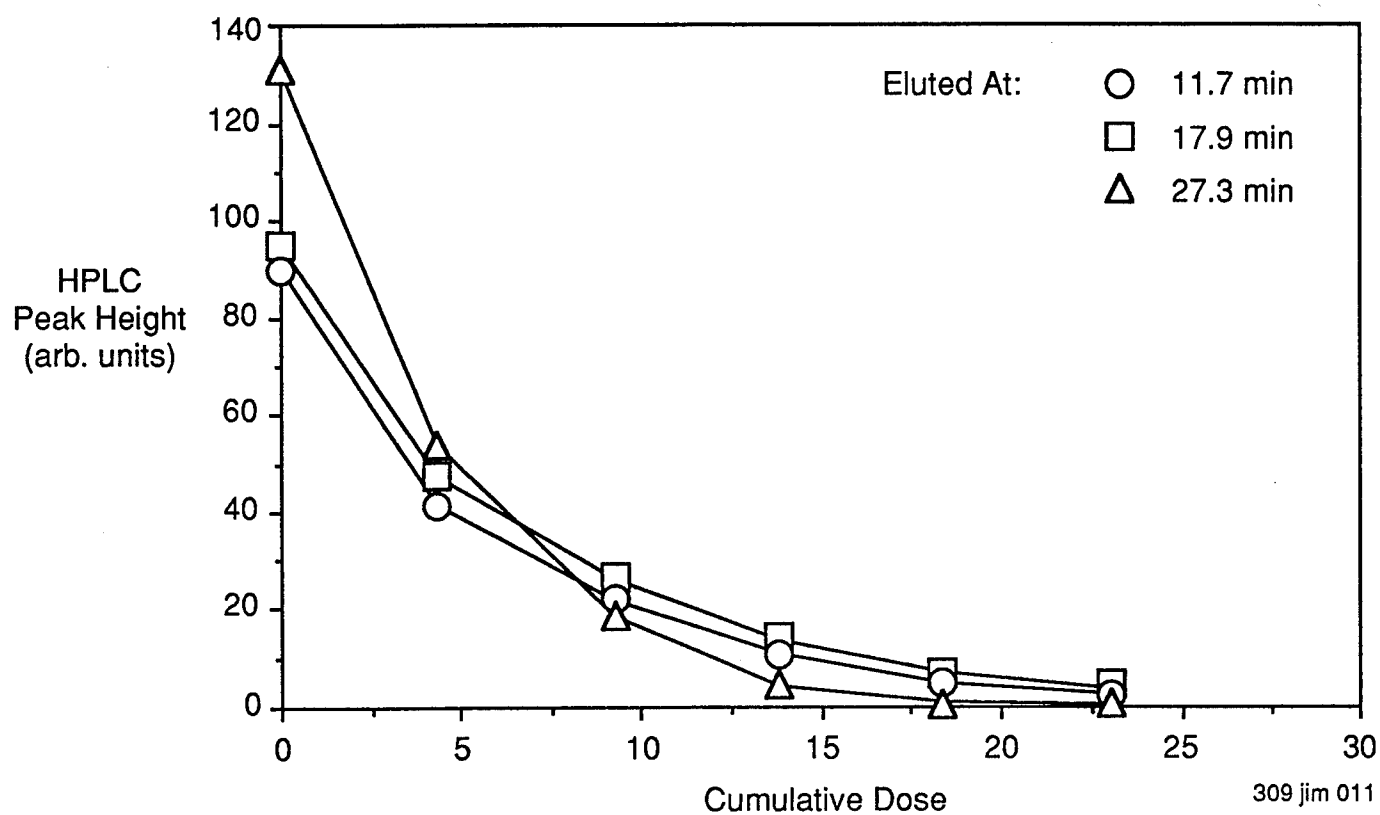


Figure 24: Red water species destruction with increasing radiolysis dosage: MOD 0.5 test of 11/11/92
(a) linear plot

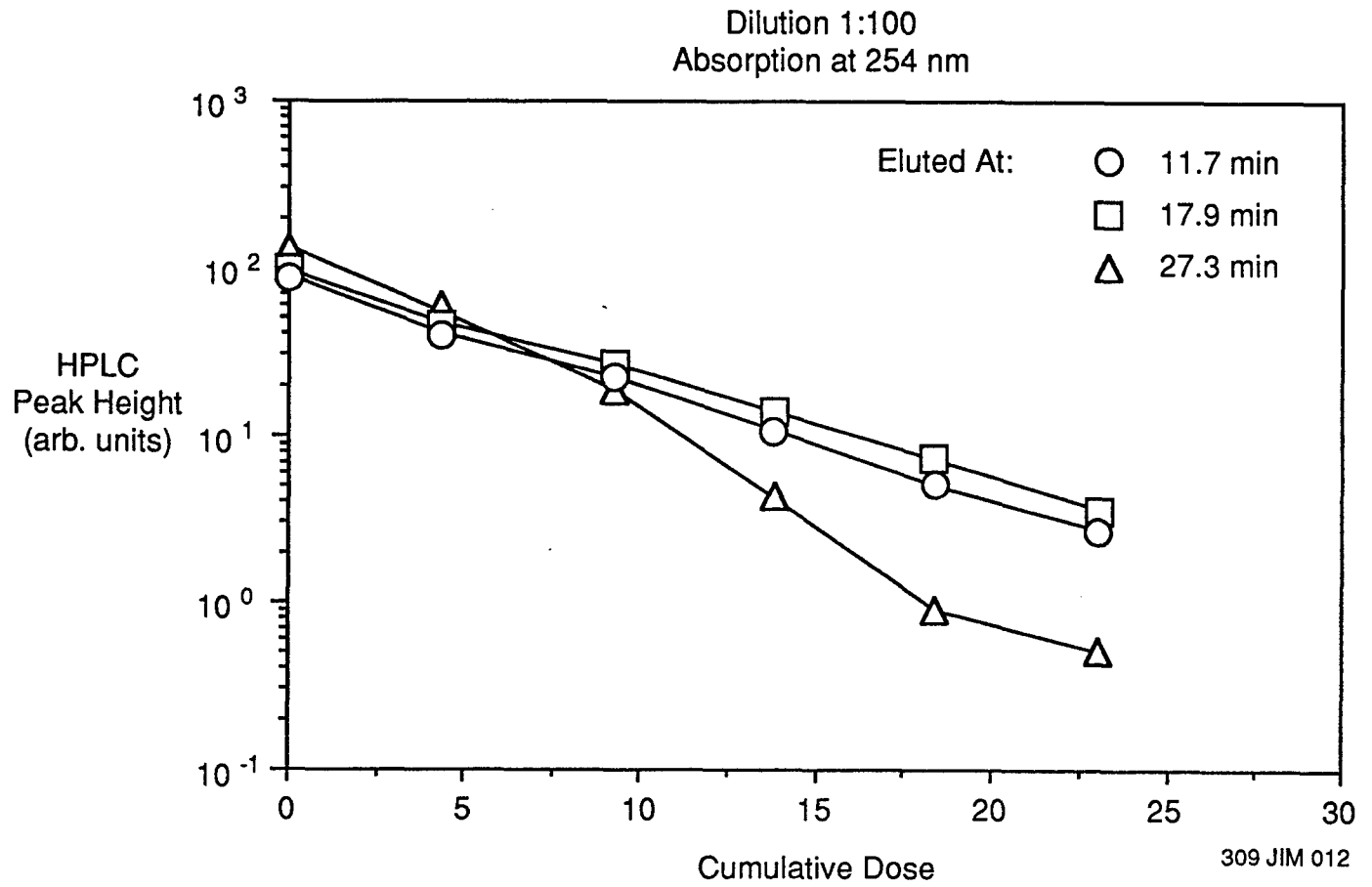


Figure 24: (b) Semilog plot

samples in Fig. 18 indicates color comparison to unirradiated diluted standards provides a fair indication of contaminant destruction. It is useful to compare relative contaminant destruction effectiveness between Figures 22 and 24. At 1:10 dilution a dose of 8.9 MRads produces 22.5% reduction in the 27.3 min elution peak. At 1:100 dilution a dose of 9.2 MRads produces 86% reduction in the 27.3 min elution peak. Although fractional reduction is more effective at the higher dilution, clearly the absolute destruction effectiveness is higher at the lower dilution.

5.1.2 Mod 0.5 VOC Tests

Three volatile organic contaminants benzene, toluene and trichloroethylene were selected in the first test segment on the basis of some or all of the following: they are building blocks for TNT and red water contaminants; there exists some data base for comparison; they are targeted contaminants which are frequently present in ground water and waste water. Radiolysis studies in some cases (benzene and toluene) were also conducted with the addition of hydrogen peroxide to the source contaminated water. The selected concentrations produced stoichiometric mixes based on the assumption that the organic contaminant would reduce to carbon dioxide and water. High initial contaminant concentrations were selected (400 ppm) to simplify handling, cleanliness and analysis resolution in this first evaluation of the induction linear accelerator technology applied to water decontamination. Moreover high initial concentrations are most relevant to the

study of red water decontamination. A further motivation to the study of high contamination levels is the ease of achieving high dose levels with the present apparatus.

A summary of Mod 0.5 tests is presented in Table 9. Runs of 10/28 and 10/29/92 were a series where contaminated water passed only once through the radiolysis cell. Runs of 11/15 through 11/19/92 are in five groups. Within each group the contaminated water was passed through the radiolysis cell six or seven times. A portion was retained for each pass as indicated by differences in processed mass between passes. Processed water has therefore a dosage for it's pass (differential) and a cumulative dosage for this and all previous passes as shown. Runs in Table 9a are included for completeness although we and presumably the analysis laboratory were in the process of learning how to handle high concentrations of VOCs in water solution. Quantitative chemical analysis is discussed below and qualitative features are discussed here.

Four of the five cumulatively irradiated groups showed changes in color and the formation of a cloudy precipitate as dose accumulation increased. In three of these cases the cloudiness peaked and then decreased as dose accumulation increased. In one of these cases the amber coloration also peaked and then decreased nearly to zero as dose accumulation increased. These features are discussed here with as visual aids.

The source for run Group 11/15/92 contained 200 ppm. each of benzene and toluene dissolved in HPLC grade water. Figure 25 shows irradiated samples at increasing

Table 9.a: VOC radiolysis tests summary: MOD 0.5

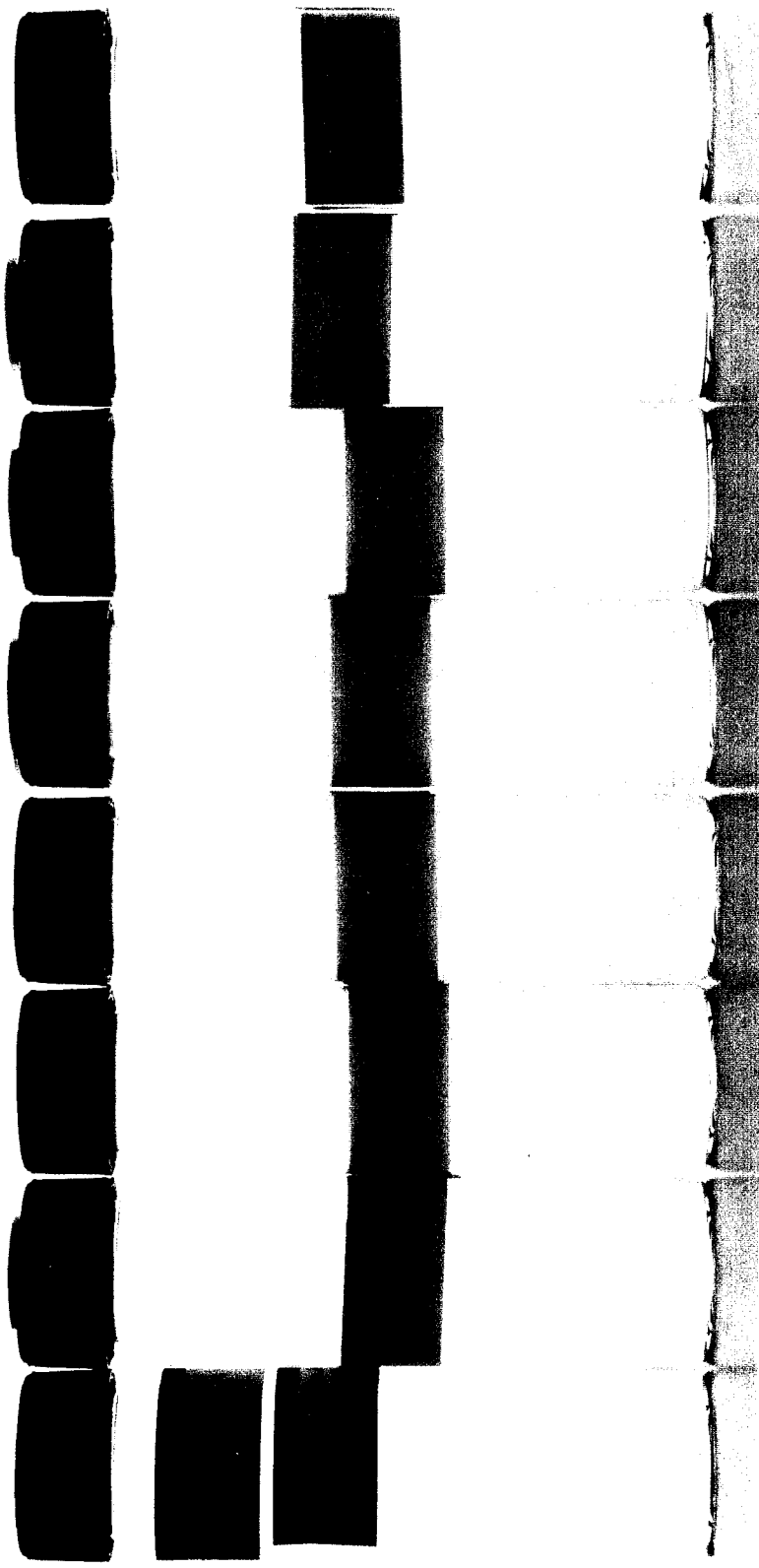
Source Composition Run Identification Number	Pulse Rate (Hz)	Run Time (sec)	Processed Mass (g)	Dose- Differential (MRad)	Dose- Cumulative (MRad)	Evolved Gas (cc)	TC (ppm)	Gc - Ms Resid Source (ppm)	GC - MS Other (ppm)
100 ppm Benzene 10/28/92-P1 10/28/92-P2	21	440	109	—	1.4			2.9	
	6.9	435	109	—	0.45			0.6 1.3	
100 ppm Benzene + Stoich. Hydrogen Peroxide 10/29/92-P1 10/29/92-P2 10/29/92-P3	21	455	90	—	1.22				
	6.9	—	88	—	0.41				
	21	500	124	—	1.21				

309 jim 013

Table 9.b: VOC radiolysis tests summary: MOD 0.5

Source Composition Run Identification Number	Pulse Rate (Hz)	Run Time (sec)	Processed Mass (g)	Dose- Differential (MRad)	Dose- Cumulative (MRad)	Evolved Gas (cc)	TC (ppm)	TC Source Scaled (ppm)	GC - MS Resid Source (ppm)	GC - MS Other (ppm)
200 ppm Benzene + 200 ppm Toluene										
11/15/92-P1	12	1020	738	0.70	0.70	30	330	360	210/290	
11/15/92-P2	12	780	564	0.64	1.34	30	250		140/110	
11/15/92-P3	12	645	472	0.64	1.98	30				
11/15/92-P4	12	520	375	0.57	2.55	20				
11/15/92-P5	12	400	293	0.57	3.12	20	240		14/11	
11/15/92-P6	25	285	202	1.35	4.47	—				
11/15/92-P7	50 ⁽¹⁾	160	116	1.60	6.07	15	500(400)	550(440)	540(510)	0
400 ppm Toluene										
11/17/92-P1	12	970	694	0.66	0.66	—	190		130	
11/17/92-P2	12	820	584	0.68	1.34	35	190		57	7.2 C ₆ H ₆
11/17/92-P3	25	660	469	1.35	2.69	35	210		30	
11/17/92-P4	25	530	373	1.35	4.04	25				
11/17/92-P5	25	400	285	1.35	5.39	20	190		1.3	0.1 C ₆ H ₆
11/17/92-P6	25	205	147	1.35	6.74	15				
400 ppm Benzene										
11/18/92-P1	12	1000	707	0.66	0.66	20	380(250)	410(270)	330(360)	0
11/18/92-P2	12	840	598	0.59	1.25	20	280		230	1.4 C ₇ H ₈
11/18/92-P3	12	700	493	0.54	1.79	20	280		150	
11/18/92-P4	25	560	392	1.18	2.97	20	280		47	0.8 C ₇ H ₈
11/18/92-P5	25	410	282	1.35	4.32	15	250		1.5	0.7 C ₇ H ₈
11/18/92-P6	25	200	144	1.30	5.62	10		430	470	
400 ppm Toluene + Stoich. Hydrogen Peroxide										
11/18/92-P1A	12	1000	706	0.46	0.46	5	390		93	
11/18/92-P2A	12	835	593	0.44	0.90	15	260		35	
11/18/92-P3A	25	695	488	0.89	1.79	25	260			
11/18/92-P4A	25	550	391	0.89	2.68	20	260		1.0	0.1 C ₆ H ₆
11/18/92-P5A	25	395	276	1.21	3.89	25				
11/18/92-P6A	25	200	144	1.33	5.22	15	200		0	
400 ppm Trichloroethylene										
11/19/92-P1	12	950	703	0.64	0.64	20	120	660	590	3.3 C ₂ H ₂ Cl ₂
11/19/92-P2	12	800	595	0.66	1.30	20	49		110	3.1 C ₂ H ₂ Cl ₂
11/19/92-P3	25	660	490	1.38	2.68	35	48		44	0.5 C ₂ H ₂ Cl ₂
11/19/92-P4	25	510	379	1.33	4.01	30	48		16	
11/19/92-P5	25	305	233	1.40	5.41	20	35		0.8	0.5 C ₇ H ₈
11/19/92-P6	25	150	112	1.43	6.84	15				

(1) Pulses Missing



Source	Irradiated Samples: Differential Dose/Cumulative Dose (MRAD)				
0.70	0.64	0.64	0.57	0.57	1.60
0.70	1.34	1.98	2.55	3.12	6.07

Figure 25: Toluene - 200 ppm + Benzene - 200 ppm in Water Irradiated by an Electron Beam
 252 jm 005
 SCIENCE RESEARCH LABORATORY

cumulative dose levels. The formation of cloudy precipitate and amber color are evident with a maximum in both at about 2.5 MRad and a significant decrease in both with further dose accumulation to 6.07 MRad. The source for Group 11/17/92 contained 400 ppm of toluene. Figure 26 shows a peak in both amber color and in cloudy precipitate at a cumulative dose of about 2.7 MRad and a decrease in both with additional dose accumulation to 6.74 MRad. The source for Group 11/18/92 contained 400 ppm of benzene. Figure 27 shows only very slight cloudiness was produced by irradiation although precipitate is evident for the three lowest dose levels. Amber color has a maximum at a cumulative dose of about 3.0 MRad. The source for Group 11/18/92-A contained 400 ppm of toluene plus a stoichiometric concentration of hydrogen peroxide (2660 ppm). Figure 28 shows only a slight trace of cloudiness at a cumulative dose of about 0.9 MRad and a peak in amber color also at this level. With increasing cumulative dose to 5.22 MRad the solution returns almost to its original clarity. Trichloroethylene at 400 ppm was cumulatively irradiated as shown in Table 3b. At all dose levels the samples showed no color change, no cloudiness and no precipitate.

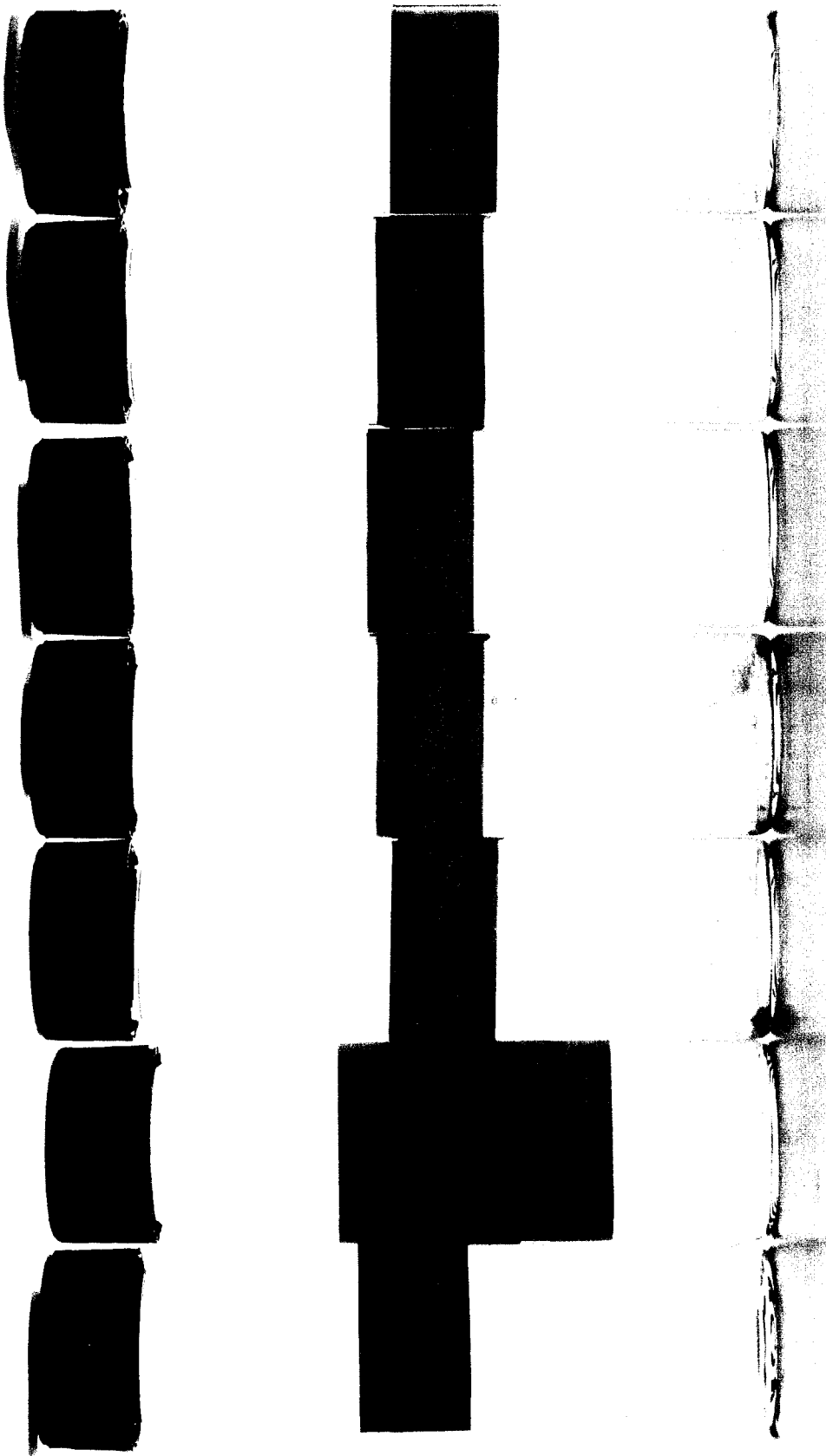
After storage for several weeks at approximately 34°F some precipitate settled in the clouded samples; however the qualitative features described above were unchanged. The settled precipitate ranged in color from white to brown and both color and quantity scaled roughly with color and cloudiness of the sample.



Source **Irradiated Samples: Differential Dose/Cumulative Dose (MRAD)**

0.66	0.68	1.35	1.35	1.35	1.35
0.66	1.34	2.69	4.04	5.39	6.74

Figure 26: Toluene - 400 ppm - in Water Irradiated by an Electron Beam



Source

Irradiated Samples: Differential Dose/Cumulative Dose (MRAD)

0.66	0.59	0.54	1.18	1.35	1.30
0.66	1.25	1.79	2.97	4.32	5.62

Figure 27: Benzene - 400 ppm - in Water Irradiated by an Electron Beam

252 jm 003

SCIENCE RESEARCH LABORATORY



Source **Irradiated Samples: Differential Dose/Cumulative Dose (MRAD)**

0.46	0.44	0.89	0.89	1.21	1.33
0.46	0.90	1.79	2.68	3.89	5.22

Figure 28: Toluene - 400 ppm + Stoichiometric Hydrogen Peroxide in Water Irradiated by an Electron Beam

252 jm 002

SCIENCE RESEARCH LABORATORY

The main point to these visual observations is that significant chemical processes are likely being caused by these high dosages of electron beam radiation. A comparison of toluene groups with and without hydrogen peroxide suggests that the peroxide may accelerate the progression to the final chemical state. These indicators were sought to provide guidance in selection of test matrix elements since the turn around time for quantitative analysis was too long to provide such guidance.

Substantial quantities of gas were generated from the contaminated water as a result of radiolysis. Although no gas analysis was performed it is useful to assess the possible loss of dissolved VOCs to the vapor phase. Estimates of evolved gas in Table 9b are based in each case on a visual comparison of gas within the transparent test pouch with the measured volume (weight) of water in the same pouch. Consider now Group 11/18/92 where 400 ppm, or 0.312 g, of benzene was dissolved in an initial 779 g of water. If benzene were present at its vapor pressure at room temperature, 80 Torr, throughout the evolved gas generated during the entire run sequence, 105 cc, this would correspond to 0.035 g of benzene. One concludes that in this most pessimistic case the loss of benzene to the vapor phase would cause a small, 11%, error in estimates of VOC destruction at these high dose levels. This estimate is pessimistic (excessive) since the gaseous concentration would be as high as the vapor pressure only if the water were saturated: saturation for benzene is 800 ppm so the present mix was initially well below saturation and decreased further as the destruction process continued. Similar arguments and conclusions apply to toluene and trichloroethylene. One may speculate on the

possible source of such large gas volumes. However the complete destruction of 0.312 g of benzene to carbon dioxide and hydrogen would produce 1.4 mg of dissolved hydrogen and 278 cc of hydrogen as a gas. In light of this the amount of evolved gas might be considered small.

Total carbon (TC) and gas chromatography analysis with mass spectrometric species identification (GCMS) were conducted on several source and processed samples. Results are shown in Tables 9a and 9b. In the column GC-MS Residual Source the measured concentrations of the injected contaminant species are reported. Dual entries in Group 11/15/92 correspond to benzene and toluene respectively. Numbers in parentheses correspond to repeat analyses taken 20 days later. Comparison of GCMS benzene results in Table 9a with the prepared source sample of 100 ppm benzene shows a great disparity in absolute concentrations although relative decrease with increased radiolysis dose is as expected. Presumably as a result of increased experience in VOC handling later tests in Table 9b show much better agreement between prepared source and GCMS source results. Still there are significant differences between prepared source concentrations and GCMS results which overestimate toluene by an average of 30% and trichloroethylene by 50% and slightly underestimate benzene by 5%. These differences may be explained in part by handling associated with in some cases repeated dilution's to achieve the GCMS calibration range of 10 to 160 ppb. With the experience of the present data base we expect that in the future we can anticipate residual concentration versus radiolysis dose to achieve the calibration range for nearly all samples by single dilutions conducted at SRL.

Results of total carbon analysis are also shown in Table 9b. Removal of dissolved CO₂ by sparging prior to analysis was not a viable option since the VOCs would be lost in the process. Consequently total carbon was analyzed rather than total organic carbon. Source results are shown after scaling to the equivalent weight of organic compound on the basis of composition and atomic weights (TC Source Scaled). Scaled source results show fair agreement when compared directly with source GC-MS results. A significant decrease is shown in each group after the first radiolysis pass followed in each group by very little change after each succeeding pass. Stability of carbon in solution is easily explained since it may exist in product compounds or as dissolved carbon dioxide. The significant decrease after the first pass is difficult to explain. Total carbon losses from solution after the first pass range from 70 to 260 ppm. If it were to depart as carbon dioxide gas the associated gas volumes would range from 120 to 430 cc. However, the total evolved gas after the first radiolysis pass in this gas tight system only from 5 to 30 cc. Specific radiolysis products were not analyzed at this time, although a variety of VOCs were analyzed as listed in Table 6. Identified trace species listed in Table 9b (GC-MS Other) which are primary species in other groups may simply be residue from previous runs. The production of dichloroethylene in Group 11/19/92 appears to be followed by rapid destruction with increased dosage.

GCMS measurements of residual source concentrations at various dose levels have been normalized by their respective unirradiated source GCMS values. These are plotted in Figures 29 through 31 as fraction remaining of source contaminant at increasing levels

of cumulative dose. Benzene Groups 11/15/92 and 11/18/92 are plotted in Figure 29 in a format where a first order process would follow a straight line. These tests were conducted at initial concentrations of 200 ppm (mixed with 200 ppm of toluene) and 400 ppm and a linear fit would suggest a destruction effectiveness of 2.5 MRads per decade. Toluene Groups 11/15/92, 11/17/92 and 11/18/92-A are plotted in Figure 30. The third group had hydrogen peroxide added. A linear fit to the solid symbols would suggest a destruction effectiveness of two MRads per decade, whereas, with peroxide added the effectiveness clearly improves to approximately one MRad per decade. In all three cases the initial slopes are more steeply negative which suggests higher effectiveness at higher contaminant concentrations. Similar comments apply to trichloroethylene results plotted in Figure 31.

In view of results reported in Table 9b the single pulse dose rate of 0.36 MRads (see Table 5) was perhaps too large for two reasons. First the total differential dose per radiolysis treatment in many cases was below 0.66 MRads which implies on average the contaminated water experienced less than two radiolysis pulses per cell transit. Since fully developed laminar flow has flow speeds which range from zero to 150% of the mean between walls and channel center one may expect significant differences in dose for different flow elements due to large differences in dwell time. This alone would not significantly bias results if the fractional reduction in contaminants were small for each cell transit, since, after several passes, the cumulative dose would tend to be much more uniform. However post run analyses reported in Table 9b show contaminant destruction

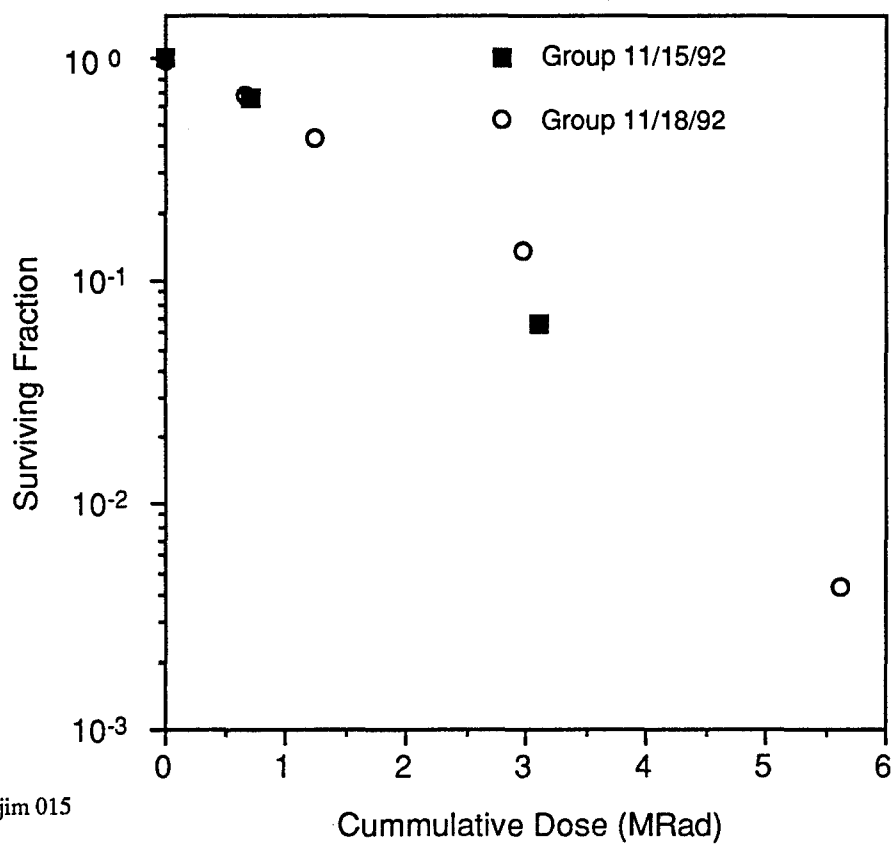


Figure 29: Destruction of benzene by pulsed electron beam irradiation: MOD 0.5

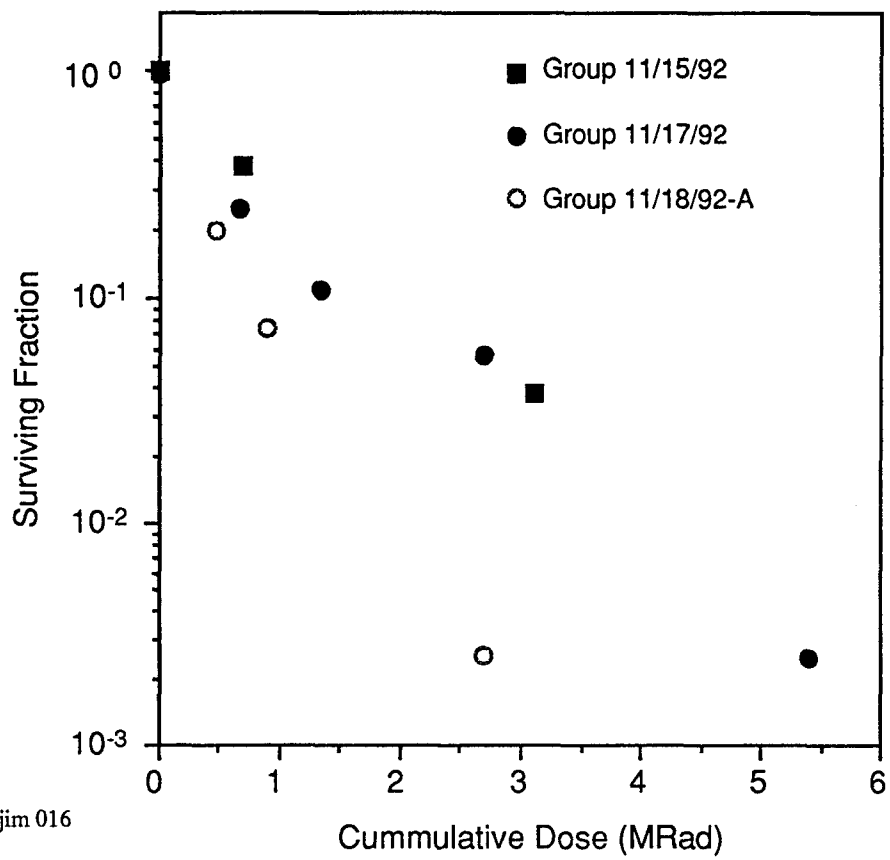


Figure 30: Destruction of toluene by pulsed electron beam irradiation: MOD 0.5

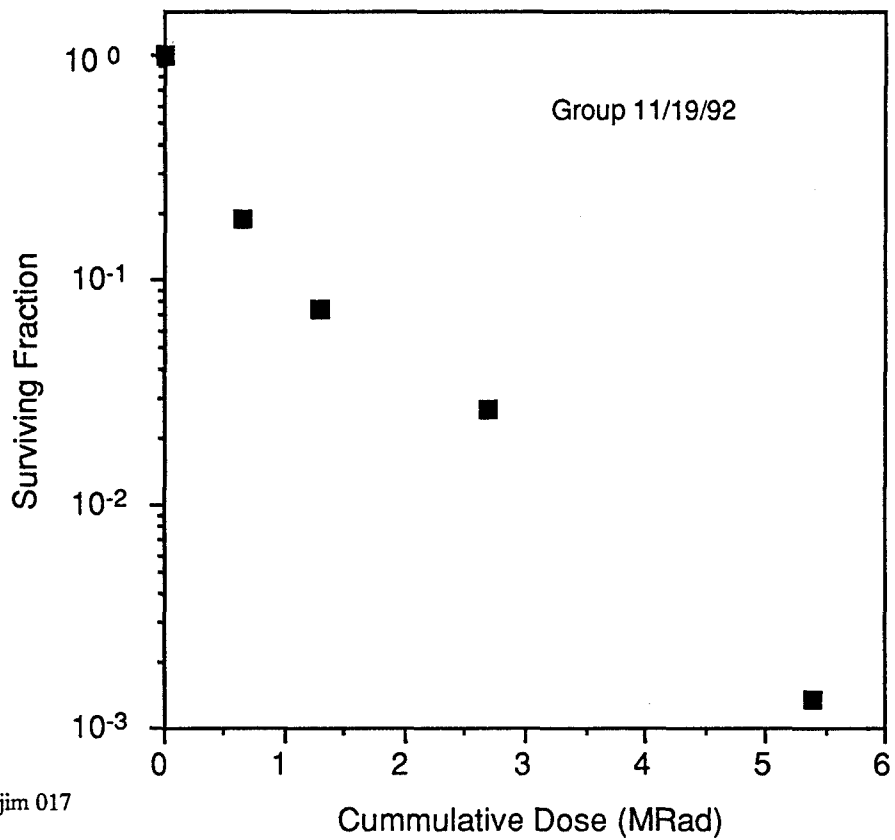


Figure 31: Destruction of trichloroethylene by pulsed electron beam irradiation: MOD 0.5

levels per pass as high as 80%. In such cases one might argue that destruction may have been much higher to water which received the mean dosage and that surviving contaminants come from regions which received little or no irradiation. In other words these conditions may cause an overestimate in the dosage required to effect a given degree of destruction. Selection of a high single pulse dosage in these preliminary tests was dictated by a variety of test constraints including time limitations and scheduling with concurrent tests. Modifications in the Mod 1.5 test apparatus and operating conditions, as already described, resolved these issues prior to the second test segment.

5.2 Mod 1.5 Experimental Results

Tests during the second segment explored the effects of dose rate on destruction efficiency, at 7×10^{11} and 1.4×10^{11} Rads/sec, and also broadened the study of efficiency dependence on initial contaminant concentrations down to 40 ppm. One test series was conducted with undiluted red water to complement the studies with water dilution reported above. Benzene was studied at two dose rates and at three initial concentrations, 400, 100 and 40 ppm. To broaden the range of VOC initial concentrations one test series examined methylene chloride destruction at an initial concentration of 5,000 ppm. Red water decontamination was evaluated by color change. VOCs destruction was evaluated by GCMS as described above. Mass balance assessment by total carbon analysis was carried out for the first test segment and results showed preservation of carbon in soluble forms to a factor of approximately 2.5 while source contaminant concentrations were

reduced by nearly three decades. Consequently to conserve resources this analysis was not performed in the second test segment. Here, as in the first test segment, accelerator radiolysis operation exceeded ten hours with an accumulation of over one million pulses over a period of several weeks with no difficulties in system performance and no apparent deterioration of the foil window. Temperature rise of the contaminated water in passage through the radiolysis cell was again the primary basis for dose determination. In this test segment direct radiometric measurements were also conducted in three intervals as described in Section 4.1.

A representative record of water temperature rise between radiolysis cell entry and exit (T_3-T_2) and of the temperature difference between cell entry and cell wall (T_2-T_9) are shown in Figure 32 as upper and lower traces respectively. This red water run, referred to as Run 12/02/93-P2, extended 900 sec during which 688 g (46 cc/min) of contaminated water was irradiated at a pulse rate of 31 Hz. The event sequence is: start red water flow and electron beam simultaneously ($t=0+100$ sec), end electron beam pulsing and simultaneous switch from red water to purge water flow ($t=0+1,000$ sec), stop purge water flow ($t=0+1120$ sec). Cooling water flow operated continuously. The temperature rise through the radiolysis channel is 20.1°C (Gain=200, $52 \mu\text{v}/^\circ\text{C}$). Conduction loss from cell water to cell structure and in turn to the cooled support structure was determined in separate tests and heating of foil and channel walls by the electron beam was estimated at 10%. With accounting for these two effects the steady state water temperature rise under adiabatic wall conditions was determined as 24.3°C .

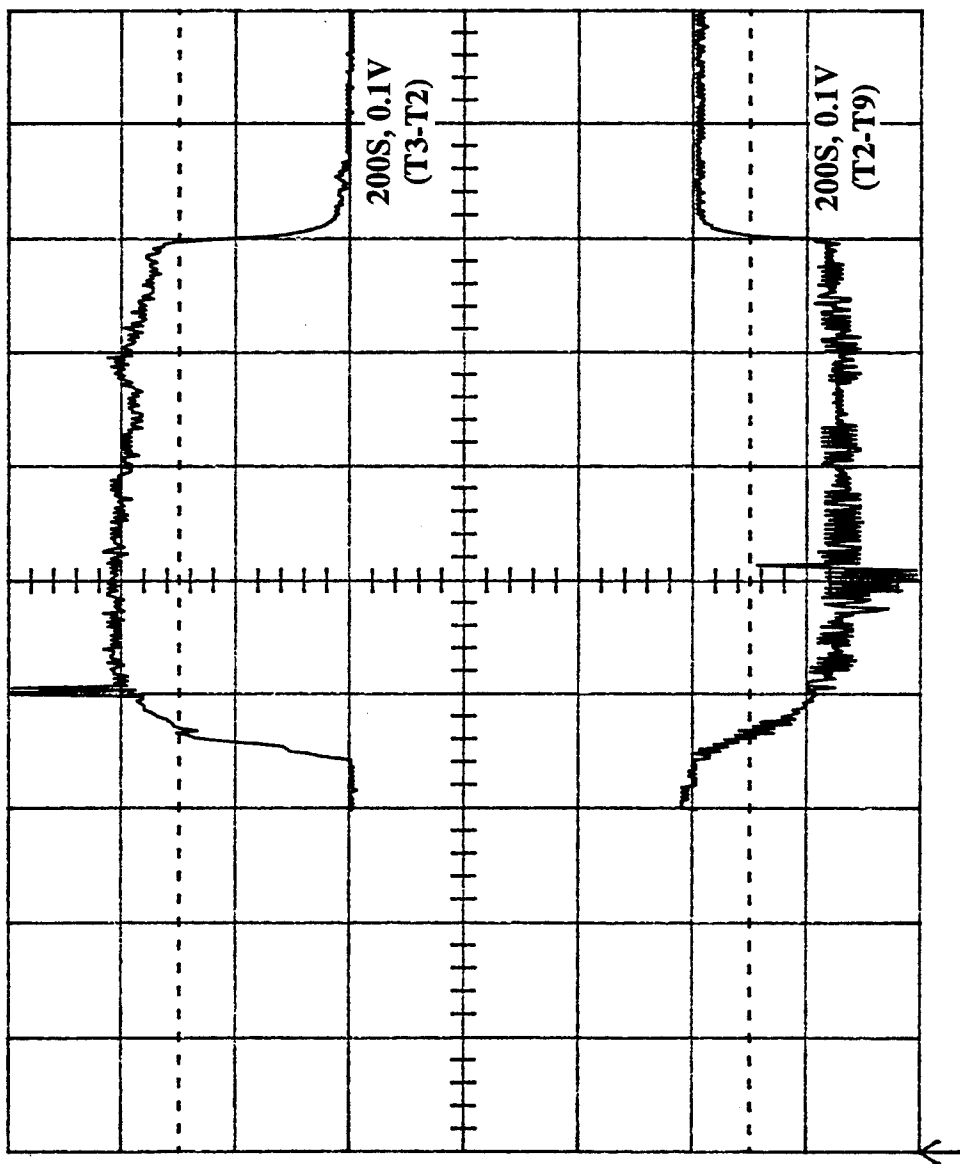


Figure 32: Water temperature rise through the cell (top) and cell inlet - cell wall temp. Difference (bottom).

This corresponds to a dose per pass of 10.2 MRads which was typical for red water tests. For VOV tests the dose per pass was of course much lower.

5.2.1 Mod 1.5 Red Water Tests

A second sample (approx. 1 kg) of undiluted red water was obtained for tests during this second segment early in 1993 by the same sources as the first sample. The specific gravity of this sample was approximately 1.15. Radiolysis tests were conducted with the red water undiluted and with no oxidizing additive. The sample was passed repeatedly through the closed flowing system with an average dose of 10.5 MRads applied in each pass. The dose rate for these tests was approximately 7×10^{11} Rads/sec. With 19 passes in total the accumulated dosage was 200 MRads. Samples of red water with no irradiation and with a dose of 200 MRads were each diluted 1:100 with water and were then compared to reference samples at dilutions of 1:100 and 1:333. This comparison showed no color change in the red water as a result of irradiation. On the basis of our earlier correlation between color change and HPLC measured contaminant destruction we concluded that no significant destruction of contaminants occurred as a result of 200 MRads of electron beam irradiation. One may speculate that recombination may play a role in contaminant survival in undiluted red water. Clearly either dilution or addition of an oxidizing agent is desirable for effective decontamination.

5.2.2 Mod 1.55 VOC Tests

During the second test segment seven test series were conducted with VOCs dissolved in water: (1) initial concentrations of 400 ppm of benzene and a dose rate of 7×10^{11} Rads/sec; (2) a duplication of the above; (3) initial concentration of 400 ppm of benzene and a diode rate of 1.4×10^{11} ; (4) initial concentration of 100 ppm of benzene and a dose rate of 7×10^{11} Rads/sec; (5) initial concentration of 100 ppm of benzene and a dose rate of 1.4×10^{11} ; (6) initial concentration of 40 ppm of benzene and a dose rate of 7×10^{11} Rads/sec; (7) initial concentration of 5000 ppm of methylene chloride and a dose rate of 7×10^{11} Rads/sec. Each group was irradiated in increments during each of six to ten passes through the radiolysis cell. Samples were taken after each pass to provide records of VOC destruction with increasing radiolysis dose up to limits ranging from four to eight MRads. Visual observations showed formation of a white cloudy precipitate which resulted from radiolysis and which increased with increased dosage for cases (1) through (5). No precipitate formed for cases (6) and (7). This precipitate appears quite stable and remains in suspension for weeks or longer. It does not appear to dissolve by water dilution. Addition of methylene chloride in increasing portions up to four parts per part of water/precipitate did not produce extraction. The methylene chloride remained clear and separated below the water/precipitate mix even after vigorous shaking. Samples were stored for possible future analysis. Only small amounts of evolved gas were observed in all tests such that dissolution to vapor does not account for a significant fraction of source contaminant or contaminant products of radiolysis.

Results of GCMS analysis of residual source contaminant concentrations are presented in Figures 33 through 37. Analyses of benzene showed no product compounds in the target list of Table 6. Since samples were diluted prior to analysis to fit the instrument range of sensitivity, 10 to 160 ppb, we may conclude none of these species were present to concentration greater than 10/160 that of benzene. Analysis of methylene chloride was done initially at concentrations well above instrument sensitivity, and repeat runs were done after appropriate additional dilutions. As a result products of radiolysis were identified and these are reported below.

Results of GCMS analysis for benzene tests are shown in Figures 33, 34 and 35. Four test series at three dose rates with initial concentrations of 400 ppm are summarized in Figure 33. Results for the highest dose rate are taken from the first test segment as reported in Figure 29-Group 11/18/92. Results at the intermediate dose rate are from the second segment and are identified with groups (1) and (2) above. Results at the lowest dose rate are identified with group (3) above. Destruction from 400 ppm to 100 ppm is not significantly dependent upon dose rate with an associated energy investment of approximately 1.6 MRads. At further increases in cumulative dose there is a clear dose rate dependence with effectiveness increasing with decreasing dose rate. These observations are summarized quantitatively in Table 10. On the basis of limited results in the first test segment we observed above that destruction varied roughly exponentially

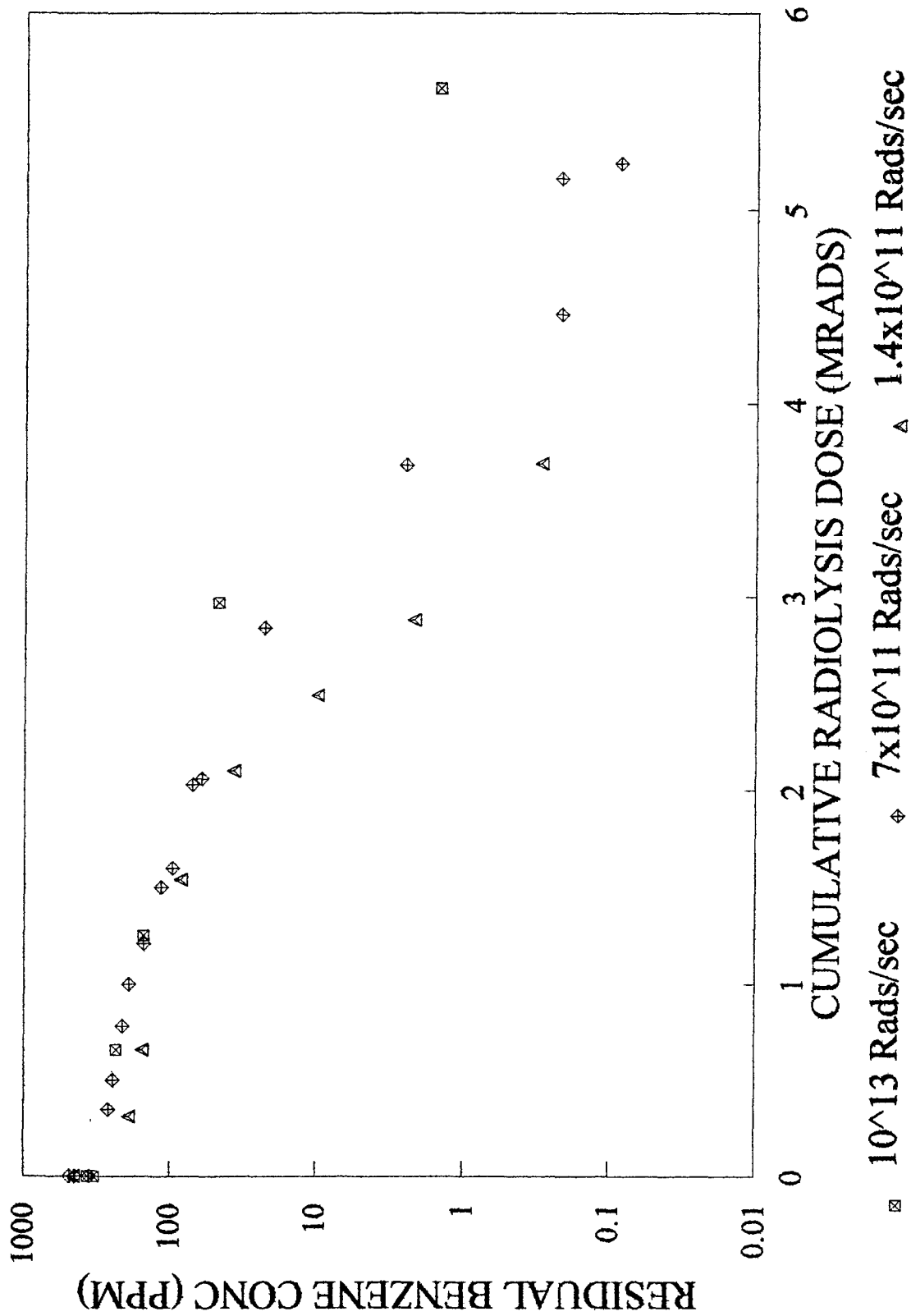


Figure 33: Radiolysis of benzene at an initial concentration of 400 ppm.

TABLE 10

Summary of Benzene Destruction by One and Two Decades
for Several Initial Concentrations and Dose Rates

Benzene Init Conc (ppm)	400	400	400	100	100	40
Dose Rate (10^{12} Rads/sec)	10	0.7	0.14	0.7	0.14	0.7
Dose for Destruction (Mrads):						
First Decade of Destruction	3.1	2.5	2.1	0.91	0.58	0.37
Second Decade of Destruction	1.7	1.0	0.62	0.45	0.33	0.36
Two Decades of Destruction	4.8	3.5	2.7	1.36	0.91	0.73

with cumulative dose. Expanded test results in Figure 33 show this is not true at lower dose rates over the broad range in destruction of more than three decades.

Results for benzene tests of groups (4) and (5) above are shown in Figure 34. For this initial concentration of 100 ppm the rates of destruction by radiolysis are much more rapid than those for 400 ppm initial concentration. Here again there is a significant dependence of rate of destruction upon dose rate with effectiveness increasing with decreasing dose rate. Residual concentration does not show exponential dependence upon cumulative dosage over the full measured range of four orders of magnitude. Destruction likely covered a broader range, however current GCMS diagnostics do not accurately resolve concentrations below 10 ppb. Certain observations for these tests are summarized in Table 10.

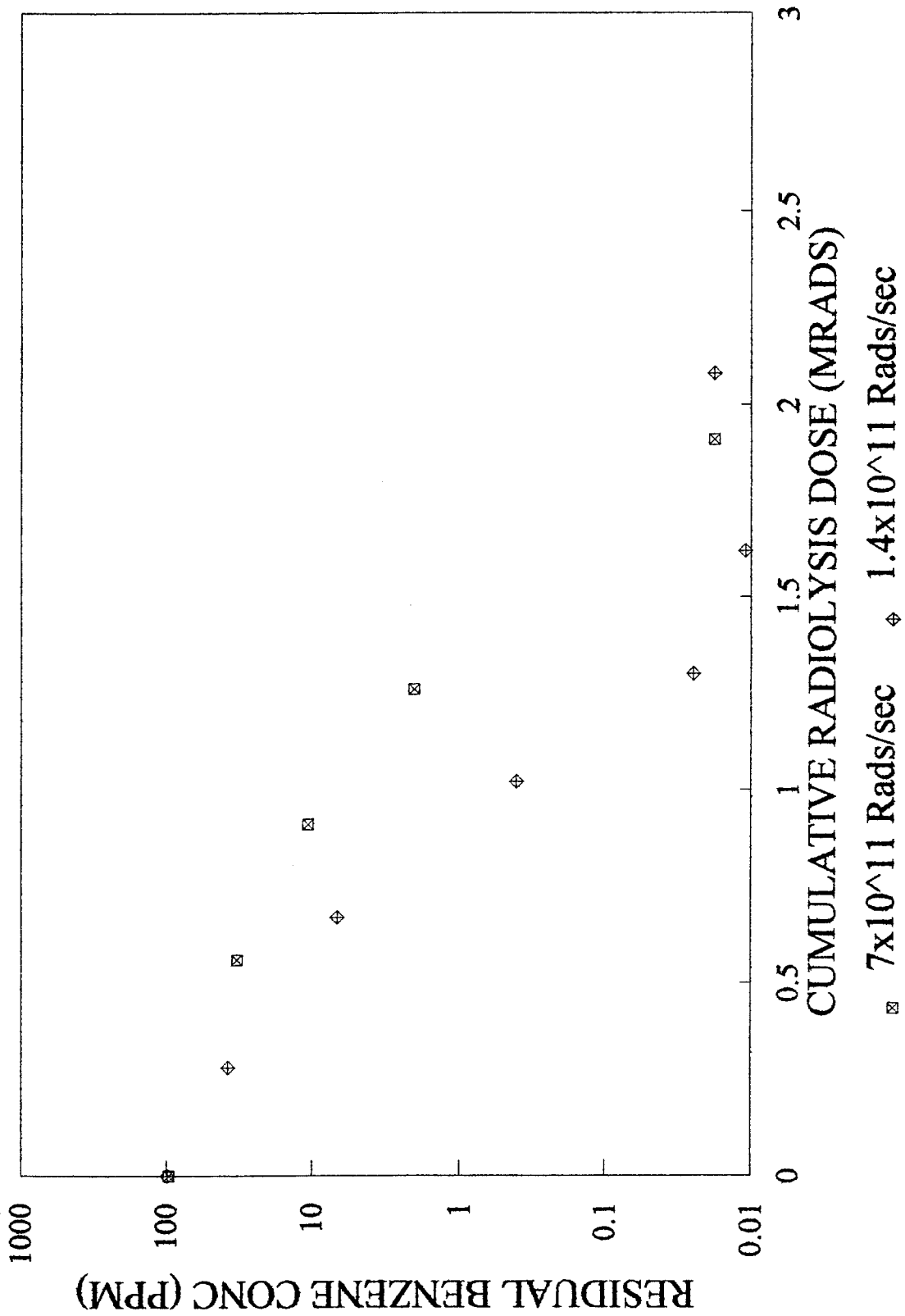


Figure 34: Radiolysis of benzene at an initial concentration of 100 ppm.

One test series was conducted at an initial benzene concentration of 40 ppm and at an intermediate dose rate of 7×10^{11} Rads/sec. These results are shown in Figure 35. Here there is a strong indication of exponential decay of concentration with increasing dosage down to the detection limit of 10 ppb. Certain features of these results are also summarized in Table 10. The Rate of destruction is even faster than those for 100 ppm initial benzene concentration. Here the constant destruction effectiveness is 0.37 MRads/decade of benzene destruction.

Results of analyses summarized in Table 10 show some interesting additional features. Reaction products, though not identified, would appear to have an influence on the continued progress of destruction. For example the dose for the second decade of destruction in the second column (i.e. reduction from 40 ppm to 4 ppm) of 1.0 Mrads is much larger than the 0.37 MRad dose for destruction from 40 ppm to 4 ppm in the last column. The dosages for one and two decades of destruction are similar for 100 ppm/ 0.7×10^{12} Rads/sec and for 40 ppm/ 1.4×10^{12} Rads/sec. Trends in the above table are summarized as: required radiolysis dose per decade of destruction increases with increasing contaminant initial concentration and with increasing dose rate; required dose per unit mass of contaminant destruction decreases with increasing contaminant initial concentration. In all benzene studies (cases 1-6) destruction was observed over a range of three to four orders of magnitude.

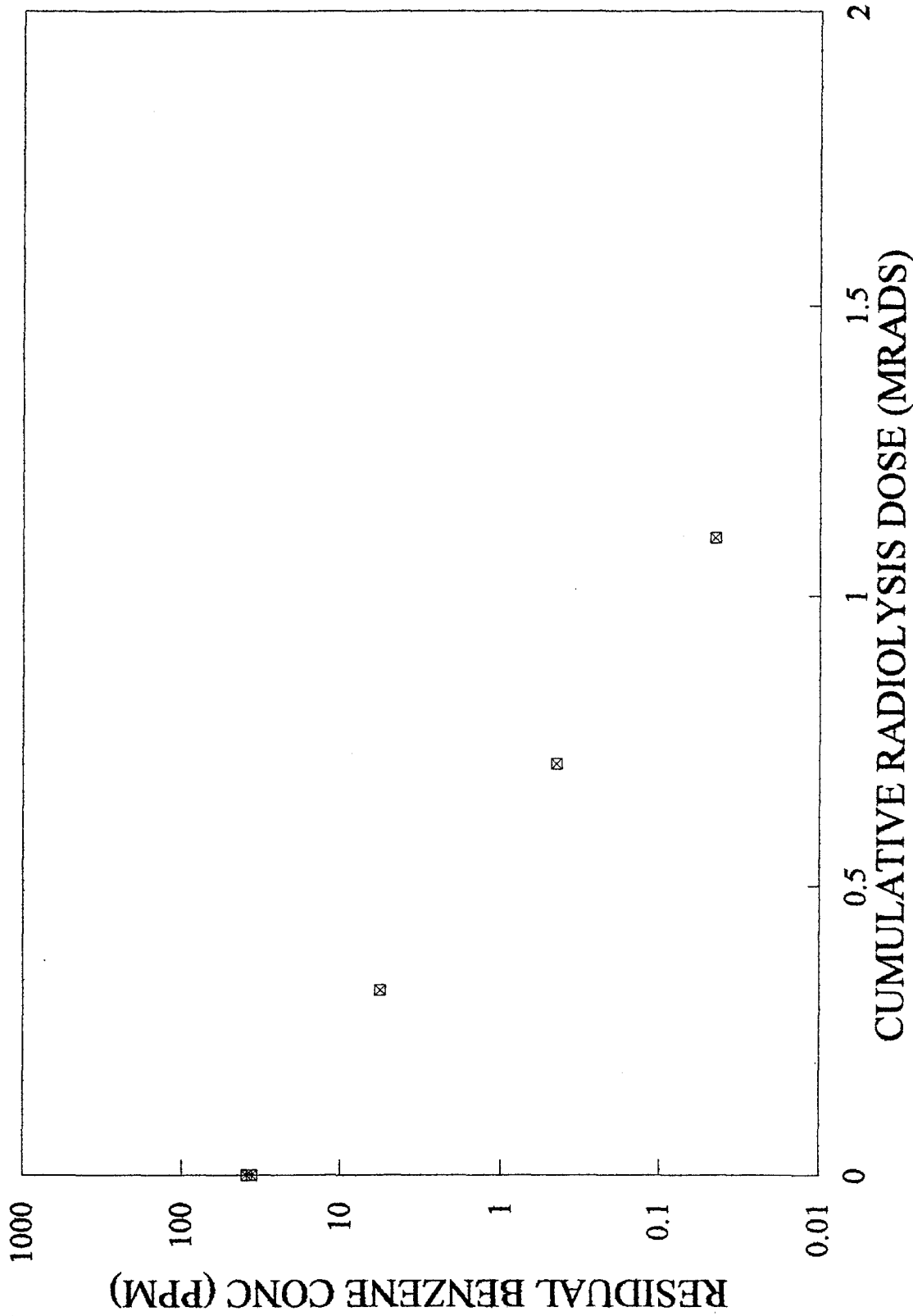


Figure 35: Radiolysis of benzene; initial concentration 40 ppm; 7×10^{11} Rads/sec.

It is useful to compare these studies at 100 and at 40 ppm initial benzene concentrations with the work of D. Savage.⁽⁵⁾ She studied benzene destruction by electron beam radiolysis at an initial concentration of 100 ppm and observed exponential dependence on dosage with an effectiveness of 0.47 MRads/decade of benzene destruction. Results in column 5 (i.e. the lower dose rate) of Table 10 compare favorably with her work. Destruction of benzene in water by electron beam radiolysis was also studied by Nickelsen et. al.,⁽¹⁷⁾ but at lower initial concentrations. They also observed a strong dependence in rate of destruction as a function of initial concentration and the same trend of decreasing effectiveness with increasing concentration. At their highest reported initial benzene concentration of 6 ppm a dosage of 0.15 MRads was required to produce a factor of ten reduction. In view of the variation in effectiveness with initial concentration our observation of 0.37 MRads/decade compares favorably with this value. The important point to these comparisons is that studies in Refs. 5 and 17 used continuous electron beams with dose rates many orders of magnitude lower than those in the current study. Consequently it is important to determine if linear induction accelerator technology does or does not incur a penalty in efficiency as a result of its inherently high dose rates. Tests reported above suggest that, although dose rate is observed to influence destruction effectiveness, operation at the low end of what is practical for this linear induction accelerator does not cause a penalty in destruction efficiency when compared with studies using continuous electron beam accelerators at low dose rates. Both studies in Ref. 5 and Ref. 17 reported measurements of creation and destruction of products from the radiolysis of benzene. Both studies used HPLC analysis and observed significant product

concentrations in comparison to surviving benzene. This is consistent with the absence of detectable radiolysis products in the current work since the observed products were not in the target list of Table 6. Savage recorded the creation and destruction of phenol and biphenyl. Nickelsen recorded the concentrations of phenyl and six additional products. At a dosage of 0.2 MRads they observed destruction of each of these products to concentrations below 200 ppb. Since there are strong similarities in benzene destruction between the current work and that of these researchers, we may assume there are strong similarities in the creation and destruction of radiolysis products as well. We have not pursued detailed studies of product formation at this time since our current focus is on the comparison of accelerator technologies and the development of a reliable and cost effective radiolysis system.

One test series was conducted with methylene chloride at an initial concentration of 5,000 ppm and at a radiolysis dose rate of 7×10^{11} Rads/sec. In these tests the source contaminant (DCM) and several products were identified in the target list of Table 6, 1,2-Dichloroethane (DCE), 1,1,2-Trichloroethane (TCEA), Trichloroethene (TCEE), 1,1,2,2-Tetrachloroethane (TETCEA) and Chloroform (CLFORM). Results of these tests are shown in Figure 36. Missing product data points at various dosages does not indicate their absence. Samples at different dosages were prediluted to different strengths and missing data points indicate dilution below their detectability. The trend of reduced destruction effectiveness with increasing initial contaminant concentration is evident when these results are compared with red water results and benzene results. A maximum dose

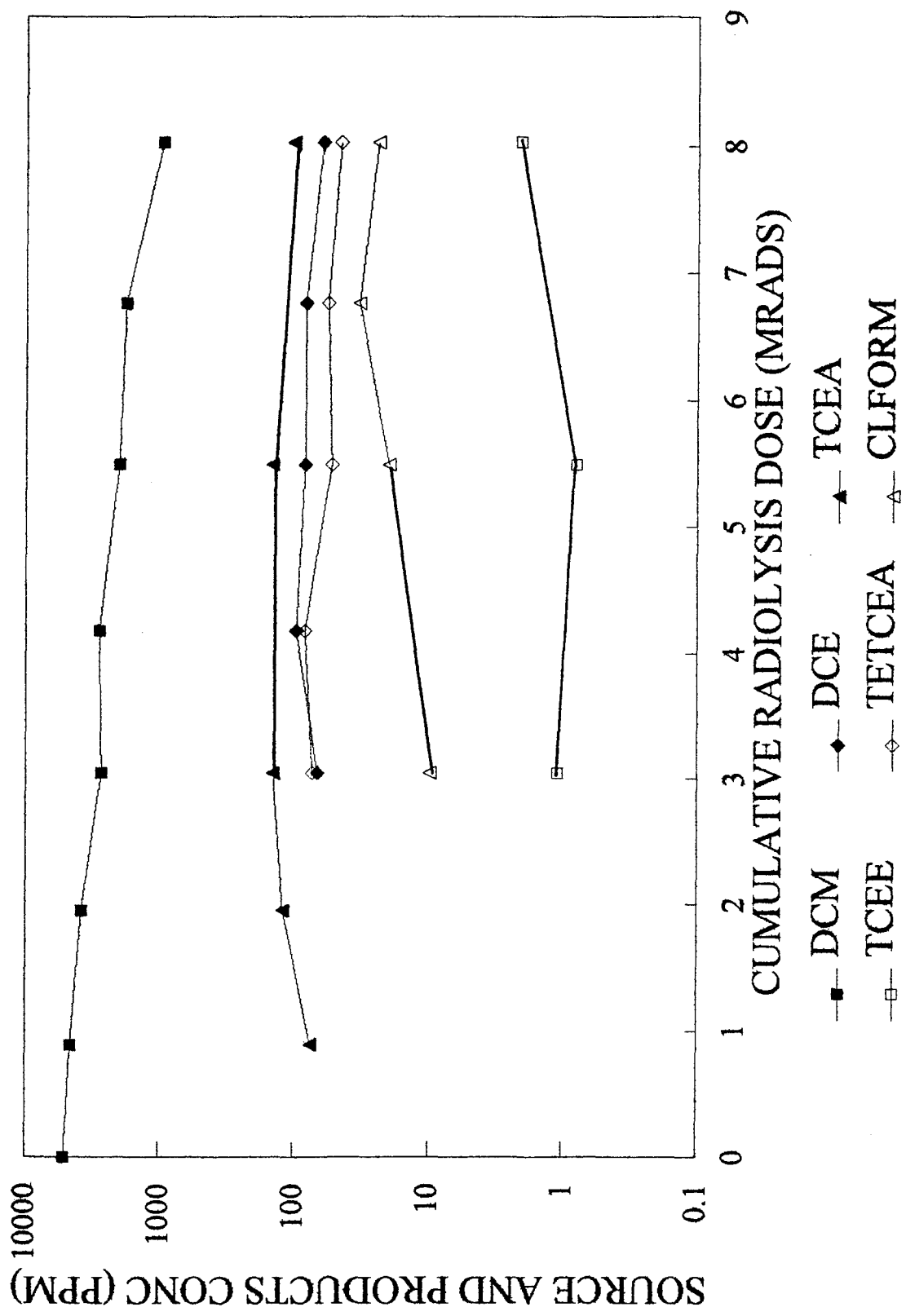


Figure 36: Methylene chloride; initial concentration 5000 ppm; 7×10^{11} Rads/sec.

of 8.0 MRads causes a reduction in DCM by 81%. Still the destruction efficiency based on unit mass of contaminant is higher than any of the benzene cases since the DCM initial concentration was 5,000 ppm. Products of radiolysis appear at low to moderate dosages and do not decrease significantly over the dose range of the study. The combined concentrations of all products do not exceed 15% of the surviving concentration of DCM over the dosage range. It is informative to do an accounting of atomic species as source contaminant and as products. The molar concentrations of chlorine, hydrogen and carbon-times-two are equal by definition in the source DCM at all dosages. This is shown in Figure 37. Irregularities in these plots result from missing data points in Figure 36; addition of interpolated values has shown that these plots then become quite smooth. The combined product molar concentrations of chlorine, hydrogen and carbon-times-two are also shown. If all destroyed source DCM went to the identified products the total concentrations of these three atomic species would be invariant. This does not occur, therefore there are presumably unidentified additional product species. However it is interesting to note that the composite composition of identified species closely matches the source chemical composition. In other words, at all dosages the concentrations of Cl, H and C are approximately in the ratios of 1/1/0.5. In fact carbon is seen to be in slightly higher concentration and this is highlighted by computing the "missing" concentrations of Cl and H which would complete this composition balance. These are called free Cl and free H in Figure 37 and these "missing" portions are seen to be a decade lower than the measured product concentrations. The pH of irradiated samples increased monotonically from 6.5 to approximately 2.0 at 8 MRads. This suggests that a significant portion of

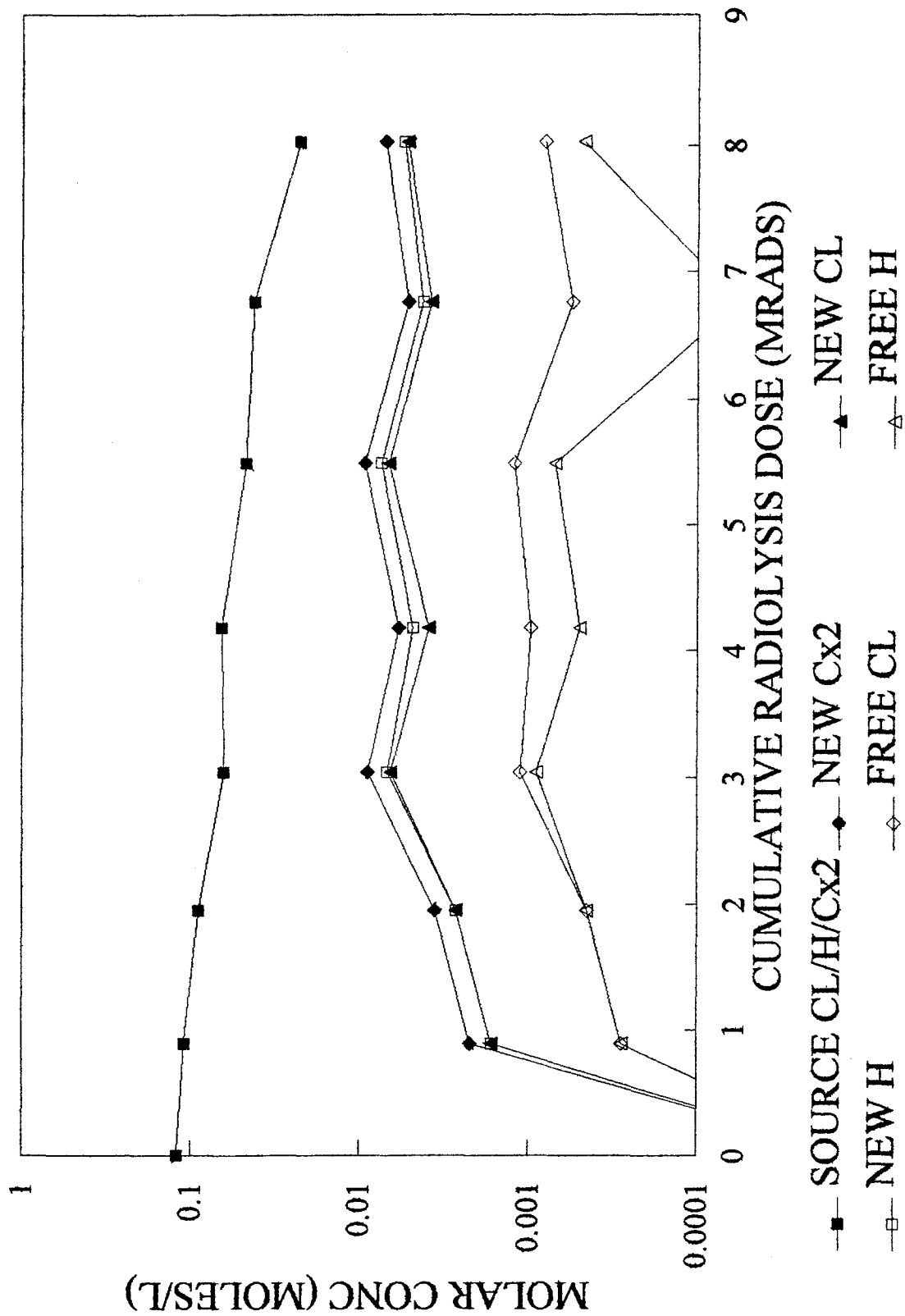


Figure 37: Methylene chloride; initial concentration 5000 ppm; 7×10^{11} Rads/sec.

product hydrogen and chlorine may exist as hydrochloric acid, but the inclusion of this in the hydrogen or chlorine tally still leaves a 68% defect from the original DCM insertion. As with red water it appears that effective VOC destruction at very high concentrations may require the addition of an oxidizing agent.

6.0 PROCESS COST ANALYSIS

Cost for any water decontamination process using induction accelerator electron beam technology is directly related to the required dosage. In the absence of oxidizing additives the cost is directly proportional to dosage if the accelerator operates at full capability. This results since capital cost, cost of electricity and most operating costs scale with delivered electron beam power. With oxidizing additives the cost would scale as (reduced) power demand and the cost of additives. Cost estimates presented here do not take advantage of possible cost reduction associated with oxidizing additives since this data base is too limited. Here we develop a single point cost estimate for red water cleanup based on limited data and some speculation. We also develop process cost maps for cleanup of volatile organic compounds for initial concentrations from 400 ppm to 1.2 ppm and for destruction by one and two decades.

Total annual operating costs for an induction accelerator driven electron beam at a power of 600 kW are listed in Table 11. The capital cost is estimated at approximately \$2/Watt. The total annual operating cost is driven by the cost of electricity as seen from their ratio = 1.6. These costs are based on a conservative estimate of "wall plug" electrical efficiency of 60%. Since capital costs scale approximately as delivered power and since amortization plus power consumption are the major operating cost elements, cost for water decontamination is nearly proportional to required dosage.

Table 11: Treatment Cost for Contaminated Industrial Water

Specifications	
Beam Power	600 kW
Capital Cost (\$)	
Accelerator	\$930,000
Computer	40,000
X-Ray Shield	30,000
Flow and Auxillary Equipment	<u>150,000</u>
Total	\$1,150,000
Annual Costs (for 7920 hrs of operation)	
Amortization (10-yr., 10%)	186,000
Cathode Replacement	4,000
Capacitor Replacement/Maintenance	60,000
Foil Replacement	6,000
Power (\$0.07/kW-h)	554,000
Labor	<u>80,000</u>
Total	890,000
Electron Beam Efficiency	0.6
Electron Beam Utilization	0.8

6.1 Configuration and Operating Parameters

The configuration for a 1.5 MeV accelerator and a coupled water radiolysis cell is shown schematically in Figure 38. Operating parameters are listed in Table 12. The depth of the radiolysis channel is dictated as 0.5 cm at the electron beam voltage of 1.5 MeV. At specified gun conditions the electron beam spot size is dictated by specifying the dose rate. A dose rate of 2×10^{11} Rads/sec requires a spot size of 1200 cm². The required dose dictates the contaminated water flow rate; for example a dose of 1.0 MRads requires a throughput of 48 liters/sec. A specification of allowed foil heating defines the total foil

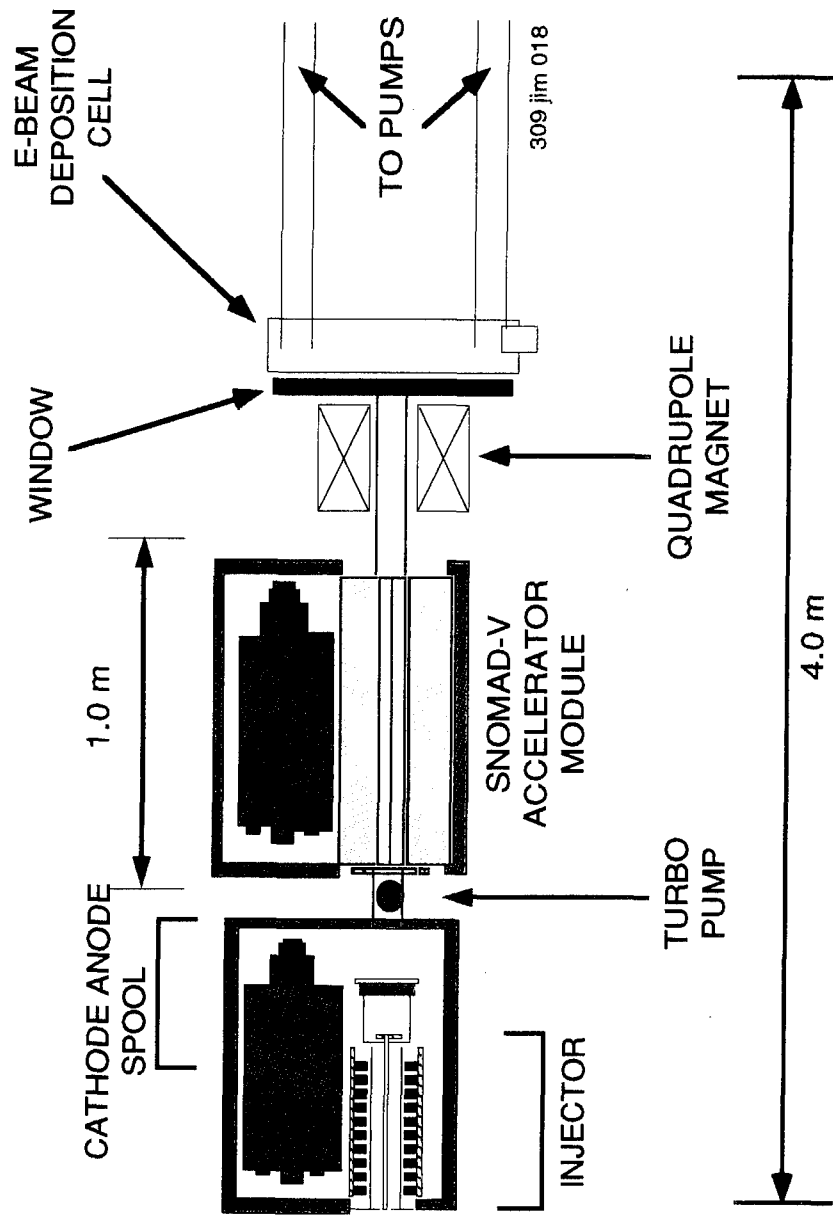


Figure 38: The electron beam treatment system consists of an induction accelerator, foil window, beam slewing magnet and electron beam deposition cell.

Table 12: Parameters for an Electron Beam Treatment System

Electron Beam Power	600 kW
Beam Voltage	1.5 MeV
Beam Current	800 Amps
Repetition Rate	10,000 pps
Pulse Length	50 nsec
Window Size	12 cm × 125 cm
Foil Thickness	4×10^{-3} cm
Foil Heat Deposition	≤ 20 Watts/cm ²

window area; for example 20 W/cm² requires a foil area of 1500 cm². This is only slightly larger than the spot size, which indicates that beam spreading by magnetic deflection is required rather than beam slewing. Foil cooling will likely be achieved by direct contact with the flowing cell water; consequently this cooling requirement is easily met. This cooling method is supported by our experience to date as was described earlier. Specification of water velocity in the radiolysis cell defines the window dimensions in the direction of and transverse to the flow; for example a specification of 1500 cm/sec requires dimensions of 24 cm by 62.5 cm respectively. This water speed corresponds to a flow dynamic pressure of approximately one atmosphere. This rule of thumb limit on velocity insures that water pressure will not add significantly to foil stress and water flow power will be moderate. Finally we have the option of multiple passes through the cell.

Multiple passes aid in flow mixing to improve dose uniformity and allow flexibility in window configuration. We have chosen a two pass arrangement to provide a window aperture of 12 cm by 125 cm.

6.2 Red Water Process Cost Estimate

Current data on destruction of red water is too limited to provide an accurate process cost estimate. A rough estimate is made here on the basis of limited data. This estimate is likely to be pessimistic since the process is not applied in combination with other procedures. For example it was shown above that the addition of hydrogen peroxide had a significant beneficial impact on the efficiency of red water decontamination; but this data base must be expanded to provide a quantitative assessment of impact on process cost.

A cost estimate for red water decontamination is developed in the following steps:

- (a) Red water at a total dissolved solids mass fraction of 0.10 is diluted 10:1 prior to radiolysis. Predilution is based on our experience of little destruction of net red water at a dosage of 200 MRads.
- (b) Destruction of contaminants is assumed to be proportional to dose over the range of 10,000 ppm to 1000 ppm at an investment of 0.003 MRads/ppm. This is based on measurements at 10:1 dilution, without peroxide addition, with observed HPLC peak reduction of 50-60% at a dose of 19.4 MRads in Figure 22.
- (c) Destruction of contaminants is assumed to be exponential with dose below 1000 ppm at an effectiveness of 12 MRads/decade. This is based on measurements of HPLC peak reductions with an effectiveness of 15

MRads/decade over an estimated range of 1000 to approximately 4 to 39 ppm in Figure 24. A 25% improvement in effectiveness is assumed at a reduced design dose rate.

- (d) For destruction to a residual concentration of 1.0 ppm the above model requires a dose of 63 MRads. Since the red water is diluted 10:1 the investment for cleanup of undiluted red water would be 630 MRads.
- (e) On the basis of costs in Table 11 and this dosage the radiolysis system of Table 12 would process 600,000 gal of red water per year (1810 gal/day) at a unit cost of \$1.50 per gallon.

The TNT facility at Radford Army Ammunitions Plant consists of two production lines each of which can manufacture 50 tons of TNT per day. The red water produced by each line was 8500 gallons per day. This is 4.7 times more than the capability of the system described in Section 6.1. Device scaling to meet these requirements is straightforward due to the modular construction of the accelerator. Addition of two 1.0 MeV modules will increase the delivered power by a factor of $3.5/1.5=2.33$. Two such systems would therefore be needed to process one line. Increased voltage is a desirable approach for power scaling since it allows an increase in radiolysis cell channel depth from 0.5 to 1.5 cm and does not increase foil heating. This large number of identical accelerator modules would likely decrease the system cost per Watt and thereby the unit decontamination cost.

The potential for cost saving by peroxide addition is interesting in view of bulk peroxide cost at \$1.00 per kg. Peroxide addition equal in weight to red water contaminants, i.e. 0.8 lb per gal, adds a cost of \$0.36 per gal which is a small fraction of our estimated decontamination cost. Comparison of our tests without peroxide and with

peroxide equal in weight to contaminants (Ref. Figs. 22 and 23) shows a dramatic increase in reduction of some HPLC peaks. This and color comparisons suggest that electron beam radiolysis with oxidizing additives should be explored further.

Cost envelopes for various waste water treatment technologies were developed by Kidman and Tsuji⁽¹⁸⁾ and are shown here in Figure 39. Incineration of red water (100,000 ppm) has a cost range of \$2.00 to \$10.00 per gallon. Our preliminary estimate for destruction by SRL electron beam technology at \$1.50 per gallon compares favorably. This is true especially when considering possible cost reductions with system optimization and with the assistance of additives.

6.3 VOCs in Water, Process Cost Estimates

Preliminary cost estimates for destruction of VOCs in water with SRL accelerator technology are shown in Figure 39. This map is based simply on assumptions of exponential decay in concentrations with dose and an effectiveness of 0.5 MRads/decade of destruction. The upper bound applies when the final concentration is 1.0 ppm as may be the requirement for discharge to the environment. The lower bound applies when the final concentration is 10 ppm as may be required when the waste water is recycled in a commercial or industrial process.

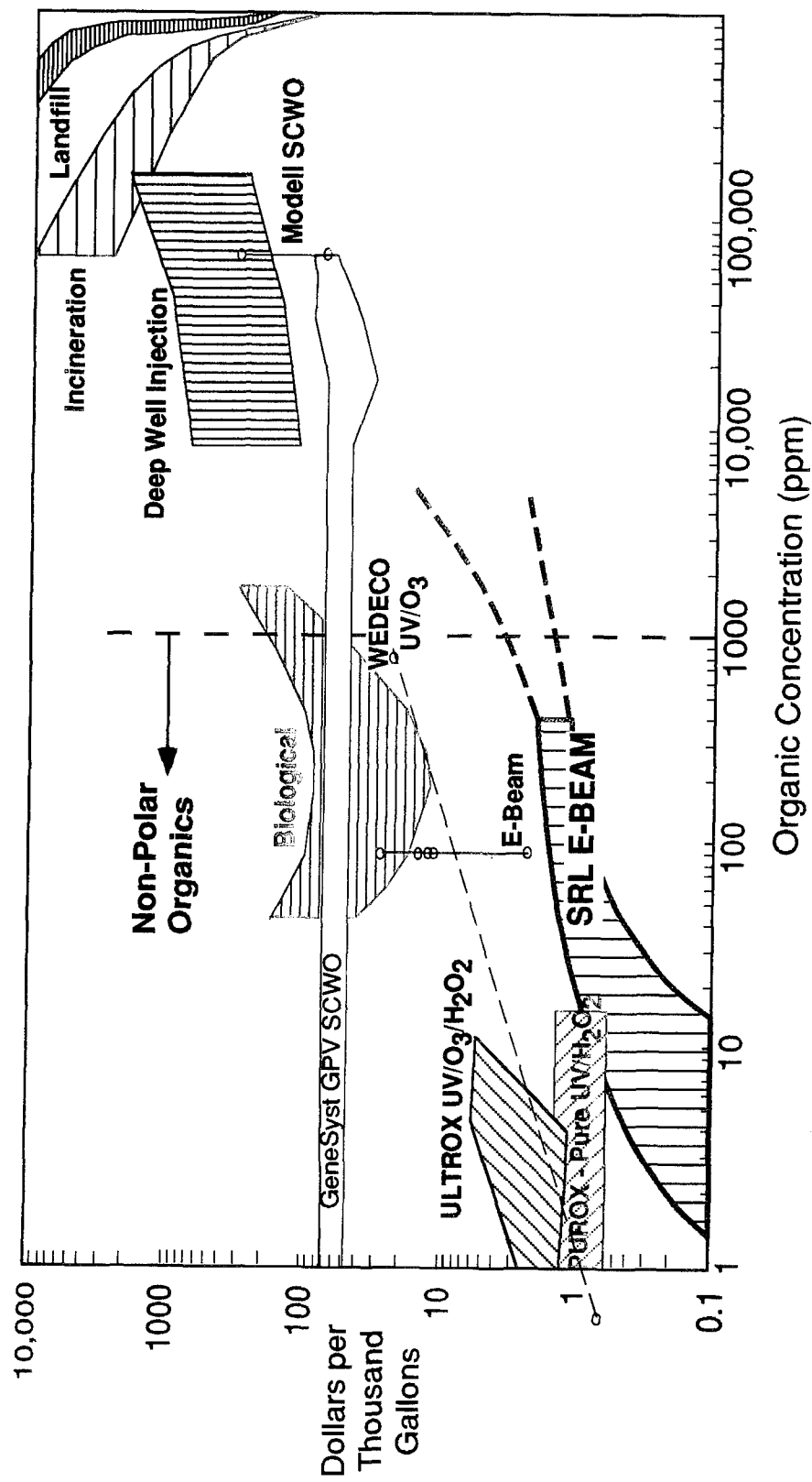


Figure 39: Cost envelopes of various waste treatment technologies.

Process costs have since been revised on the basis of additional data for benzene radiolysis as reported above. We have extended this costing to lower benzene concentrations (6 and 1.2 ppm) using results reported by Nickelsen et. al.⁽¹⁷⁾ This costing is based on dosages required for one and for two decades of destruction at several levels of initial benzene concentration. For initial concentrations of 400, 100 and 40 ppm the dosages were taken from Table 10 at the lowest dose rates for which data exists. For initial concentrations of 6 and 1.2 ppm dosages were taken from Reference 17. As described above dosage is the only remaining input necessary to establish throughput and cost for the SRL induction accelerator technology. For example reduction in benzene concentration from 40 ppm to 400 ppb requires a dose of 0.73 MRads and the associated annual processed volume is 520 Mgal/year. At an annual operating cost from Table 11 of \$890,000.00 the resulting unit cost would be \$1.72 per 1,000 gallons. In a similar manner the cost maps in Figure 40 were generated for two levels of destruction, 100× and 10×, and for five levels of initial benzene concentration.

Comparison of Figures 39 and 40 show that induction accelerator technology is substantially less expensive than competing technologies for VOC destruction over the studied range of initial concentrations. This is especially true for concentrations at the high and low extremes. Furthermore the current cost analysis is pessimistic in at least two respects. First, benzene was used as the basis for dose requirements, although a variety of VOCs require lower doses for equal destruction. This is seen by comparison of toluene and trichloroethylene in Figs. 30 and 31 with benzene in Figure 29. This has also been

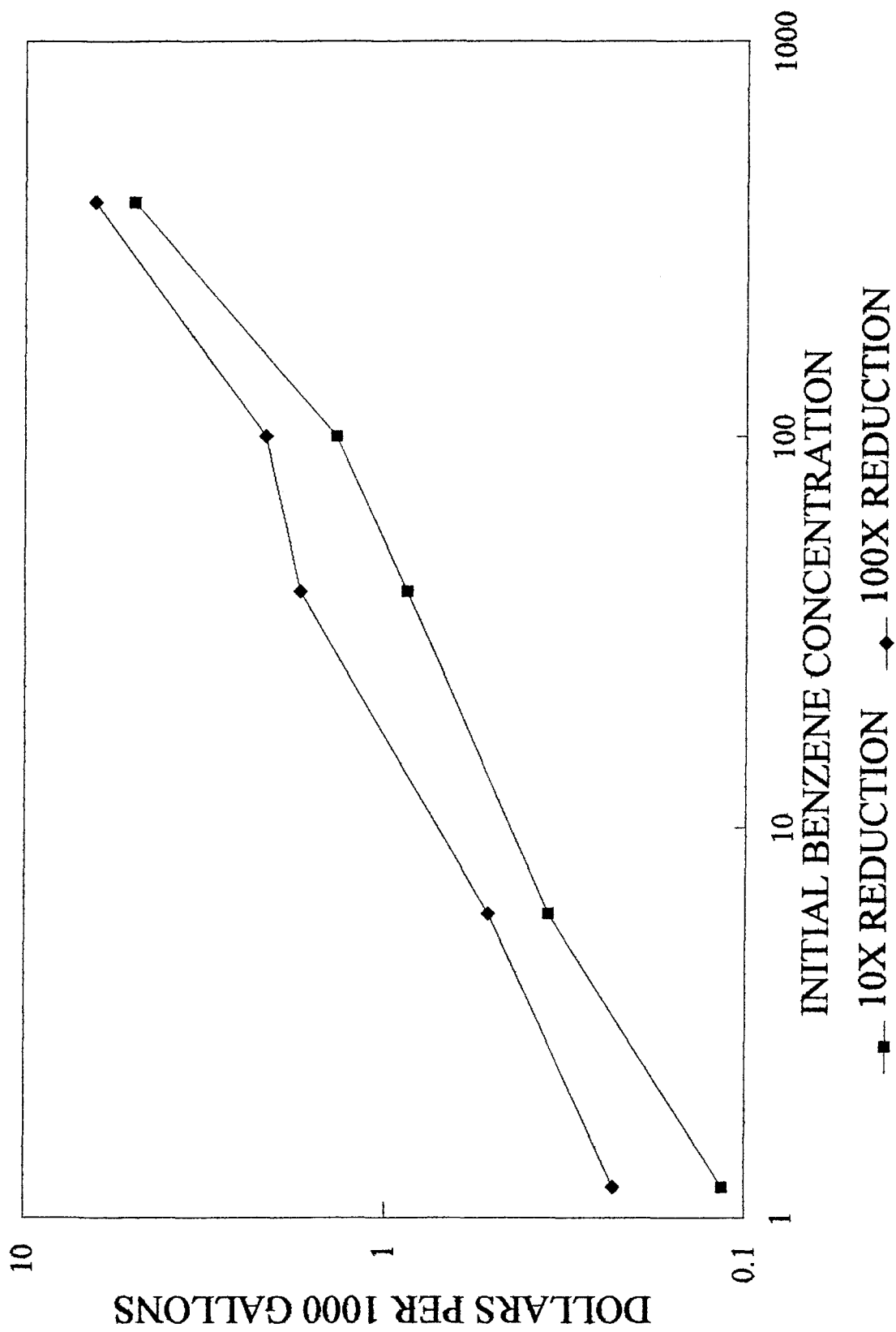


Figure 40: Cost for benzene destruction by radiolysis.

reported at lower initial concentrations in Ref. 17. Second, the data in Table 10 at 40 ppm are not at the lowest dose rate of 1.4×10^{11} Rads/sec. There would likely be a gain in projected efficiency if this data were available; in fact this is suggested by the departure of 40 ppm results from the overall cost trend in Figure 40.

7.0 SUMMARY AND CONCLUSIONS

7.1 Summary

Unwanted isomeric forms of TNT are separated from 2,4,6,TNT by reaction with sodium sulfite in several stages of sellite washing. This preferentially replaces NO_2 at asymmetric sites and renders soluble products. These are removed with wash solution and form the major constituents of process waste water. The color of red water is thought to be due primarily to these sulfonates and their complexes. U.S. military production facilities of TNT, including the primary site at (RAPP), have been closed due to lack of an environmentally acceptable method for disposal of red water. The U.S. Army is exploring the option of incineration, but they are also actively seeking more cost effective alternative technologies.

The broad objective of this research is to develop an experimental basis for evaluation of a new, low cost electron beam radiolysis process for red water decontamination. This would utilize induction accelerator technology developed at Science Research Laboratory (SRL), which is compact and modular and which has demonstrated component reliability of it's all solid state circuitry. Electron beam radiolysis has been demonstrated as an efficient means for water decontamination; however the SRL technology offers the best promise to overcome previous limitations of reliability, size, initial cost, power scalability and serviceability. The specific objectives are to determine the dependence of destruction

efficiency on initial contaminant concentrations, extent of destruction, contaminant species and on the addition of an oxidizer, hydrogen peroxide. Most importantly we explore the effect of dose rate since high dose rates are characteristic to and unique to induction accelerator technology. Primary emphasis is given to red water and to its building blocks, benzene and toluene. Limited tests were also conducted on trichloroethylene and on methylene chloride.

The test apparatus consists of a flowing contaminated water channel which is exposed to direct electron beam irradiation through a thin titanium foil window. The radiolysis cell is attached directly to a flange on SRL's SNOMAD-IV linear induction accelerator. The water flows in direct contact with the foil and thereby provides highly effective foil cooling. Each of two foils was subjected to over one million beam pulses during approximately ten hours of radiolysis operation over periods of several weeks and showed no signs of deterioration. The contaminated water flow system has sealed supply and discharge pouches which allows capture of both liquid and vapor products of radiolysis. Tests were conducted in two segments, first with the injector portion of the accelerator with an accelerating capability of 0.5 MeV and later with the addition of an accelerator module with a combined accelerating capability of 1.5 MeV. The system operated reliably during both test segments.

The primary measurement for dose determination was the water temperature rise between entry and exit of the radiolysis cell. These were complemented by periodic

dosimetry measurements with a Radiometric System supplied by Far West Technology. Both source and processed radiolysis samples were analyzed in selected cases. Red water samples were analyzed by Jordi Associates. Destruction of TNT and its isomers as well as other red water constituents was determined by high performance liquid chromatography (HPLC) with UV absorption detection. Red water composition was found to be complex, as expected, with at least thirty distinguishable peaks. Samples of symmetric TNT and of four of its five isomers were obtained and analyzed and identified in the HPLC traces. VOC samples were analyzed by Energy and Environmental Engineering Inc. Destruction of VOC was determined by gas chromatographic analysis and mass spectrometric detection (GCMS) and in some cases mass balance assessment was done by total carbon analysis.

Studies on red water were conducted on the neet product as delivered and at dilutions of 10:1 and 100:1, at electron beam dose rates of 10^{13} and 7×10^{11} and 1.4×10^{11} Rads/sec, and in one case with the addition of hydrogen peroxide. Tests on the neet product showed no significant contaminant destruction at cumulative dose levels to 200 Mrads. At a dilution of 10:1 contaminant destruction was observed from bleaching and from HPLC analysis. Destruction was approximately proportional to dose with a reduction of 50-60% at the maximum dose of 19 Mrads. At a dilution of 10:1 and with the addition of hydrogen peroxide, destruction efficiency was increased dramatically for some eluted peaks and only moderately for others, and bleaching effectiveness was significantly increased. At a dilution of 100:1 contaminant destruction followed

approximately exponential dependence on dosage, with eluted peak reductions by factors of 25 and greater at dosages to 23 Mrads, and with corresponding dramatic color reduction. Color change (bleaching) due to radiolysis was determined to provide a fair quantitative assessment of the destruction of major eluted peaks in the HPLC analysis.

VOCs in water were irradiated at initial concentrations of 5000, 400, 100 and 40 ppm. Effect of dose rate on destruction efficiency was examined at 10^{13} , 7×10^{11} and 1.4×10^{11} Rads/sec; in general lower dose rates produced increased destruction efficiency. Benzene destruction efficiencies at the lower dose rates are in fair agreement with studies at other laboratories where dose rates were many orders of magnitude lower. This observation is very important to the practical implementation of induction accelerator technology since high dose rates inherent and unique to its operation. A summary of benzene tests is presented in Table 10 where dependencies of destruction efficiency on initial concentration and on dose rate are evident.

System operational features have been developed for full scale applications to decontamination of red water and of VOCs. An example is presented for a required dose of 1.0 Mrads. It illustrates practical performance requirements in terms of foil heating, foil area, flow pump power and flow rate. Process costs have been developed, which indicate that red water decontamination by electron beam radiolysis may compete to advantage with incineration and VOCs decontamination by radiolysis has considerable cost advantages over all competing processes. These observations apply specifically to the

induction accelerator technology developed at this laboratory, which has low capital cost, solid state circuitry, modular design and demonstrated component reliability.

A chemical reaction model has been developed for the decomposition of red water and on this basis an initial cost estimate for decontamination was developed as \$0.45 to \$2.00 per gallon. Results of red water radiolysis measurements were subsequently used to develop a cost estimate of \$1.50 per gallon at a process rate of 1810 gallons per day. Comparison with estimates for cost of incineration shows radiolysis to be competitive, but not dramatically less expensive. Radiolysis by SRL's induction accelerator technology offers much greater cost advantages for contamination at lower concentrations, such as are present in pink water (i.e. waste water from munitions handling rather than explosives manufacturing) or in industrial waste water streams. This is illustrated in our analysis of VOCs decontamination.

Costs for destruction of VOCs by electron beam radiolysis were developed from measurements for benzene conducted at SRL and at Florida International University. These estimates are presented in Figure 40 and are compared to costs for alternative technologies in Figure 39. Comparisons show that induction accelerator technology is substantially less expensive, and it offers very high flow processing capability. For example, reduction of benzene from 40 ppm to 400 ppb would cost approximately \$1.72 per 1000 gallons at a processing capacity of 520 Mgal/year. Lower costs may be realized for VOCs which are more readily destroyed than benzene and there is potential for

somewhat improved destruction efficiency at dose rates lower than those reported above. One may conclude that induction accelerator technology offers a promising alternative to destruction of a wide variety of waterborne contaminants over broad ranges of concentrations.

7.2 Conclusions

Key questions addressed in this study are: (1) What is the efficiency and projected cost for electron beam decontamination of red water and other waste water streams? (2) Does induction accelerator technology with associated high electron irradiation dose rates influence process efficiency? Reported results show that dose rate indeed affects decontamination efficiency. However, dose rates, at the lower end of the range which is practical for large scale induction accelerator systems, are as efficient as competing continuous electron beam systems. Said simply, no significant penalty is implicit in the application of this compact, reliable and low cost technology. The projected dose requirements for red water decontamination is 630 Mrads with a projected treatment cost of \$1.50 per gallon. This is comparable to the cost of incineration; consequently this technology does not present an attractive alternative. It may, however, offer an attractive means for decontamination of pink water which has composite contaminant concentrations of order 200 ppm. This observation is based on reported studies of a variety of volatile organics at concentrations between 40 and 400 ppm. Here the dosages required for reductions by a factor of ten range between 0.73 and 2.7 Mrads and the associated treatment costs are projected as \$1.70 to \$6.40 per thousand gallons. This is much less

costly than competing conventional and advanced technologies. Induction accelerator technology as developed at SRL would, therefore, offer a cost effective system which is scalable to hundreds of millions of gallons per year.

REFERENCES

- (1) Metcalf & Eddy, Inc., *Wastewater Engineering: Treatment, Disposal and Reuse*, McGraw Hill, N.Y. (1989).
- (2) R.W. Coutant, T. Zwick and B.C. Kim, **Removal of Volatile Organics from Humidified Air Streams by Absorption**, DITC Report AD-A 192 435 (1987).
- (3) **Hazardous Waste Conference**; R.L. Levine, Director, Center for Bioengineering and Pollution Control, University of Notre Dame, Aug. 31-Sept. 3, 1992.
- (4) **Symposium on Environmental Applications of Advanced Oxidation Technology**, Myron Jones Chairman, Electric Power Research Institute and National Science Foundation Sponsors, San Francisco, CA, February 22-24, 1993.
- (5) D.E. Savage, **A Sequential Liquid Chromatography Study of the Destruction of Organic Contaminants in Water by Electron Irradiation**, Doctoral Thesis, Massachusetts Institute of Technology, Dept. Of Chemical Eng, Sept. 1992.
- (6) J.P. Moran, D. Goodman, and J. Jacob, **Reliable Low Cost Induction Accelerator System for Treatment of Contaminated Water**, See Ref. (4).
- (7) S. Faroeq, C.N. Kurucz, T.D. Waite and W.J. Cooper, **Disinfection of Waste Waters: High Energy Electrons vs. Gamma Radiation**, Accepted for publication, Water Research.
- (8) W.J. Cooper, M.G. Nickelsen, D.E. Meacham, T.D. Waite and C.N. Kurucz, **High Energy Electron Beam Irradiation: An Advanced Oxidation Process for the Treatment of Aqueous Based Organic Hazardous Wastes**, Water Poll. Res. J. of Canada, 27, No. 1, pp. 69-95, 1992.
- (9) E.W. Merrill, et. Al., **Destruction of Trace Toxic Compounds in Water and Sludge by Ionizing Radiation**, *Amer. Inst. Chem. Eng. Sym.* 74, 245 (1977), and S.W. Tay and E.W. Merrill, **Water Purification by Electron Irradiation in the Presence of Polymers**, NSF Final Report ECE-8612487 (1987).
- (10) M.R. Cleland, R.A. Fernald and S.R. Maloof, *Rad. Phys. Chem.* 24, 179 (1984).
- (11) A.K. Pikaev and V.N. Shubin, *Radiat. Phys. Chem.* 24, 77 (1984).
- (12) A. Sakumoro and T. Miyata, *Radiat. Phys. Chem.* 24 55 (1984).
- (13) I.G. Draganic and Z.D. Draganic, **The Radiation Chemistry of Water**, Academic Press, New York (1971).

- (14) W.J. Cooper, **E-Beam: The Treatment of Aqueous Based Toxic Organic Wastes**, Proceedings of Rad Tech 1992, Boston, MA (1992).
- (15) J.A. Kohlbeck, C.D. Chandler, Jr., R.L. Dickensen, **Final Engineering Report on Production Engineering Projects PE-238 and PE-289; Continuous TNT Characterization Study PE-238; Continuous TNT Process Control and Characterization Study-Extension PE-289**, Radford Army Ammunitions Plant, Hercules Inc., May 1973.
- (16) J.L. Hintze and P.J. Wagner, **TNT Wastewater Feasibility Study Phase I Laboratory Study Final Report**, Aerojet Propulsion Division, Sacramento, CA, September 1992.
- (17) M.G. Nickelsen, W.J. Cooper and L. Kaijun, **High Energy Electron Beam Generation of Oxidants for the Treatment of Benzene and Toluene in the Presence of Radical Scavengers**, Florida International University, Submitted for publication in: Water Research.
- (18) R.B. Kidman and K.S. Tsuji, **Preliminary Cost Comparison of Advanced Oxidation Processes**, Los Alamos National Laboratory LA-12221-MS, (1992).